Changes in gas-detector simulation

Rob Veenhof

RD51 collaboration and Uludağ university, Bursa, Turkey

Operating principles:

- A charged particle passes through the gas and ionises molecules;
- the electric field in the gas volume transports the ionisation electrons and provokes multiplication;
- the movement of electrons and ions leads to induced currents in electrodes.

Лев Давидович Ландау
(1908-1968)

Energy loss fluctuations

- Given a single-collision energy loss distribution $w(\epsilon)$, the distribution $f(\epsilon)$ of the energy loss ϵ after many collisions is *schematically* given by the Laplace transform:

$$L f(x,s) = \mathrm{e}^{-x\int_0^\infty (1-\mathrm{e}^{-s\epsilon}) w(\epsilon) \mathrm{d}\epsilon}$$

- Ландау showed (1944), assuming in particular:
  - thick layers: numerous small energy losses;
  - Rutherford-inspired energy loss distribution $w(\epsilon) \sim 1/\epsilon^2$;
  - neglect of the atomic structure:

$$L f(s) \approx s^s$$

Landau: too narrow for thin layers

- 2 GeV protons on an (only !) 5 cm thick Ar gas layer:

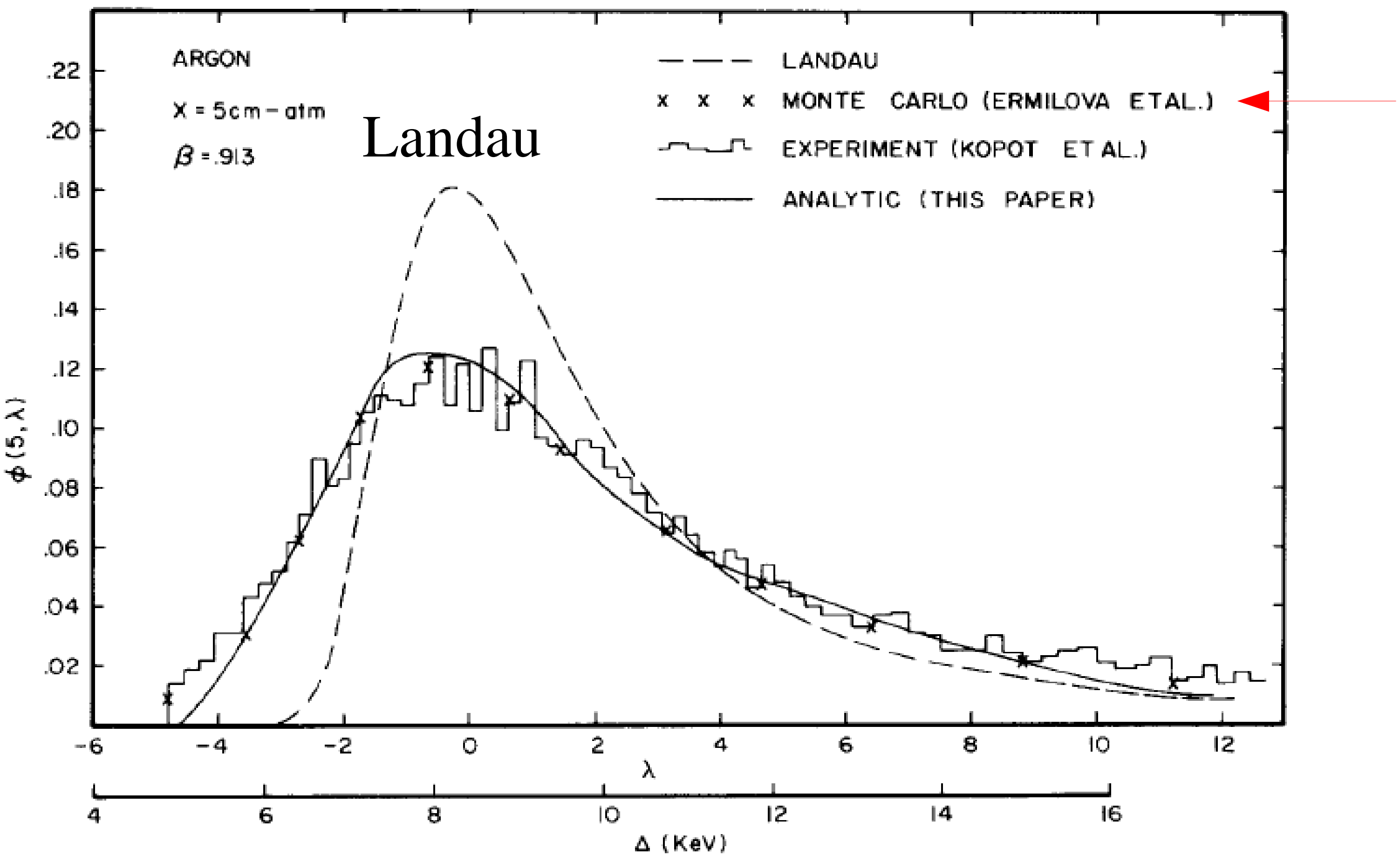

[Diagram: Richard Talman, NIM A **159** (1979) 189-211]

Virtual photon exchange model

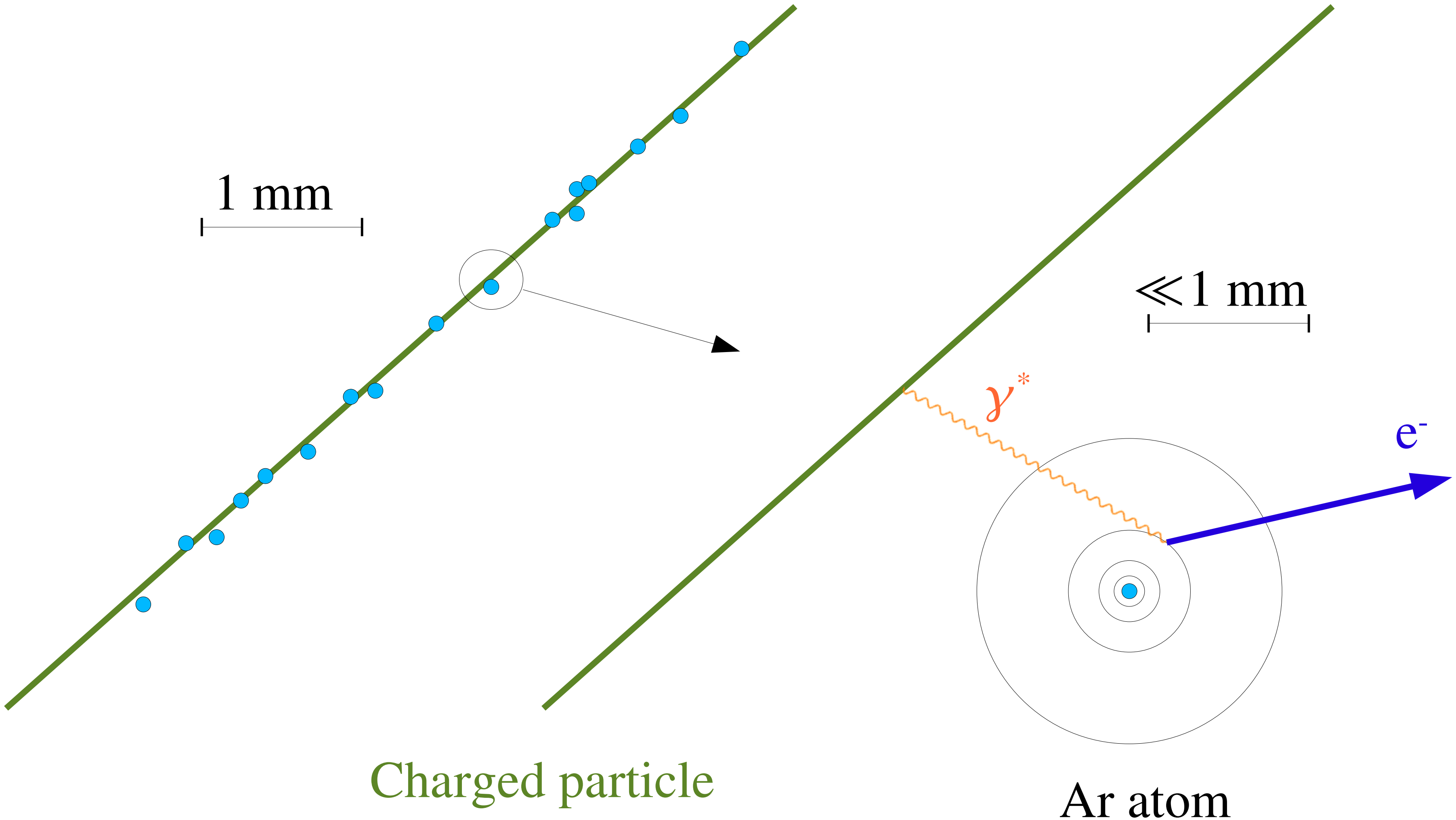

Heed

Igor Smirnov

- PAI model or absorption of real photons:

  Atom + π^- ➡ Ion^{+*} + π^- + e^- (photo-electric effect,

  Atom + γ ➡ Ion^{+*} + e^- real or virtual photon)

- Decay of excited states:

  Ion^{+*} ➡ Ion^{++} + e^- (Auger)

  Ion^{+*} ➡ Ion^{+} + γ (fluorescence)

  Ion^{+*} ➡ Ion^{+*} (Coster-Kronig)

- Processing of electrons:
  - below ionisation energy $\longrightarrow$ transport
  - photo- and Auger-electrons ("δ-electrons"):

  e^- + Atom ➡ Ion^{+} + 2 e^- (absorption of high-energy electrons)

Photo-absorption in argon

- Argon has 3 shells, hence 3 groups of lines:

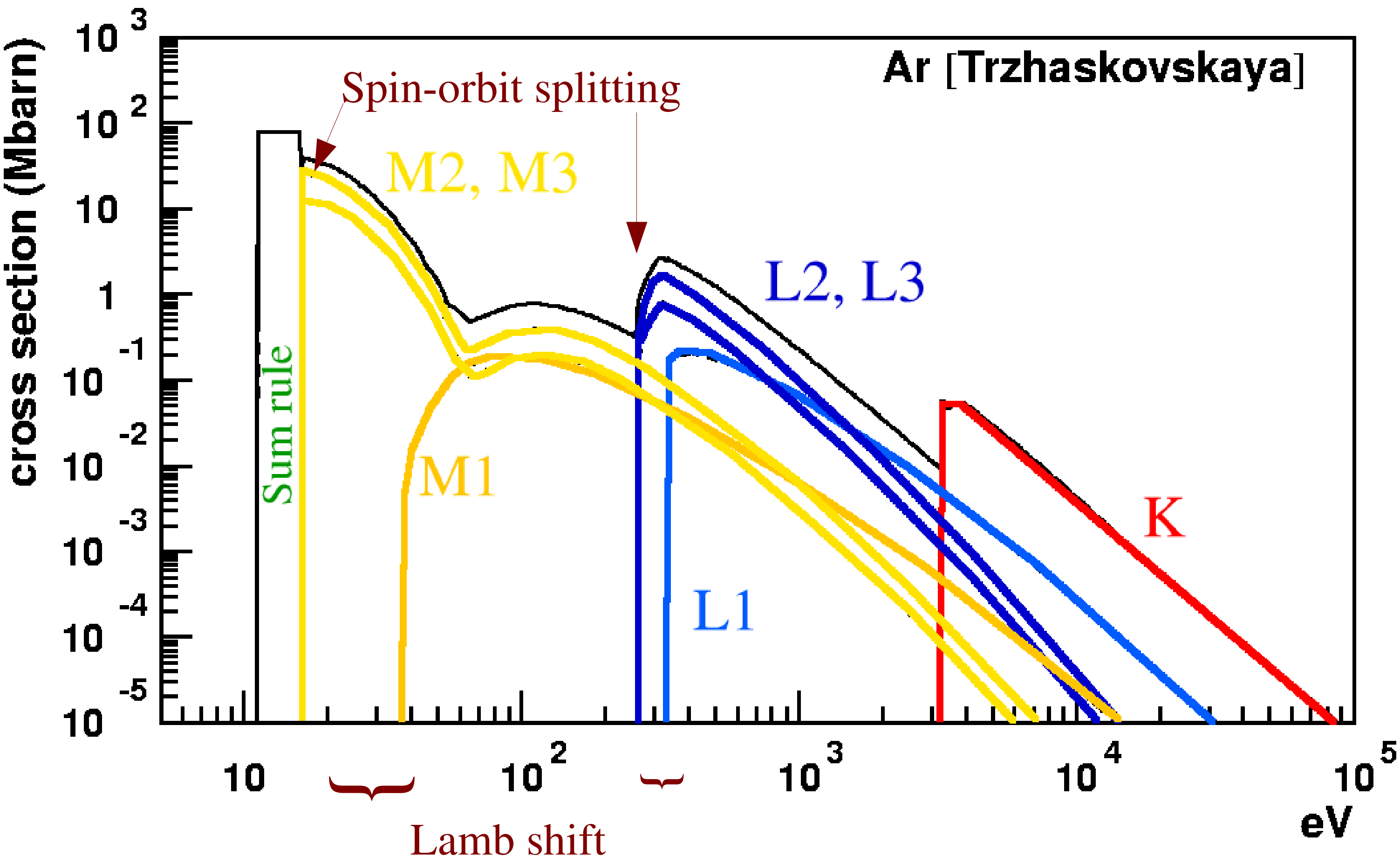

K = 1s

L1 = 2s
L2 = 2p 1/2
L3 = 2p 3/2

M1 = 3s
M2 = 3p 1/2
M3 = 3p 3/2

[Plot from Igor Smirnov]

Range of photo- and Auger-electrons

- Electrons scatter in a gas.
- Measures of the range:
  - R_{total}: total path length
  - R_p : practical range
  - $\overline{z}$: cog in direction of initial n
  - σ_x: RMS in direction of initia
  - σ_z: RMS transverse to initial

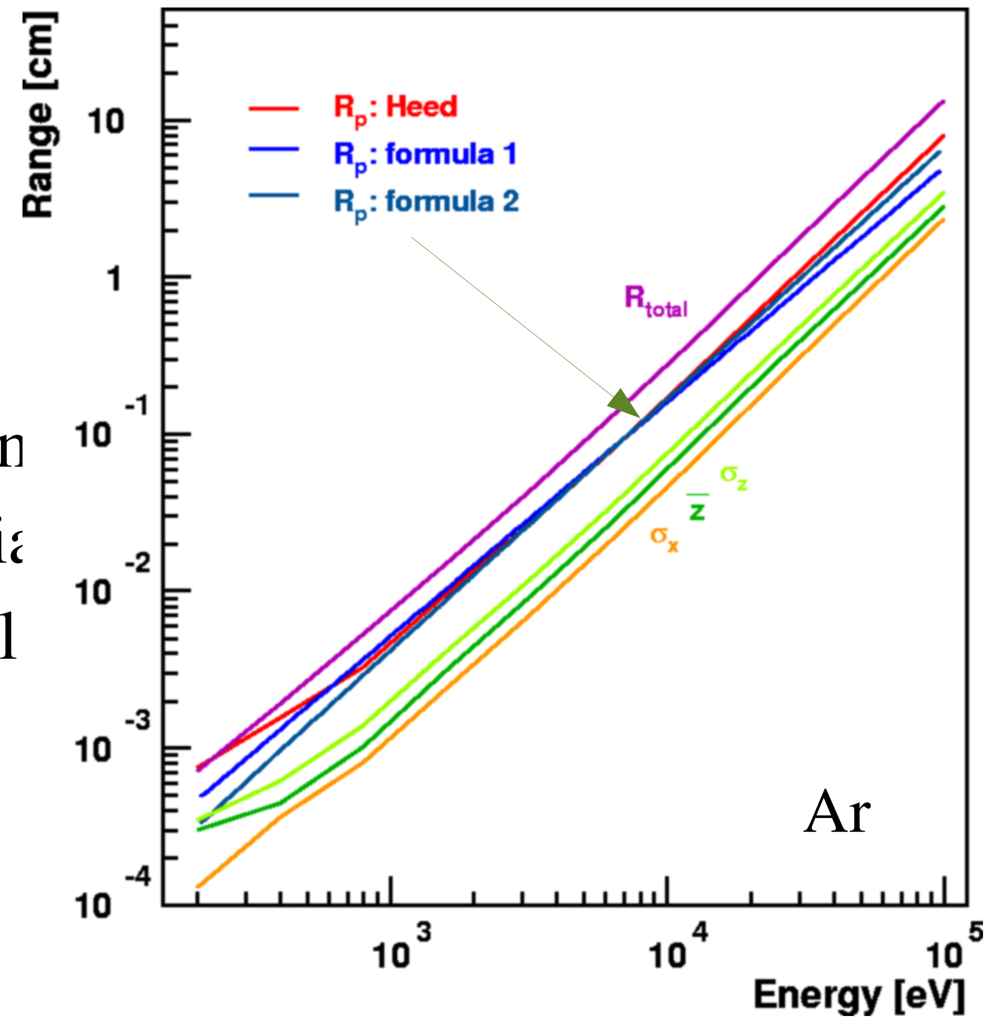

Practical range: distance at which the tangent through the inflection point of the descending portion of the depth- absorbed dose curve meets the extrapolation of the Bremsstrahlung background (ICRU report 35, 1984)

MWPC

- First gaseous tracking device
- 1968: Georges Charpak

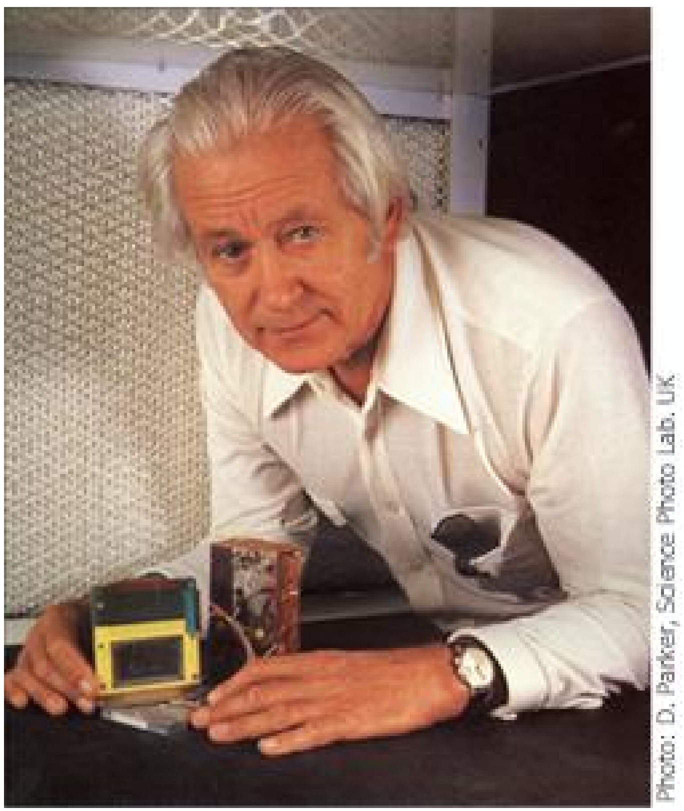

Georges Charpak

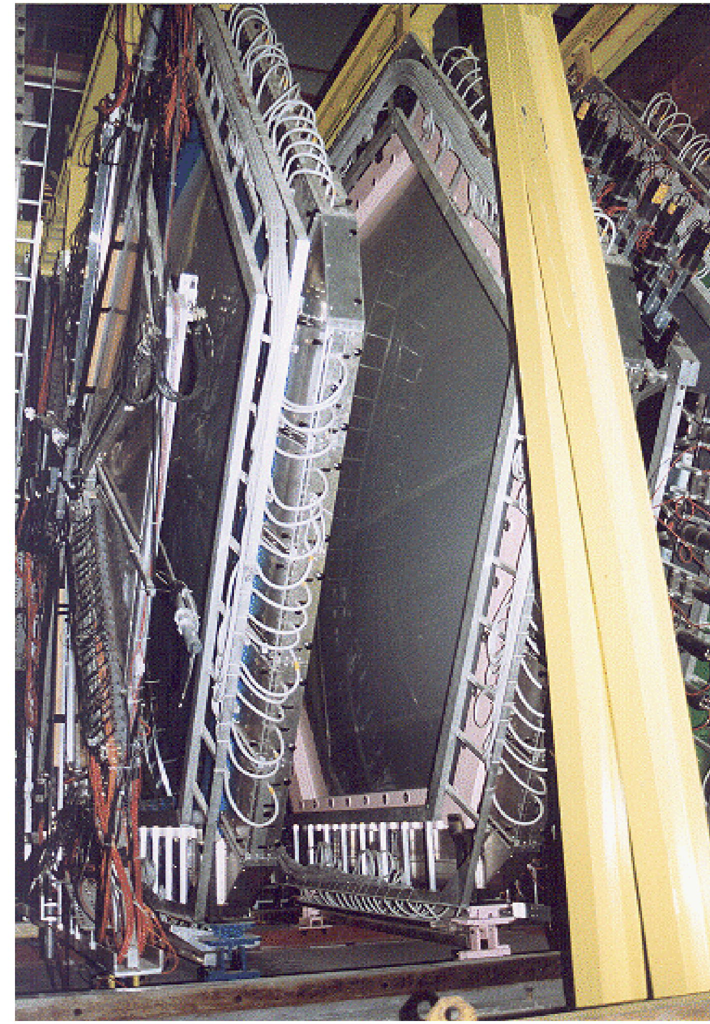

One of the NA60 muon chambers

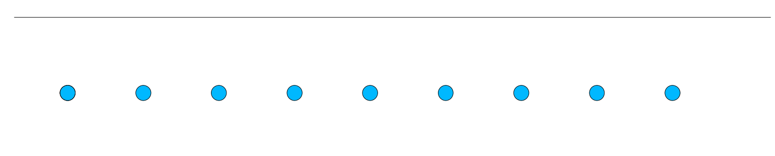

TPC

- Typically very large
- Almost empty inside
- Excellent for dealing with

- 1976: David Nygren

Alice

Star

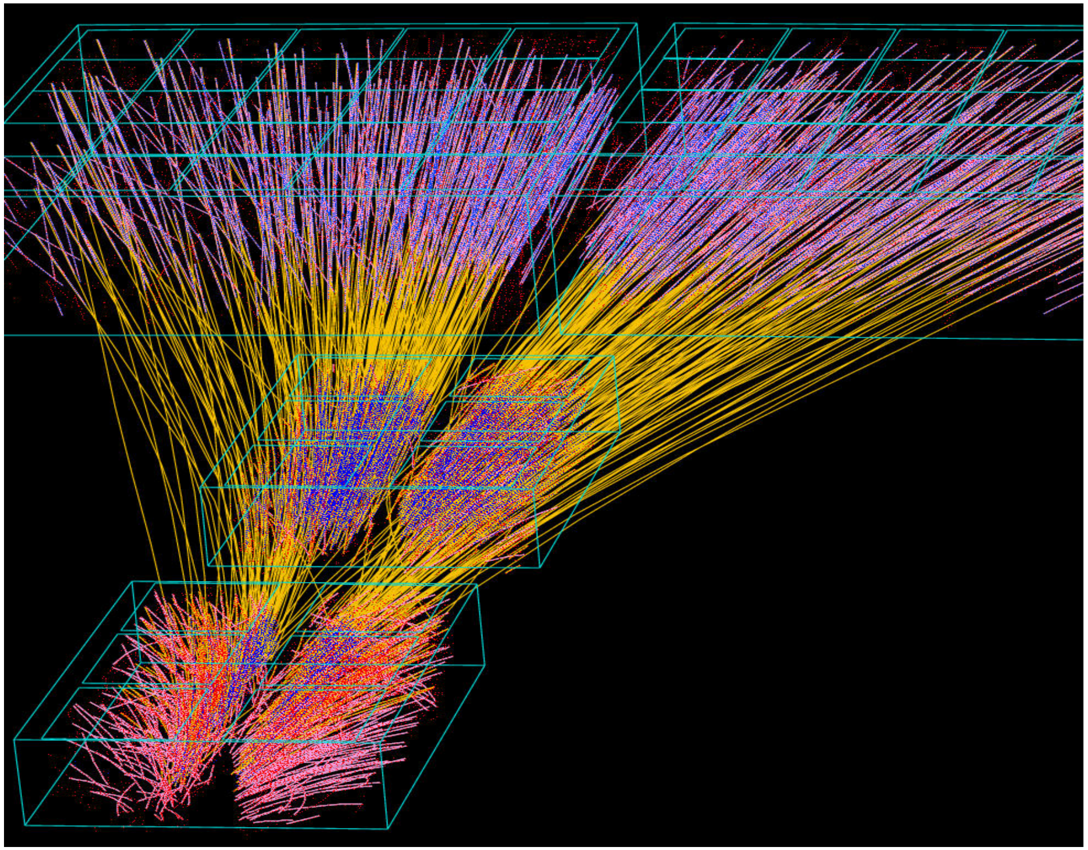

NA49

David Nygren

1749: Cauchy-Riemann equations

Jean le Rond d'Alembert
(Nov 16th 1717 –Oct 29th 1783)

- Core of the complex potential method.

- Existence of a derivative of a complex analytic function $f = u + \mathrm{i}\, v$

$$f'(z) = \frac{\partial f}{\partial x} = \frac{\partial u}{\partial x} + \mathrm{i}\frac{\partial v}{\partial x} = \frac{\partial f}{\partial \mathrm{i} y} = -\mathrm{i}\frac{\partial u}{\partial y} + \frac{\partial v}{\partial y}$$

$$\frac{\partial u}{\partial x} = \frac{\partial v}{\partial y} \qquad \frac{\partial v}{\partial x} = -\frac{\partial u}{\partial y}$$

Augustin Louis Cauchy
(Aug 21st 1789 – May 23rd 1857)

- implies that Re(*f*) is harmonic:

$$\frac{\partial^2 u}{\partial x^2} = \frac{\partial^2 v}{\partial x \partial y} = \frac{\partial^2 v}{\partial y \partial x} = \frac{-\partial^2 u}{\partial y \partial y} \qquad \frac{\partial^2 u}{\partial x^2} + \frac{\partial^2 u}{\partial y^2} = 0$$

Georg Friedrich Bernhard Riemann
(Sep 17st 1826 – Jul 20th 1866)

Conformal mappings – an example

- Schwartz-Christoffel transformation of a half-plane to the external part of a rectangle:

$$z \to \int_0^z \frac{d\xi}{\sqrt{\xi(\xi-1)(\xi-a)}} = \frac{2}{\sqrt{a}} \mathrm{sn}^{-1}\left(\sqrt{z}, \frac{1}{\sqrt{a}}\right)$$

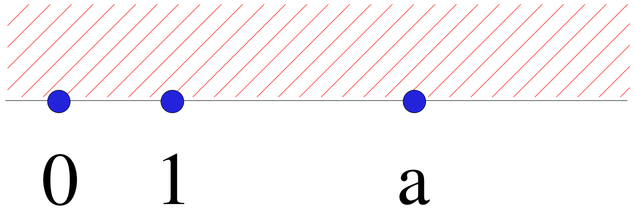

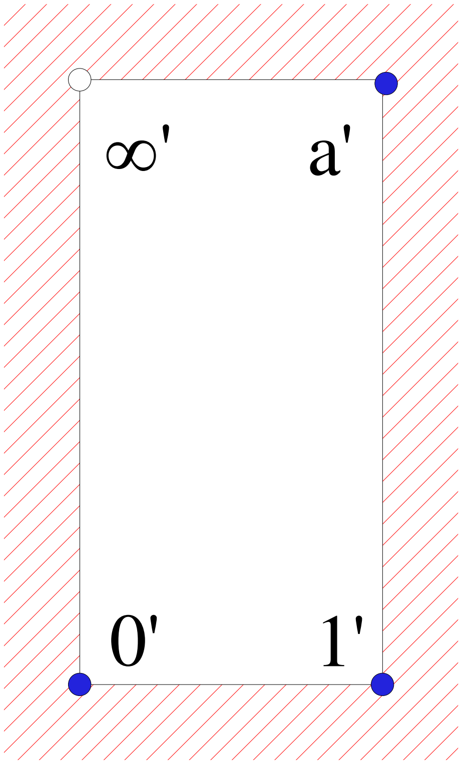

MPGD

- Micro-Pattern Gas-based Detectors
  - have small structural elements
  - use 3d electrodes to generate electric fields.

MSGC

- Built using solid-state techniques;
- good resolution;
- poor resistance to high rates.

- 1988: Anton Oed

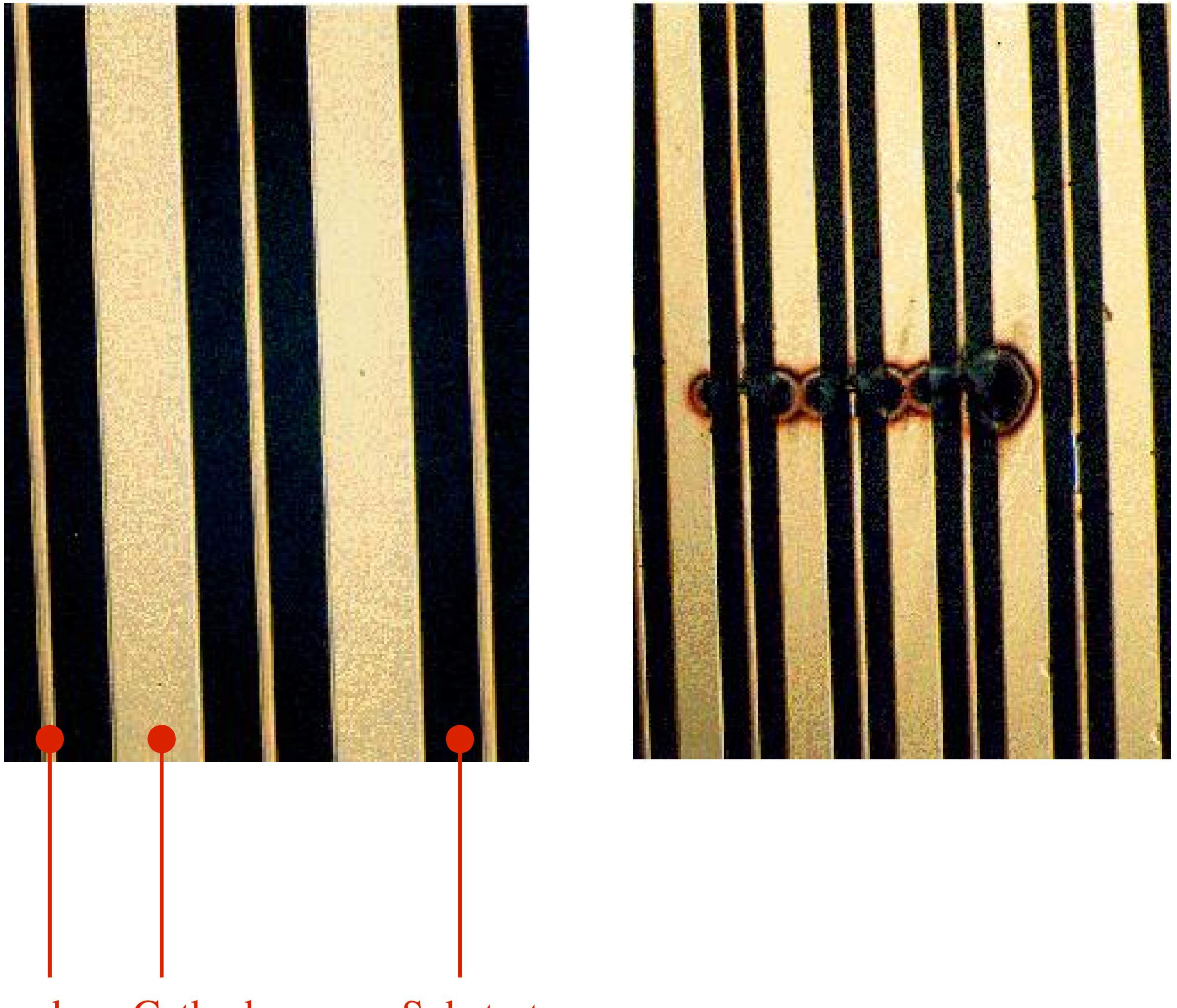

Gossip

- The “electronic bubble chamber”.

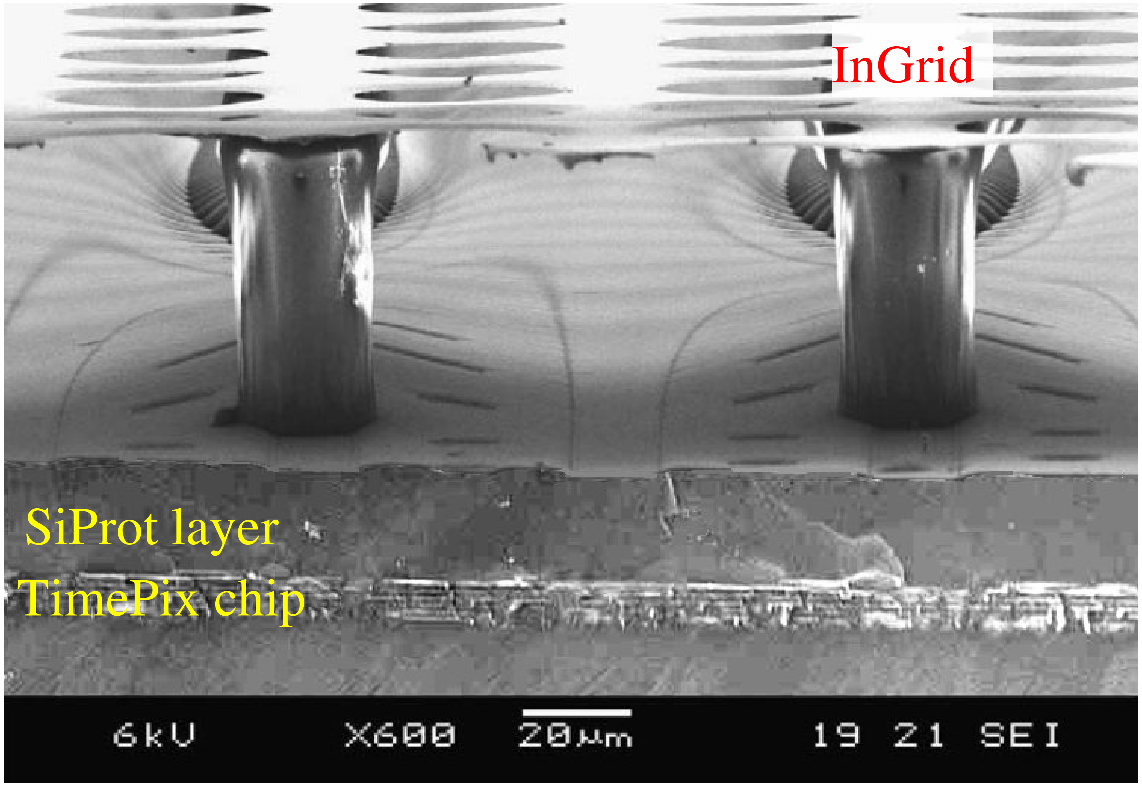

Harry van der Graaf (r)

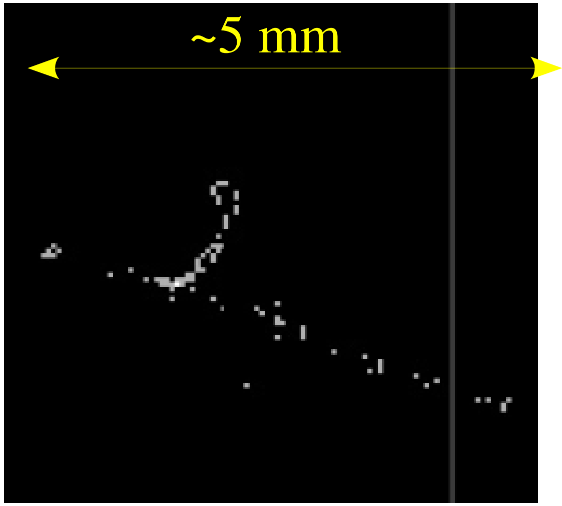

δ-electrons made visible in He/iC_4H_{10}, using a modified MediPix, ~2004.

Field calculation techniques

- Closed expressions:
  - almost all 2d structures of wires, planes + periodicities;
  - dielectrics and space/surface charge are laborious;
  - fast and precise, if applicable – not suitable for MPGDs.
- Finite elements:
  - 2d and 3d structures, with or without dielectrics;
  - several major intrinsic shortcomings.
- Integral equations or Boundary element methods:
  - equally comprehensive without the intrinsic flaws;
  - technically challenging and emerging.
- Finite differences:
  - used for iterative, time-dependent calculations.

Ιωα'ννης Αργυ'ρης

(1913-2004)

Aircraft wings – finite elements

- “*Stiffness and Deflection Analysis of Complex Structures*”, a study in the use of the finite element technique (then called “direct stiffness method”) for aircraft wing design.

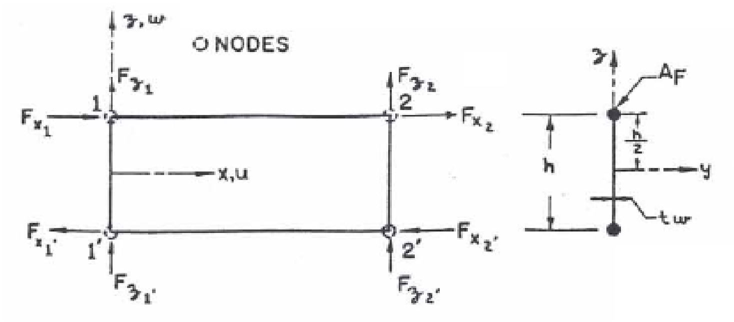

$$
[K] = \frac{6EI}{Lh^2(1+4n)}
\begin{array}{c}
\begin{matrix} u_1 & v_1 & w_1 & u_2 & v_2 & w_2 \end{matrix} \\
\begin{bmatrix}
(4/3)\,(1+n) & & & & & \\
0 & 0 & & & & \\
-(h/L) & 0 & h^2/L^2 & & & \\
(2/3)\,(1-2n) & 0 & -(h/L) & (4/3)\,(1+n) & & \\
0 & 0 & 0 & 0 & 0 & \\
h/L & 0 & -(h^2/L^2) & h/L & 0 & h^2/L^2
\end{bmatrix}
\end{array}
$$

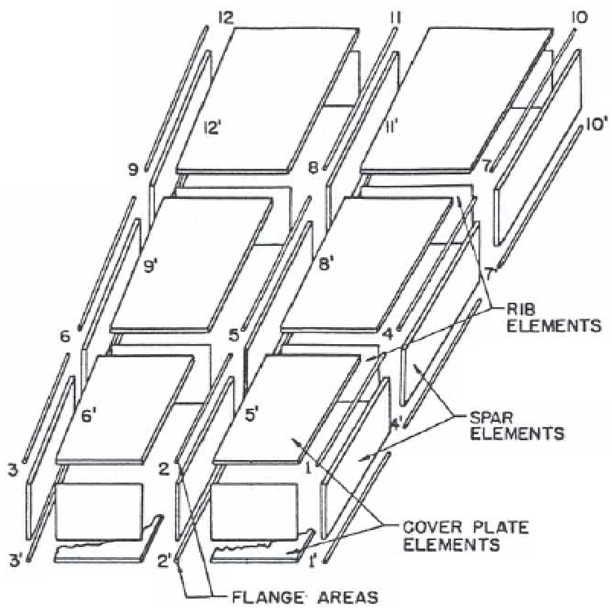

[M.J. Turner, R.W. Clough, H.C. Martin and L.J. Topp, *Stiffness and Deflection Analysis of Complex Structures*, J. Aero. Sc. **23** (1956), 805-824. MJT & LJT with Boeing.]

The price to pay for finite elements

- Finite element programs are flexible but they focus on the wrong thing: they solve V well, but we do not really need it:
  - quadratic shape functions do a fair job at approximating $V \approx \log(r)$ potentials;
  - potentials are continuous;
  - potentials and fields are not Maxwell compliant.

- E is what we use to transport charges, but:
  - gradients of quadratic shape functions are linear and not suitable to approximate $E \approx 1/r$, left alone $E \approx 1/r^2$ fields;
  - electric fields are discontinuous at element boundaries;
  - a local accuracy of ~50 % in high-field areas is not unusual.

Boundary element methods

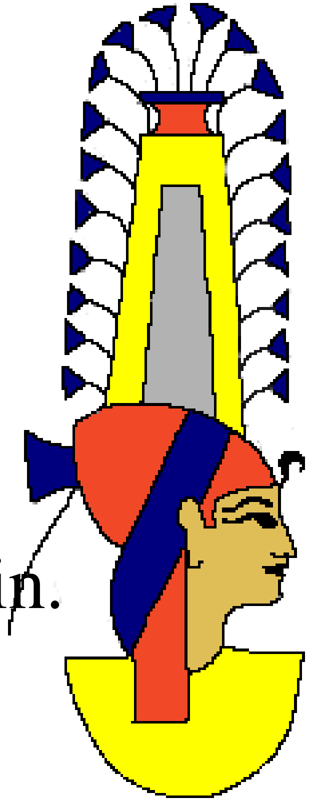

- Contrary to the finite element method, the elements are on the boundaries, not inside the problem domain. Charges are computed for the boundary elements.

- The field in the problem domain is calculated as the sum of Maxwell-compliant field functions, each extending over the entire problem domain. There are no discontinuities.

- But ... the method poses substantial numerical challenges: large non-sparse matrices and inherent singularities. The technique is time consuming.

Magboltz: e^- transport in gases

- A large number of cross sections for 60 molecules...
  - Numerous organic gases, additives, *e.g.* CO_2:
    - elastic scattering,
    - 44 inelastic cross sections (5 vibrations and 30 rotations + super-elastic and 9 polyads),
    - attachment,
    - 6 excited states and
    - 3 ionisations.
  - noble gases (He, Ne, Ar, Kr, Xe):
    - elastic scattering,
    - 44 excited states and
    - 7 ionisations.

CO_2 – vibration modes

- CO_2 is linear:
  - O – C – O
- Vibration modes are numbered V(*ijk*)
  - *i*: symmetric,
  - *j*: bending,
  - *k*: anti-symmetric.

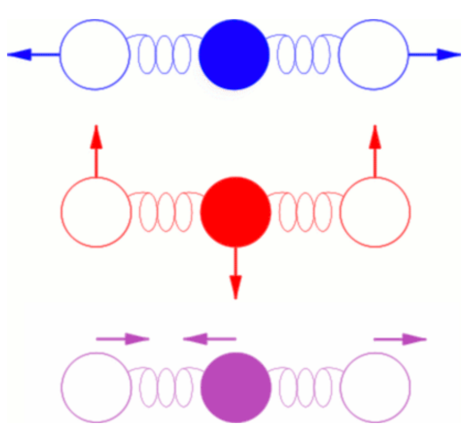

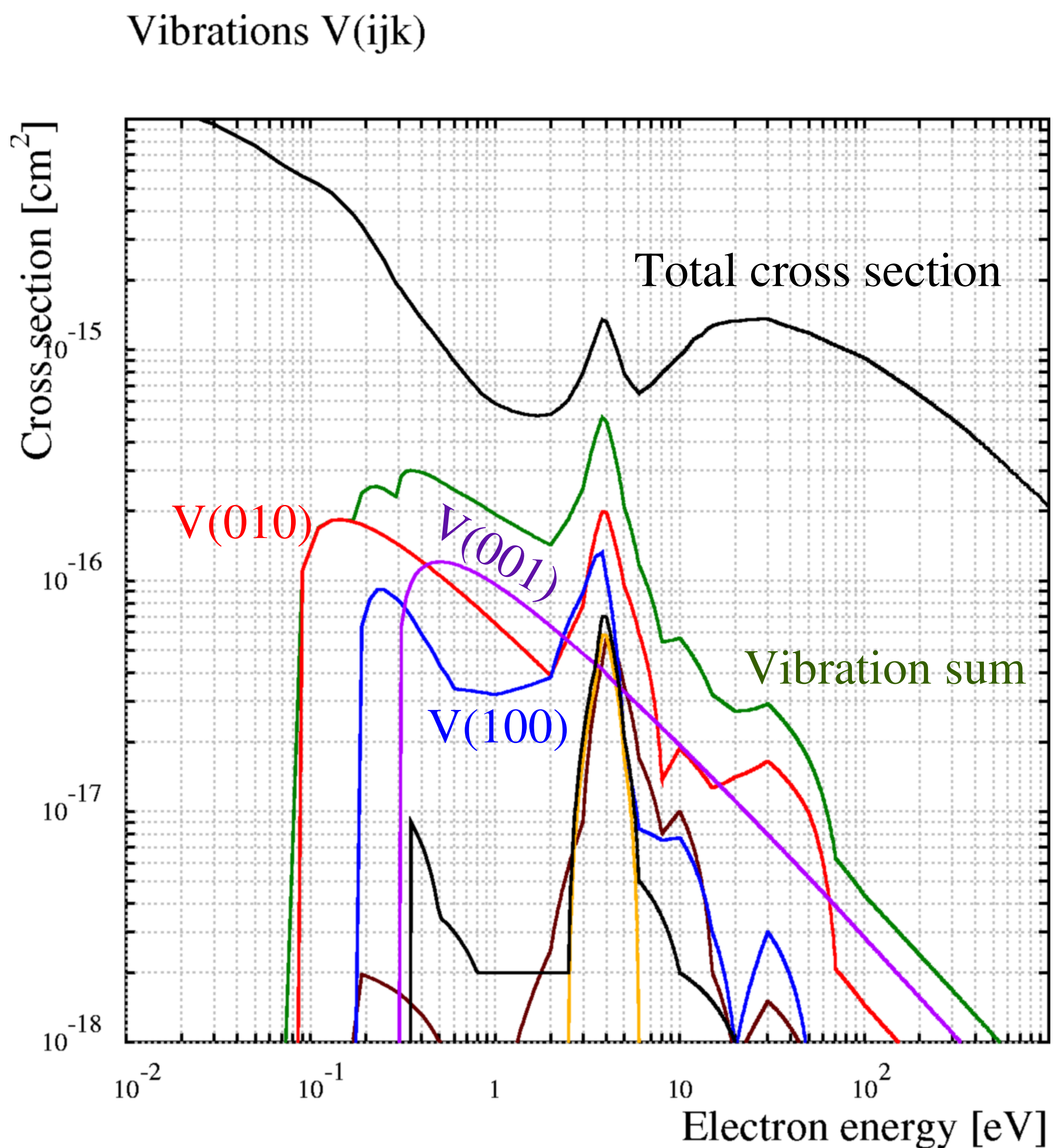

Attachment in CO_2

- CO_2 is a linear molecule:

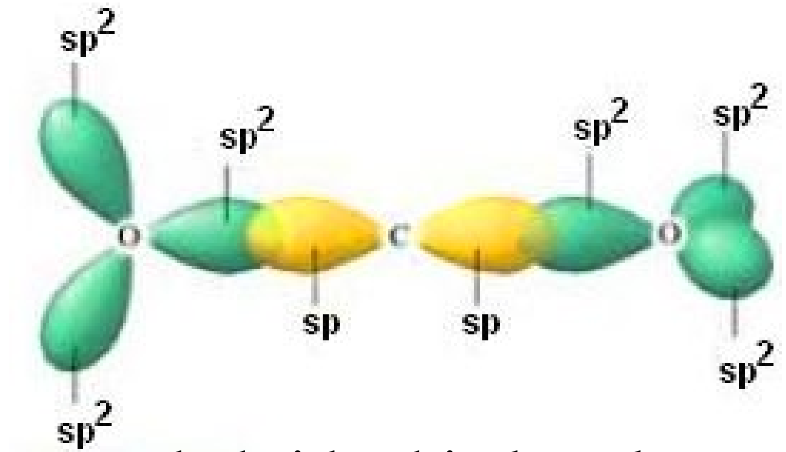

hybrid orbitals only,
p-orbitals not shown

- CO_2 with an extra e^-: instable ($\tau \ll 1$ ps, $\epsilon_{VEA} \approx$ -3.8 eV). Low energy e^- collisions produce O^-, not CO_2^-.
- With an e^- added, a bent structure (134°) is favoured. Long lifetime ($\tau \approx 90$ µs) but still *negative* electron affinity ($\epsilon_{AEA} \approx$ -0.6 eV). metastable.
- Attachment works in $[CO_2]_n$ clusters: vibration and rotation modes absorb excess energy.

σ bonds (2 times)

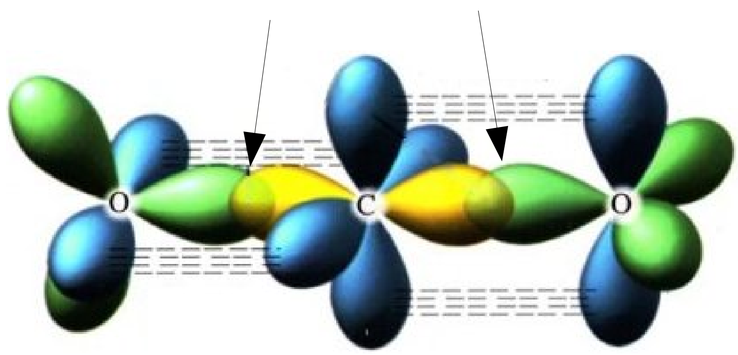

π bonds (2 times)

- [Source: presumably SS Zumdahl, Chemistry (1983) DC Heath and Company.]

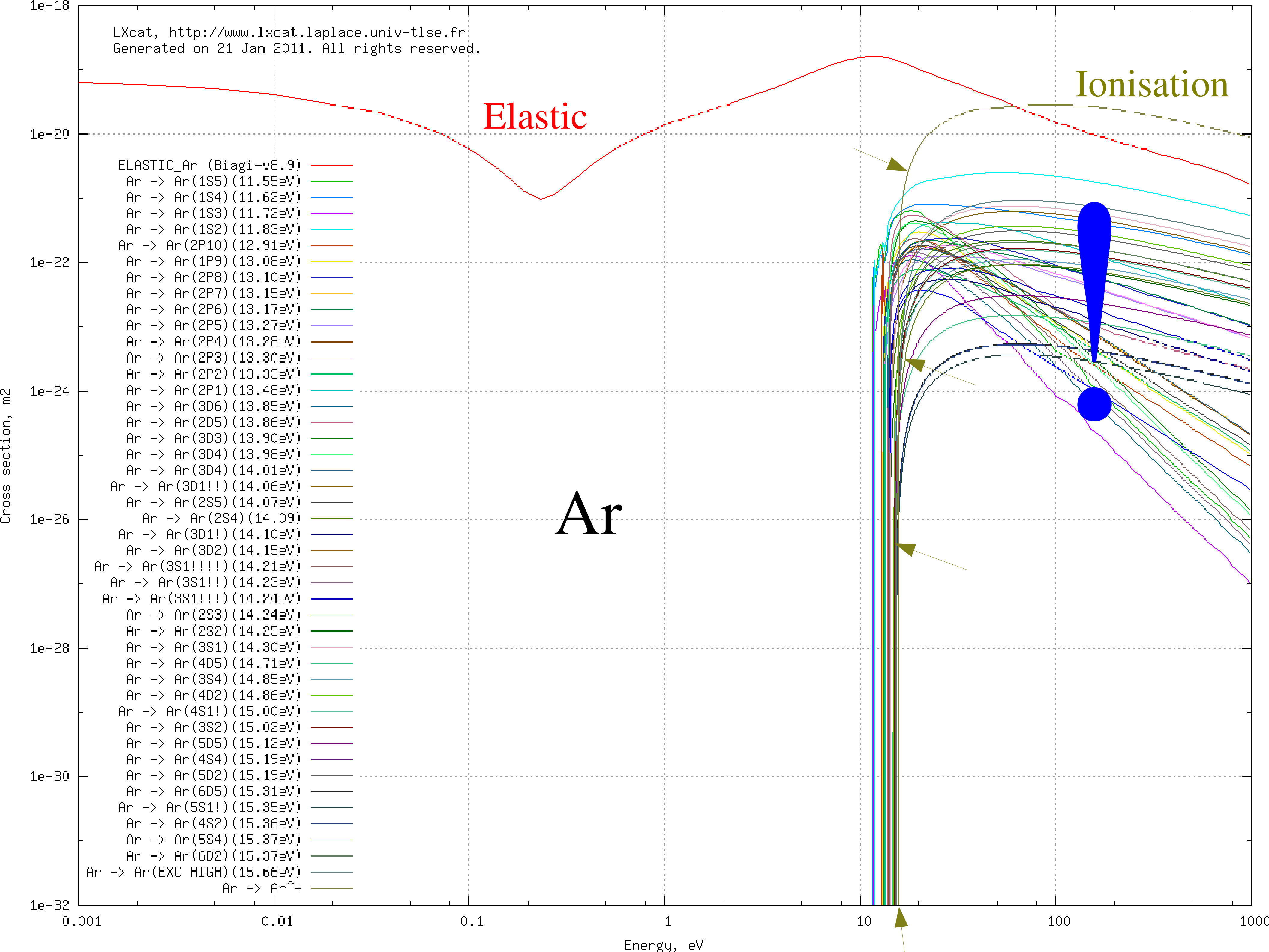
LXcat, http://www.lxcat.laplace.univ-tlse.fr
Generated on 21 Jan 2011. All rights reserved.
Elastic
Ionisation
Ar
ELASTIC_Ar (Biagi-v8.9)
Ar -> Ar(1S5)(11.55eV)
Ar -> Ar(1S4)(11.62eV)
Ar -> Ar(1S3)(11.72eV)
Ar -> Ar(1S2)(11.83eV)
Ar -> Ar(2P10)(12.91eV)
Ar -> Ar(1P9)(13.08eV)
Ar -> Ar(2P8)(13.10eV)
Ar -> Ar(2P7)(13.15eV)
Ar -> Ar(2P6)(13.17eV)
Ar -> Ar(2P5)(13.27eV)
Ar -> Ar(2P4)(13.28eV)
Ar -> Ar(2P3)(13.30eV)
Ar -> Ar(2P2)(13.33eV)
Ar -> Ar(2P1)(13.48eV)
Ar -> Ar(3D6)(13.85eV)
Ar -> Ar(2D5)(13.86eV)
Ar -> Ar(3D3)(13.90eV)
Ar -> Ar(3D4)(13.98eV)
Ar -> Ar(3D4)(14.01eV)
Ar -> Ar(3D1!!)(14.06eV)
Ar -> Ar(2S5)(14.07eV)
Ar -> Ar(2S4)(14.09)
Ar -> Ar(3D1!)(14.10eV)
Ar -> Ar(3D2)(14.15eV)
Ar -> Ar(3S1!!!!)(14.21eV)
Ar -> Ar(3S1!!)(14.23eV)
Ar -> Ar(3S1!!!)(14.24eV)
Ar -> Ar(2S3)(14.24eV)
Ar -> Ar(2S2)(14.25eV)
Ar -> Ar(3S1)(14.30eV)
Ar -> Ar(4D5)(14.71eV)
Ar -> Ar(3S4)(14.85eV)
Ar -> Ar(4D2)(14.86eV)
Ar -> Ar(4S1!)(15.00eV)
Ar -> Ar(3S2)(15.02eV)
Ar -> Ar(5D5)(15.12eV)
Ar -> Ar(4S4)(15.19eV)
Ar -> Ar(5D2)(15.19eV)
Ar -> Ar(6D5)(15.31eV)
Ar -> Ar(5S1!)(15.35eV)
Ar -> Ar(4S2)(15.36eV)
Ar -> Ar(5S4)(15.37eV)
Ar -> Ar(6D2)(15.37eV)
Ar -> Ar(EXC HIGH)(15.66eV)
Ar -> Ar^+
Cross section, m2
1e-18
1e-20
1e-22
1e-24
1e-26
1e-28
1e-30
1e-32
0.001
0.01
0.1
1
10
100
1000
Energy, eV

Ionisation through excitation

- Create excited noble gas atoms:
  - $Ar + e^- \rightarrow Ar + e^-$ (in)elastic scattering
  - $Ar + e^- \rightarrow Ar^* + e^-$ excitation
  - $Ar + e^- \rightarrow Ar^+ + 2e^-$ ionisation

e^- Energy

- Interaction with quencher:
  - $Ar^* + CO_2 \rightarrow Ar + CO_2^+ + e^-$

    if Ar^* excitation energy $>$ CO_2^+ ionisation energy
  - Quenching rate constants are comparable to hard-sphere scattering, i.e. faster than radiative decay of (esp. higher) excited states.

Pressure

- Transfer rates for Ar-CO_2, from experimental gain curves
- Hint of 3-body interactions.

[Tadeusz Kowalski and Özkan Şahin]

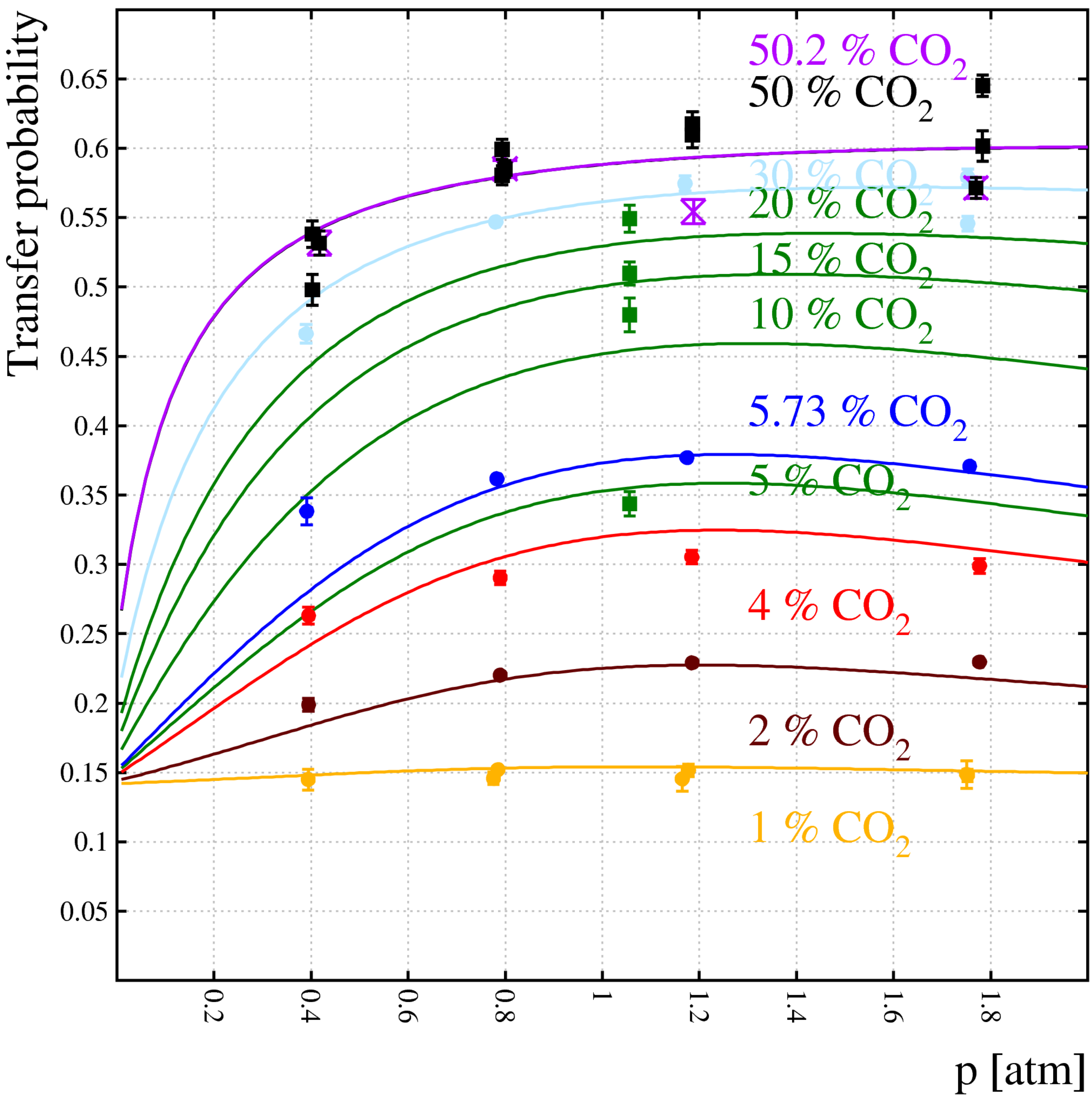

PhD students: solve this puzzle and win a fondue during your next visit to CERN.

Why does the rate fall in Ne-CO_2 ?

- Ar-CO_2 is best studied mixture

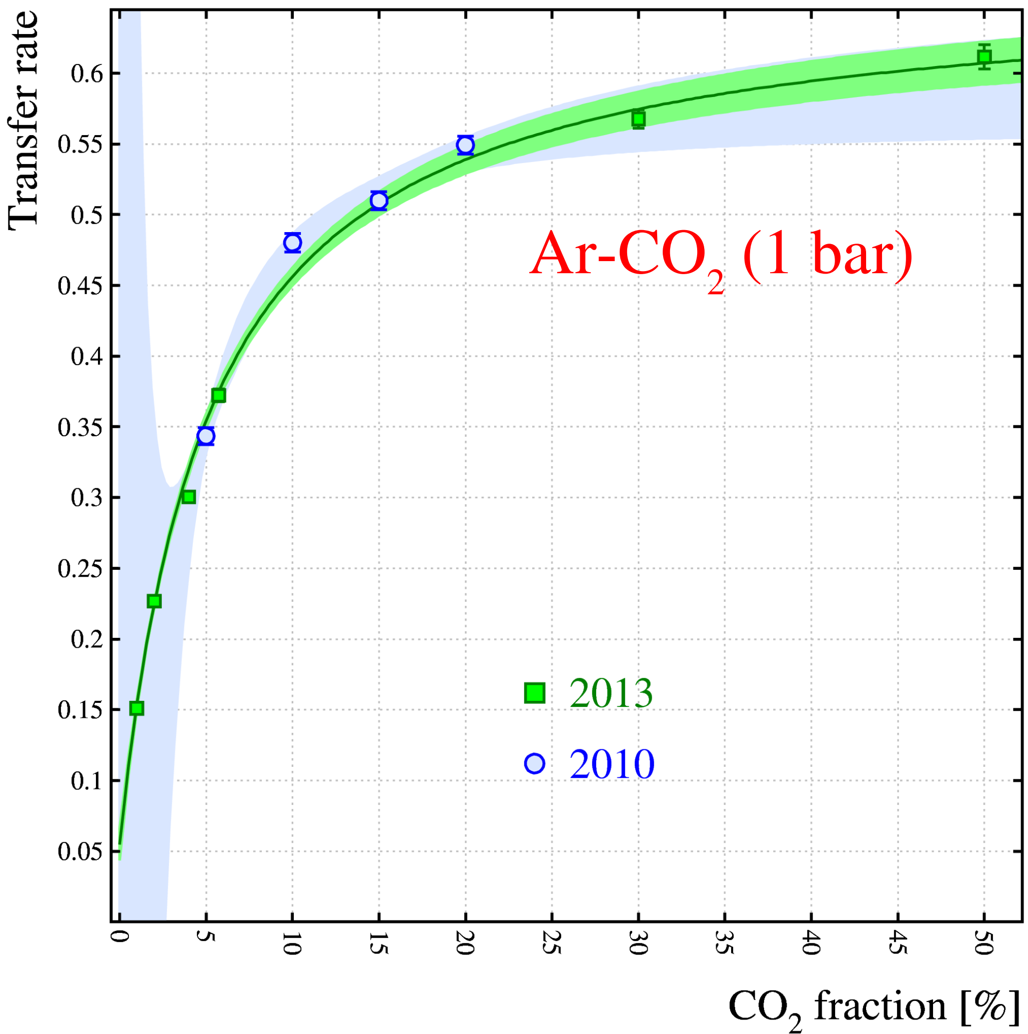

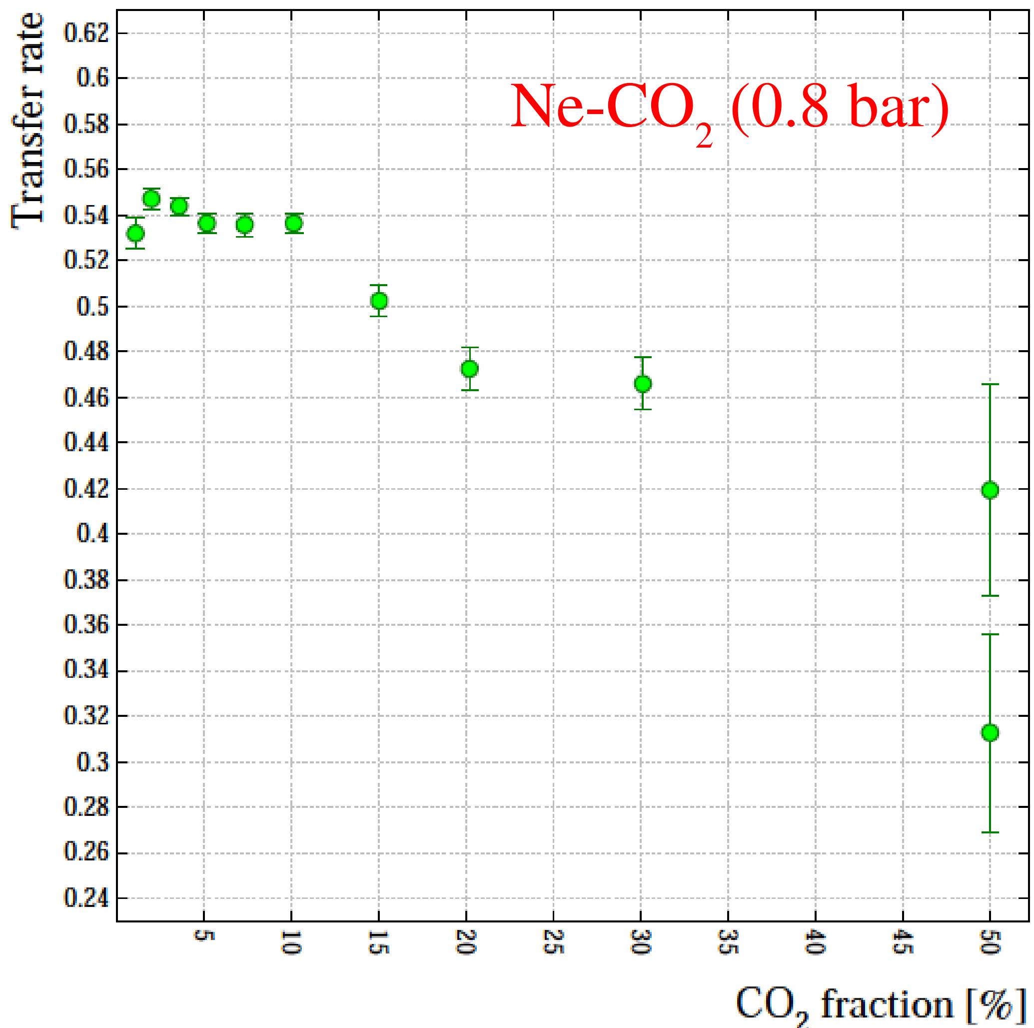

Scales: gas vs structural elements

- Recall:
  - Mean free path of e^- in argon: 2-5 μm,
  - diffusion: ~80 μm for 1 mm.
- Compare with:
  - Micromegas mesh pitch: 63.5 μm
  - GEM polyimide thickness: 50 μm
  - Micromegas wire thickness: 18 μm
  - GEM conductor thickmess: 5 μm
- Hence:
  - mean free path approaches small structural elements;
  - diffusion is not likely to be Gaussian.

e⁻ and ion⁺ trajectories

- Example (Harp): E×B effect in an enlarged ℵ read-out cell.

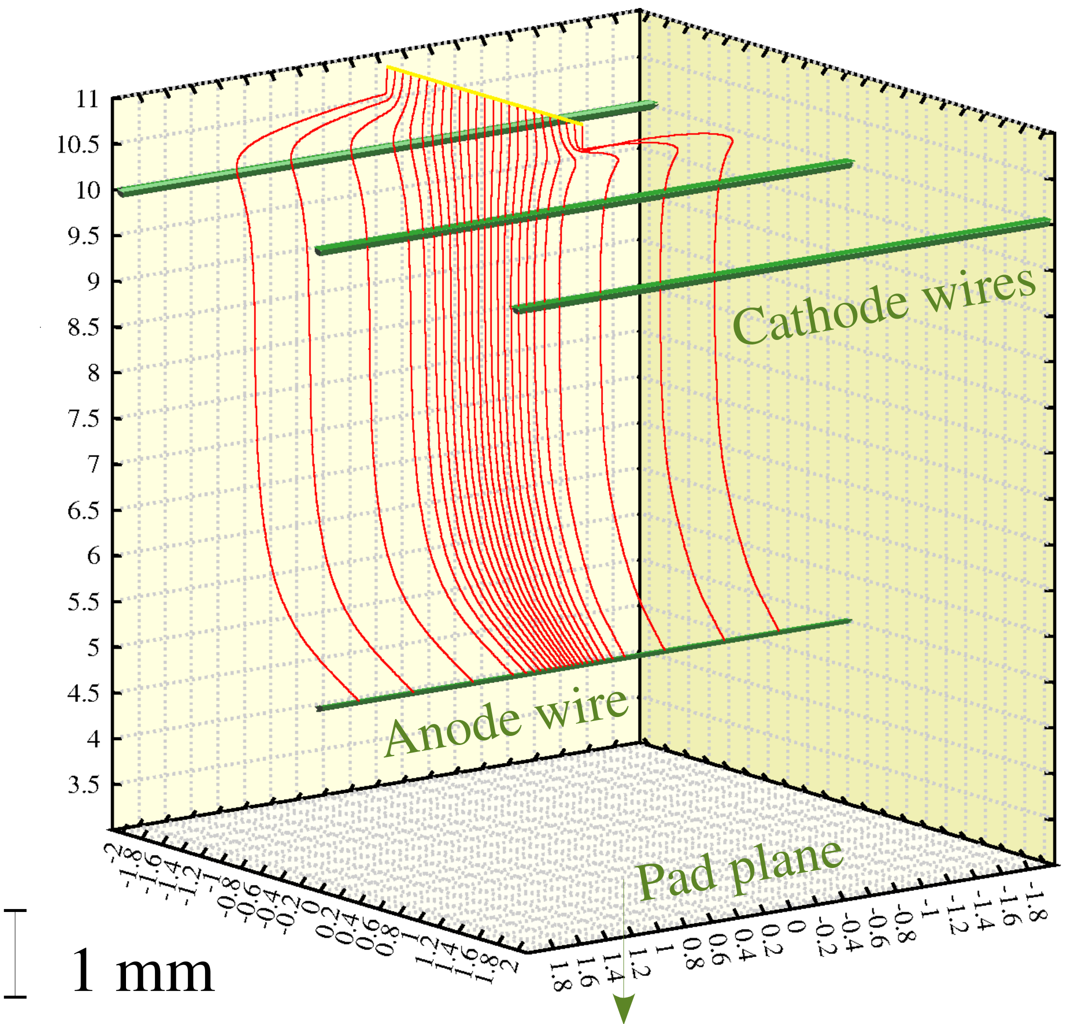

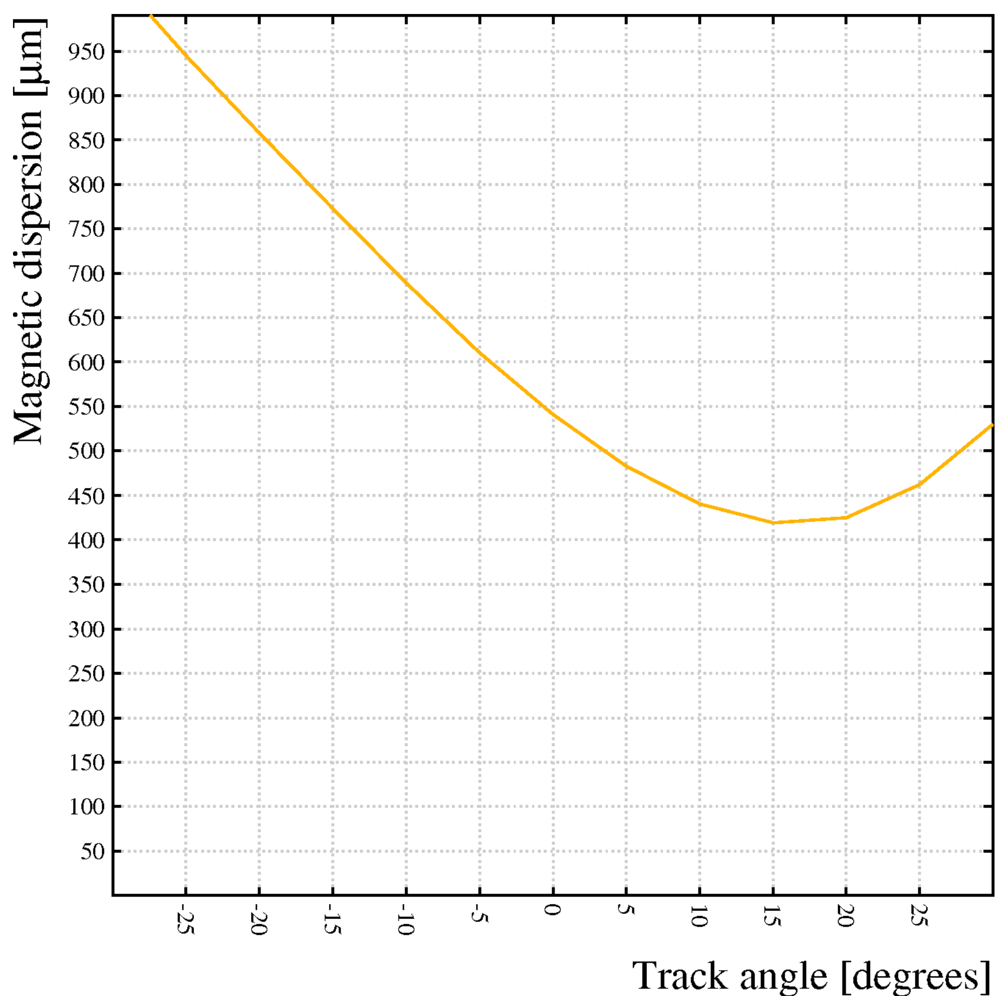

Microscopic Micromegas

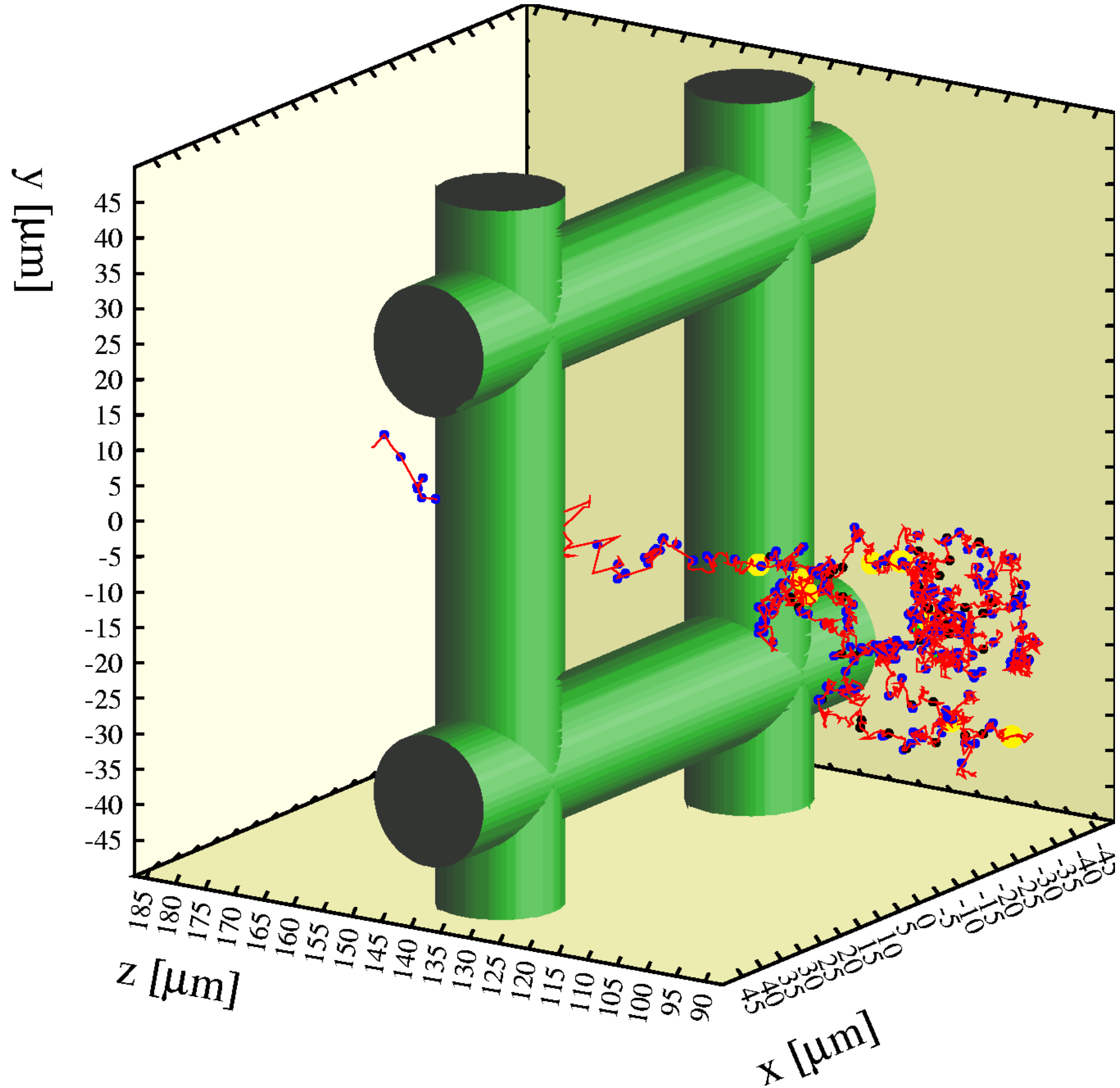

- Legend:
  - – electron
  - ○ inelastic
  - ○ excitation
  - ○ ionisation

Flux vs microscopic ?

- A diffusion-free flux argument does not reproduce the data ...

- but the microscopic approach works.

Field calculations: finite elements.

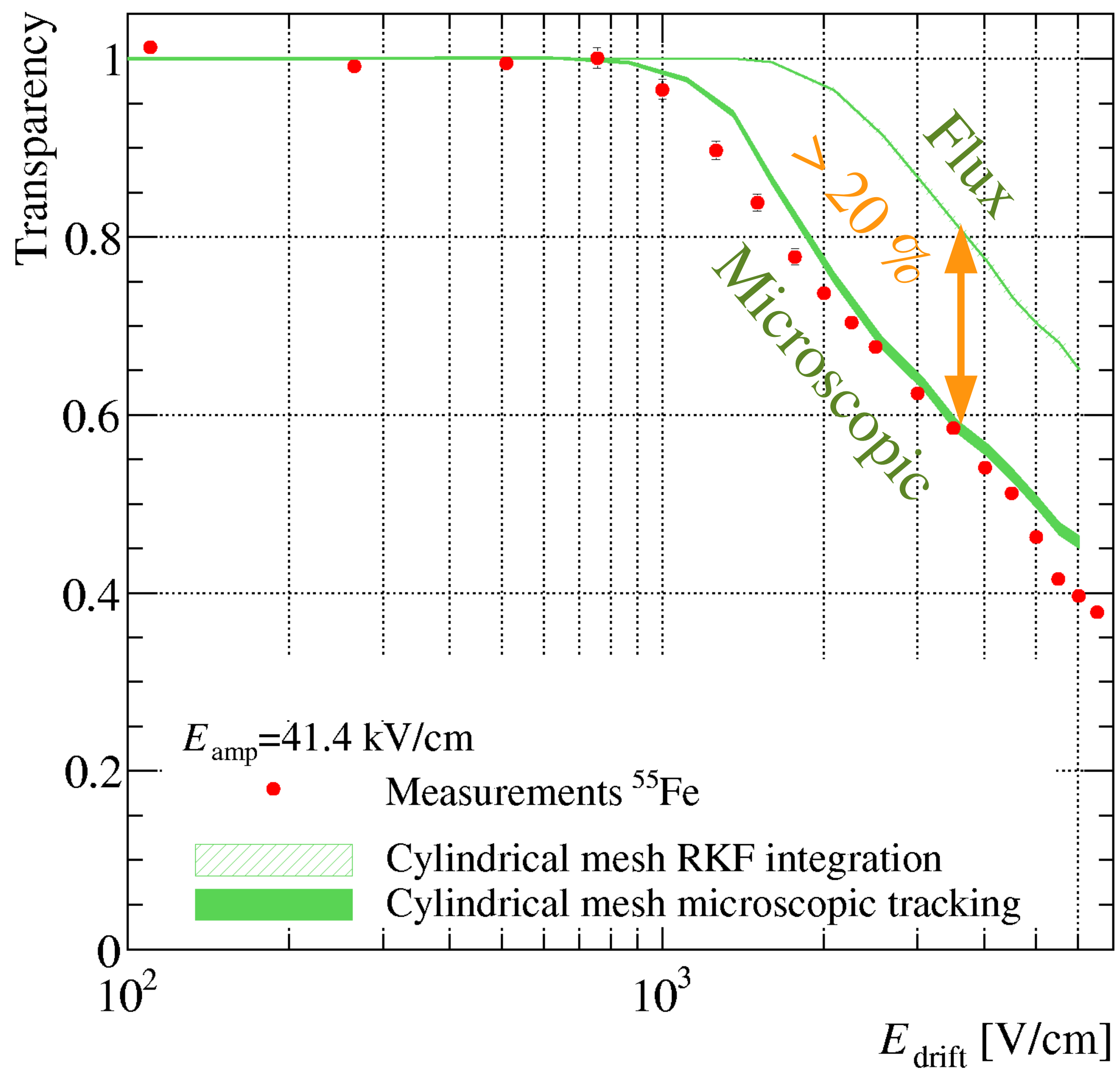

GEM, textbook

- e^- & ion^+ follow the “field lines”

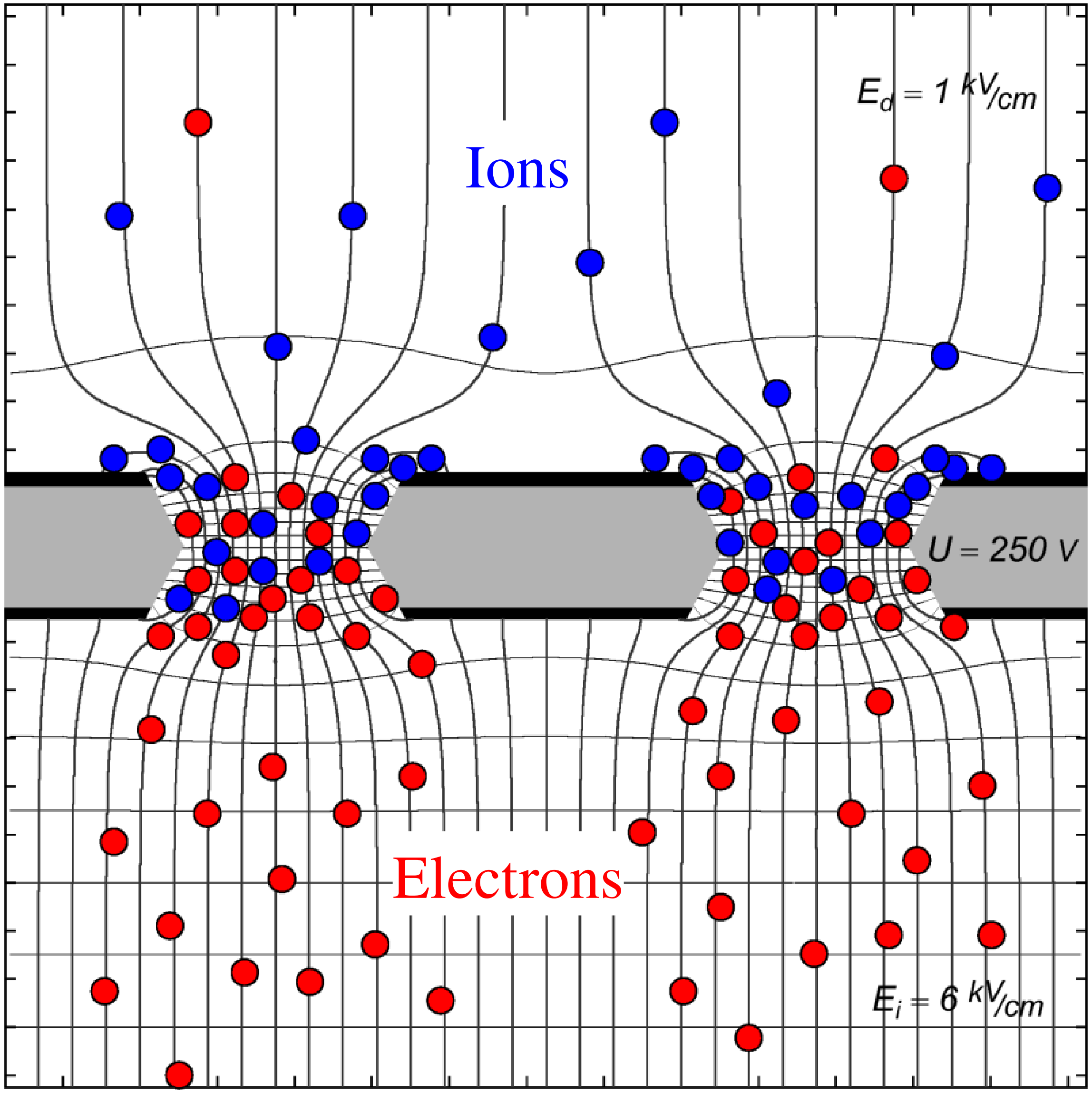

[DESY FLC/TPC, based on a CERN GDD drawing]

GEM, microscopic view

- Micropattern devices have characteristic dimensions that are comparable with the mean free path.

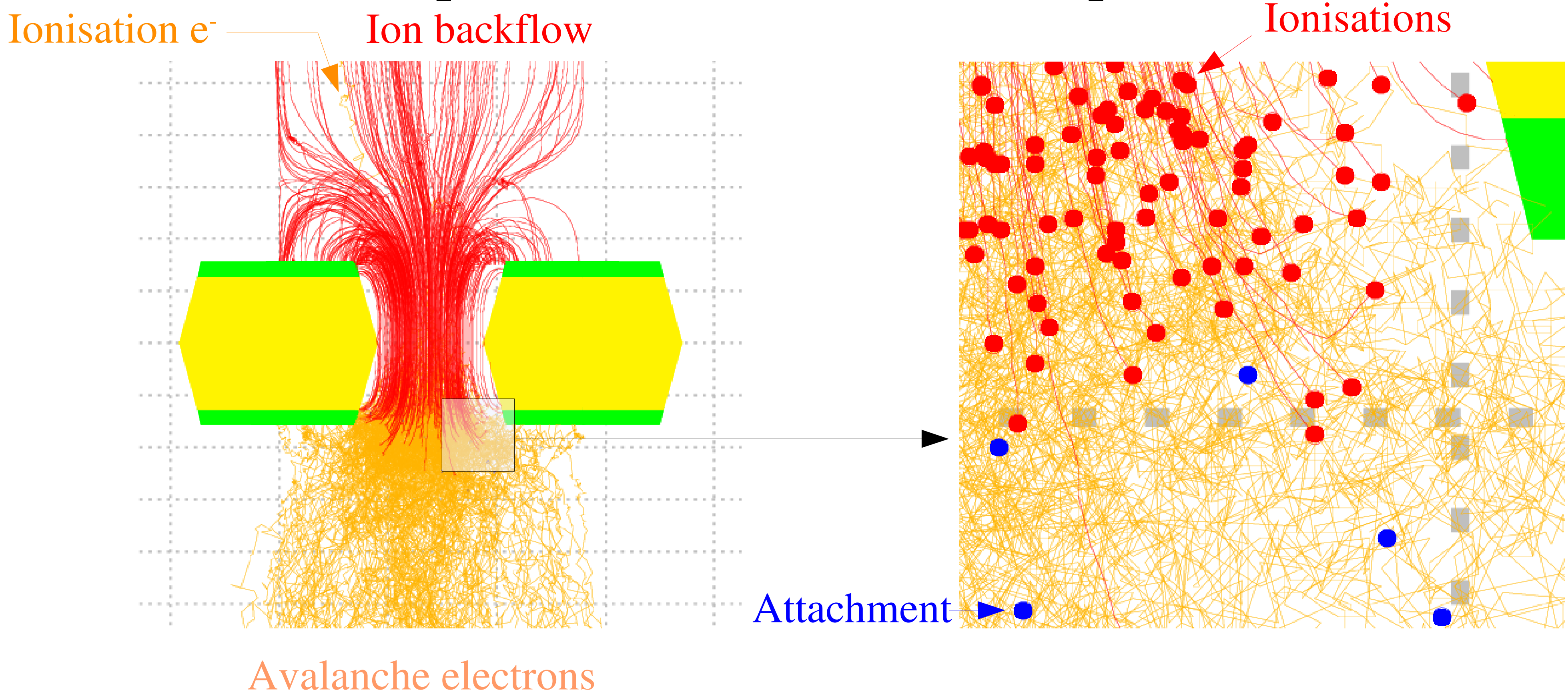

[Plot by Gabriele Croci and Matteo Alfonsi]

Avalanche regions

- Vicinity GEM anode: large multiplication,
  e^- → GEM anode, polyimide,
  ion^+ → polyimide, GEM cathode, drift region.
- Hole centre: lower fields, less multiplication,
  e^- → pad plane,
  ion^+ → drift region.

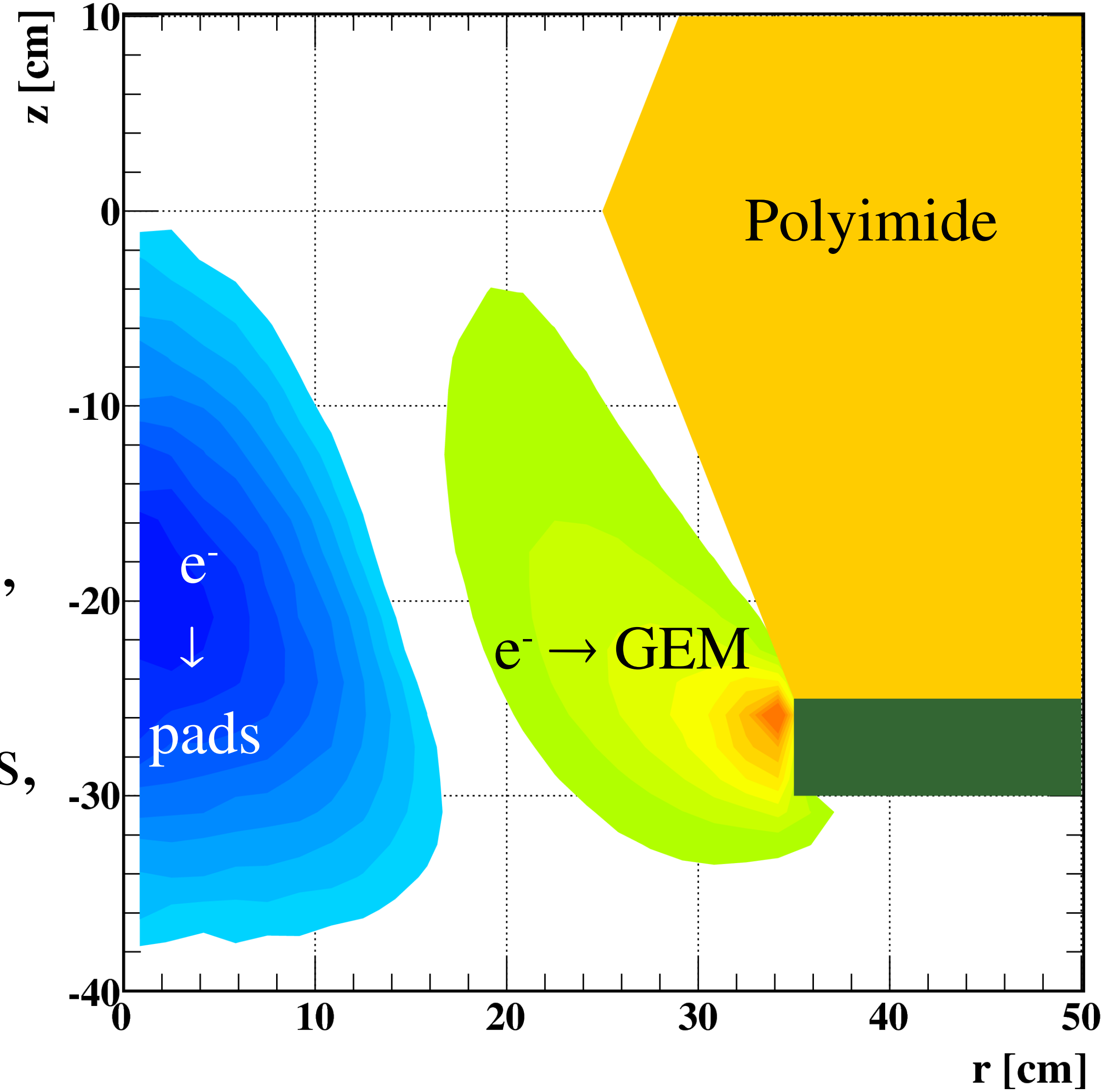

Gain calculations in a pristine GEM

- Calculations predict that G_{tot} and G_{eff} rise with increasing inner hole diameter.

- G_{eff} rises mainly because the losses of incoming electrons diminish;
- G_{tot} rises because the exit electrode becomes more accessible.

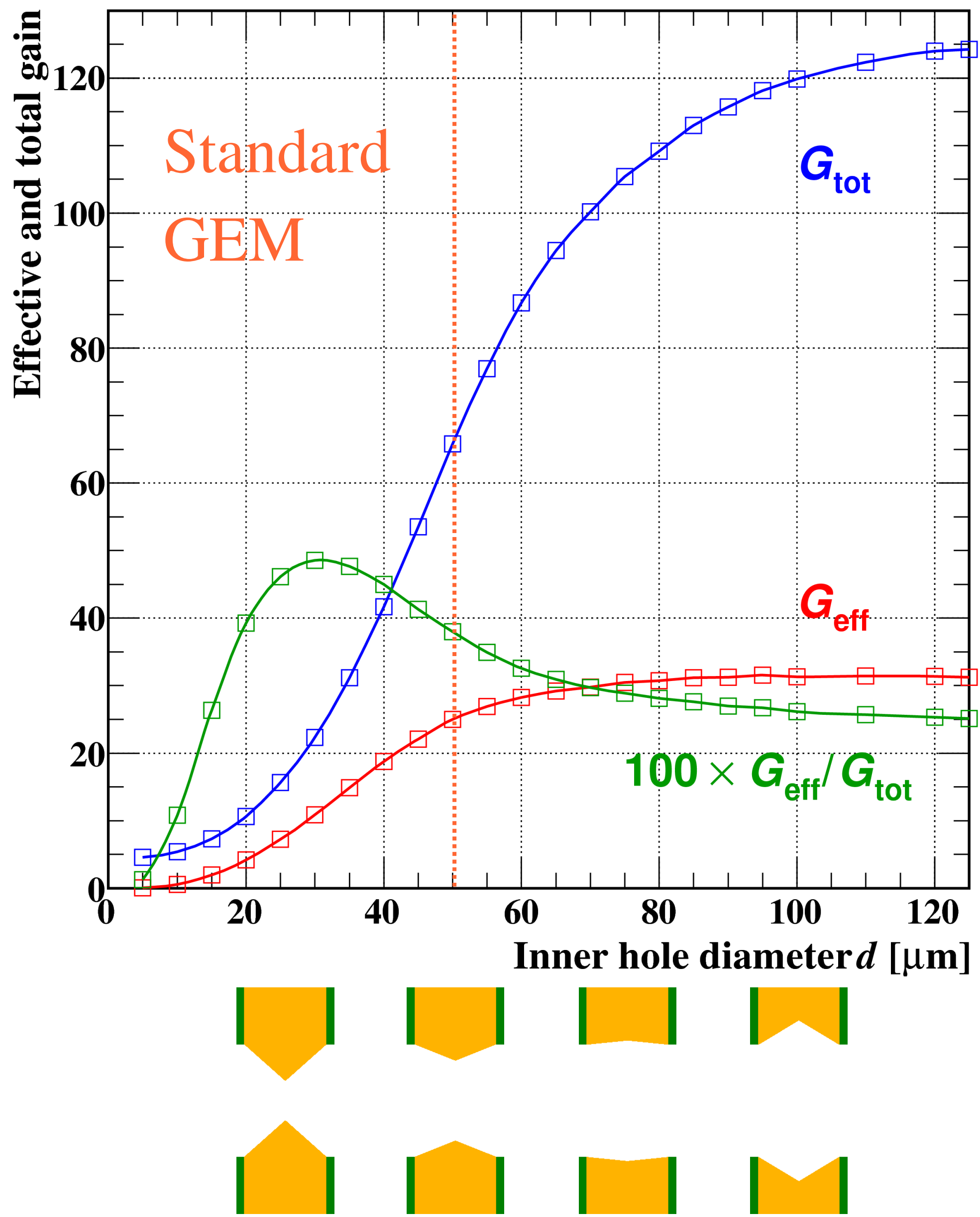

HBD data

- Measurements for 2 triple GEMs with different hole shape shows that smaller holes lead to *larger* gain !

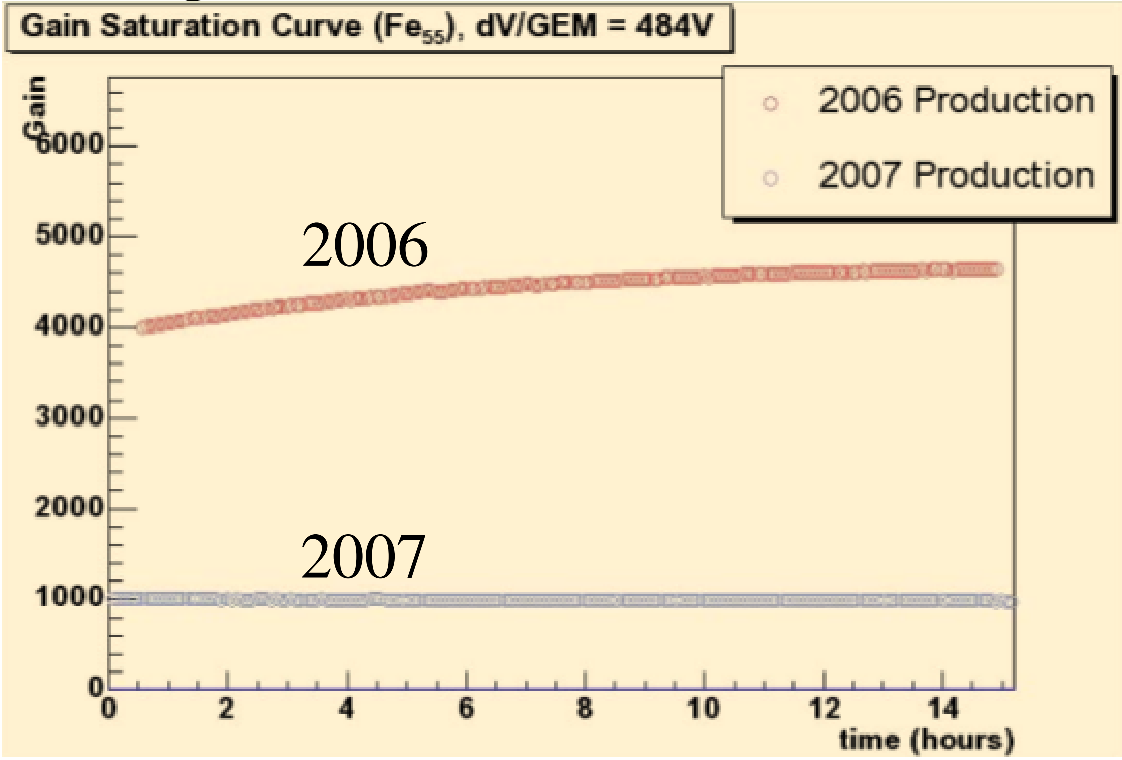

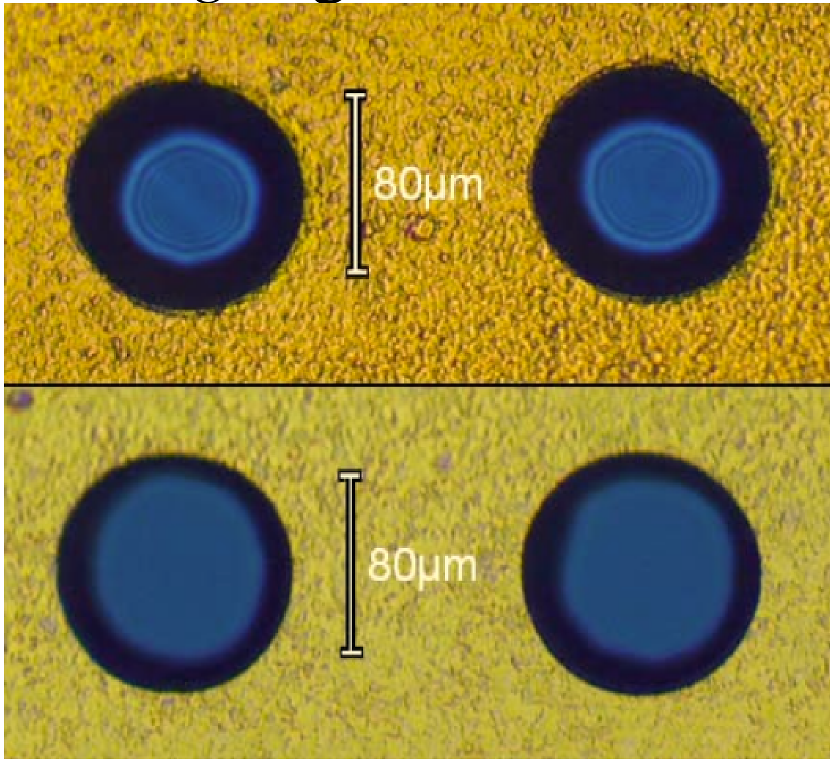

- [W. Anderson *et al.* 10.1109/NSSMIC.2007.4437147]

GEMs of various manufacturers

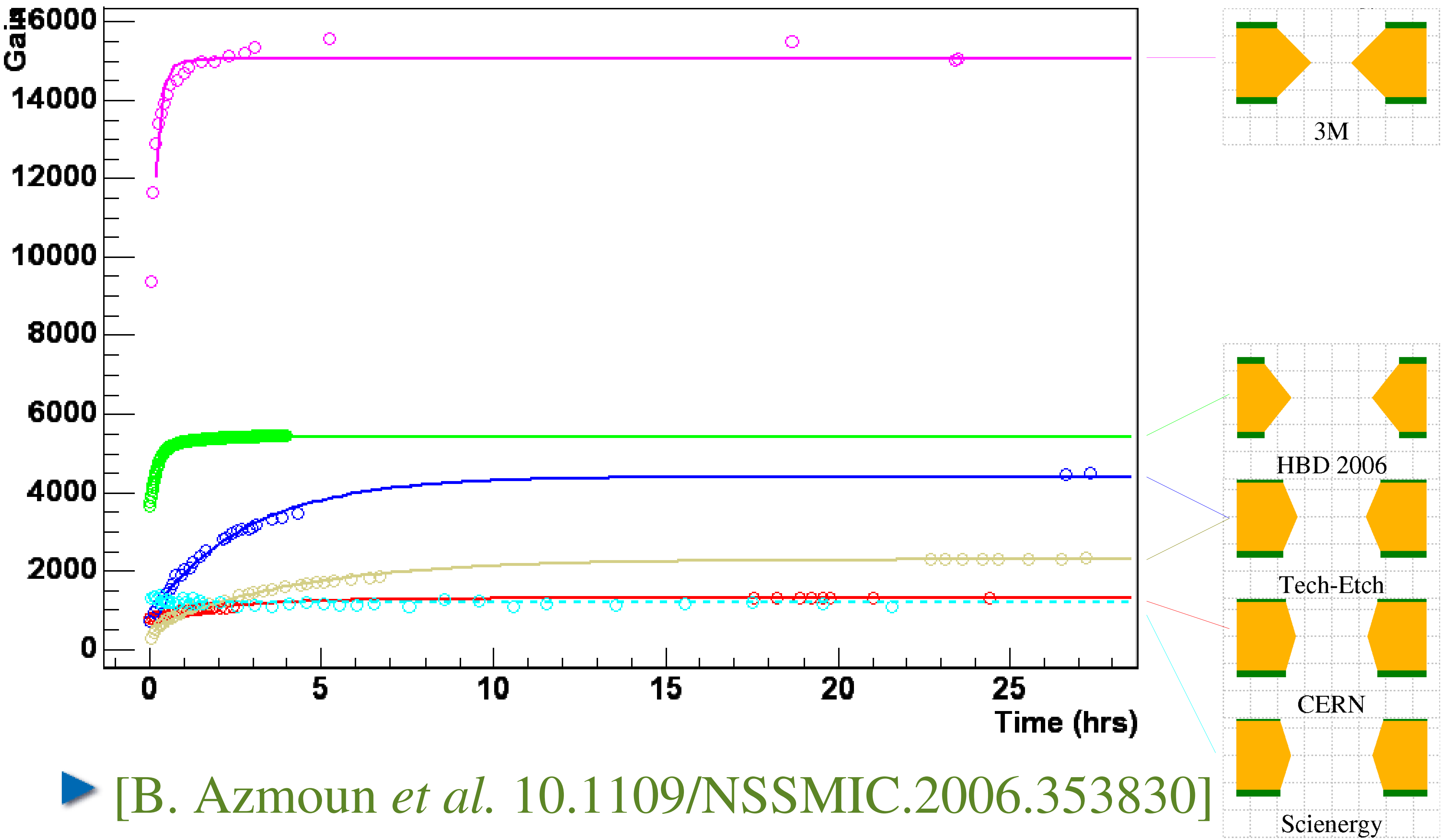

- [B. Azmoun *et al.* 10.1109/NSSMIC.2006.353830]

Effect of surface charge (V_{GEM} = 400 V)

- In a clean GEM, small holes give lower gain.
- As charge accumulates, the gain curves cross.
- Effect more pronounced at higher GEM voltage.

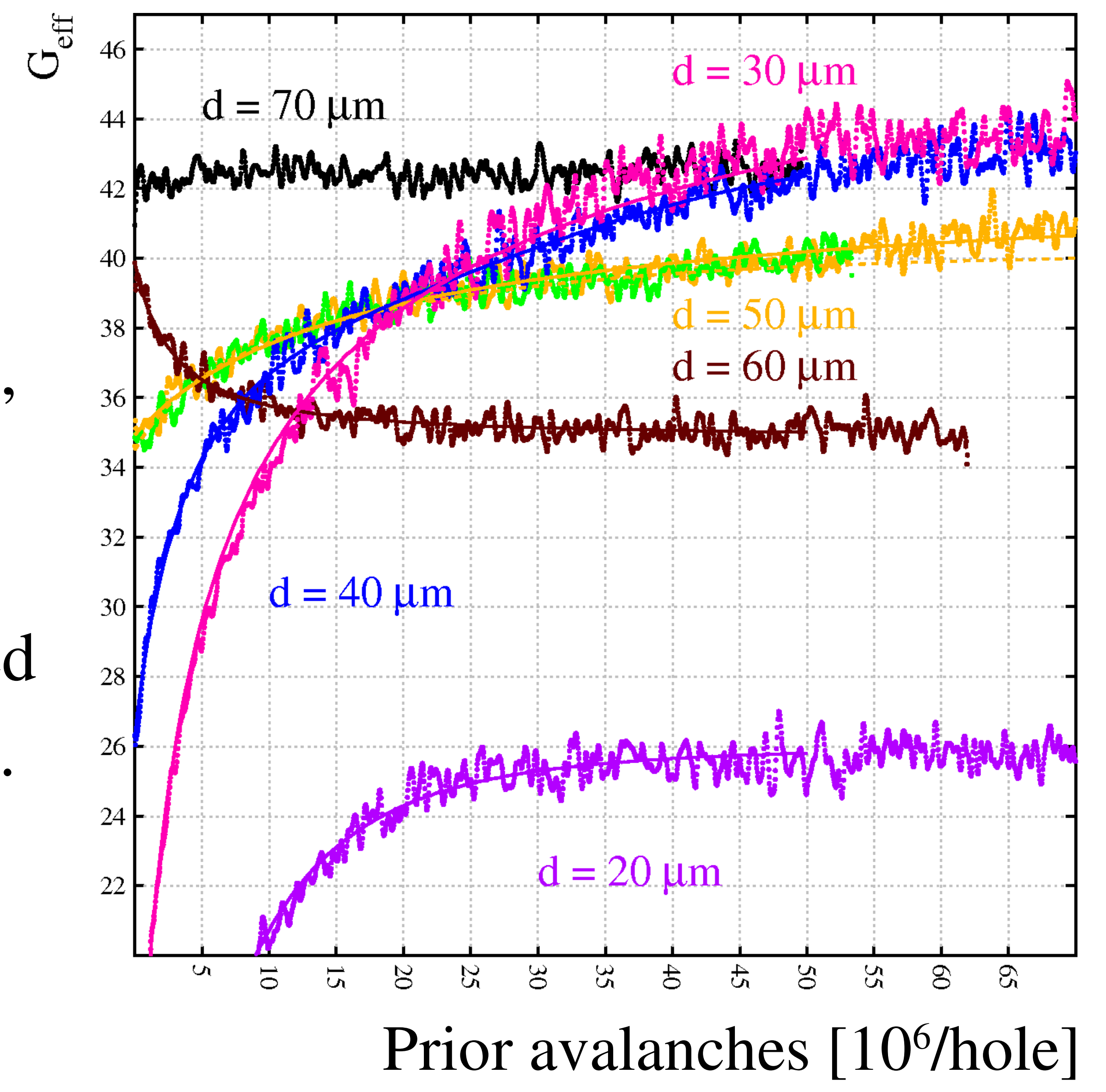

Charges in GEMs

- In GEMs, active gas comes in contact with dielectrics; in breach of a fundamental law of gas-based devices. This results in charge accumulations on the plastic which distort the field.

- Space charge may affect ion back flow: see talk of Bernhard Ketzer.

- Polyimide can contain mobile charges. These migrate through the plastic and modify the field.

Charging-up current

- When applying voltage across a new GEM, a current flows:
  - *not* constant (i.e. not a resistor)
  - decay is *not* exponential (i.e. not a capacitor);
  - decay is *not* linear (i.e. not evacuation);
  - but a *power law*.

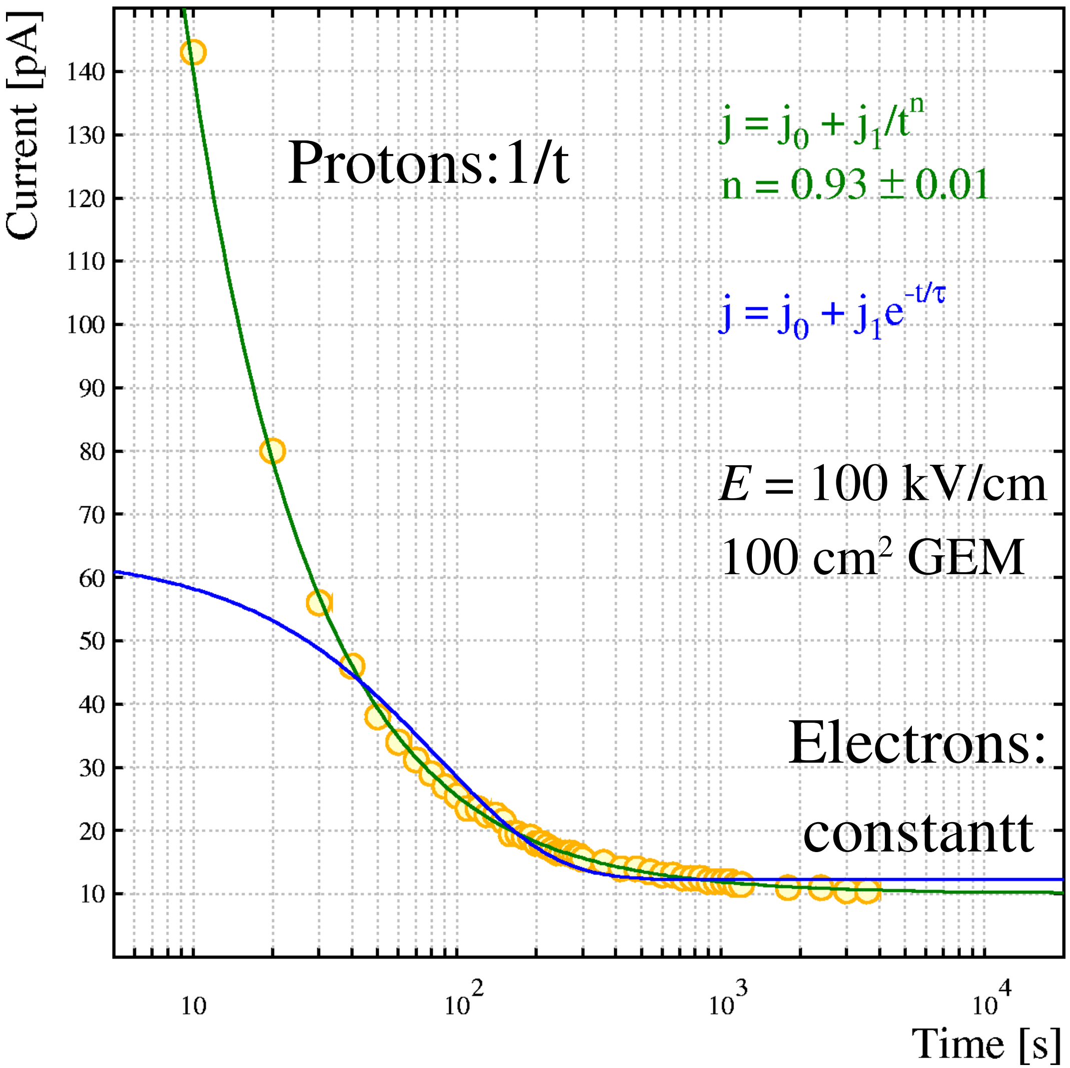

Discharge current

- The initial charge carriers stay in the polyimide, as can be seen by switching off the HV.
- The discharge current has reverse polarity and obeys a Kohlrausch law.

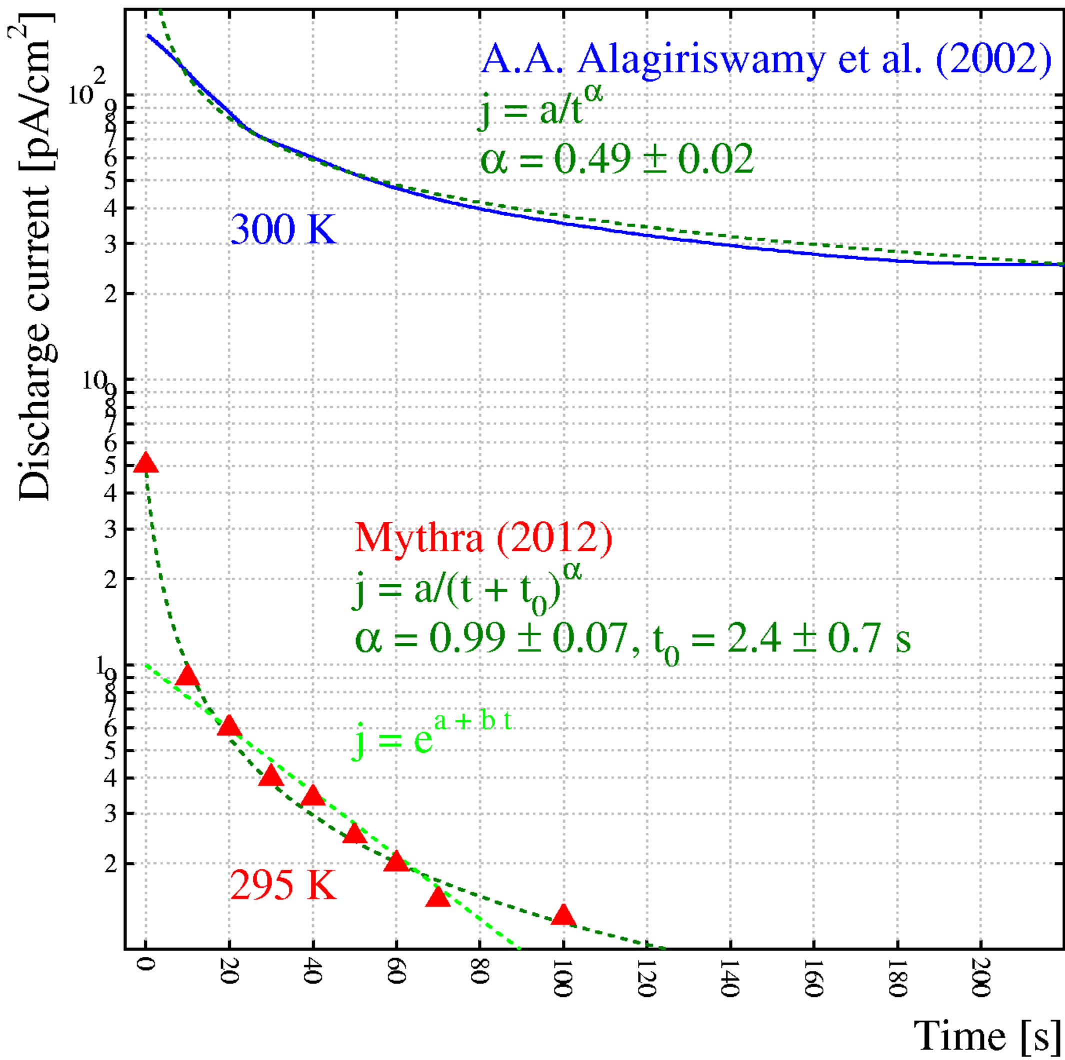

Protons: polyamic acid (PAA)

- Note the intermediate acid, i.e. an H^+ donor:

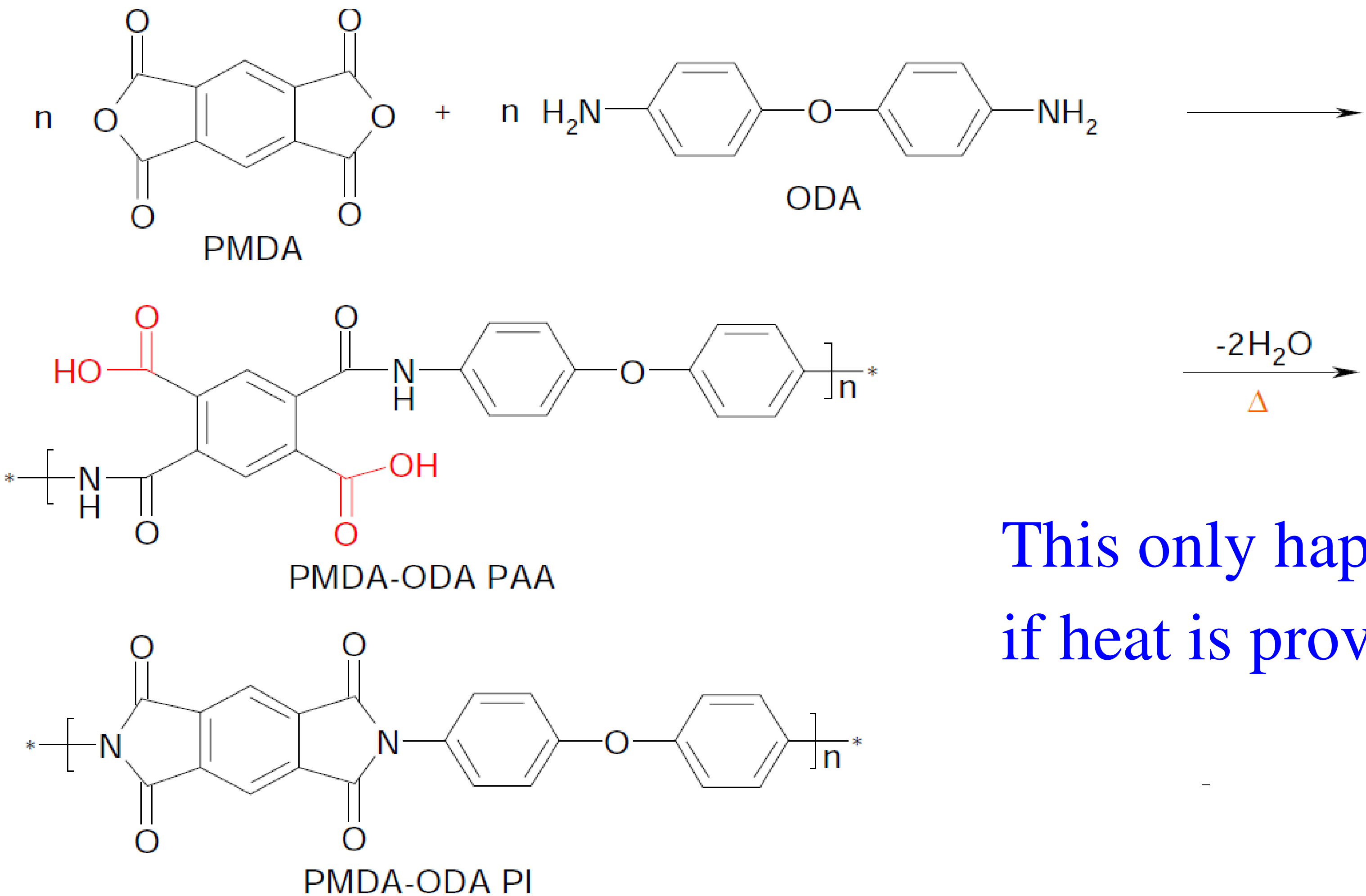

This only happens if heat is provided.

PAA → PI vs baking temperature

- The quantity of remaining PAA depends on the baking temperature.
- The proton density therefore also varies.
- [H. Oji *et al.*, Memoirs of the Synchrotron Radiation Center, Ritsumeikan University, Kyoto, Japan **8** (2006) 187-188.]

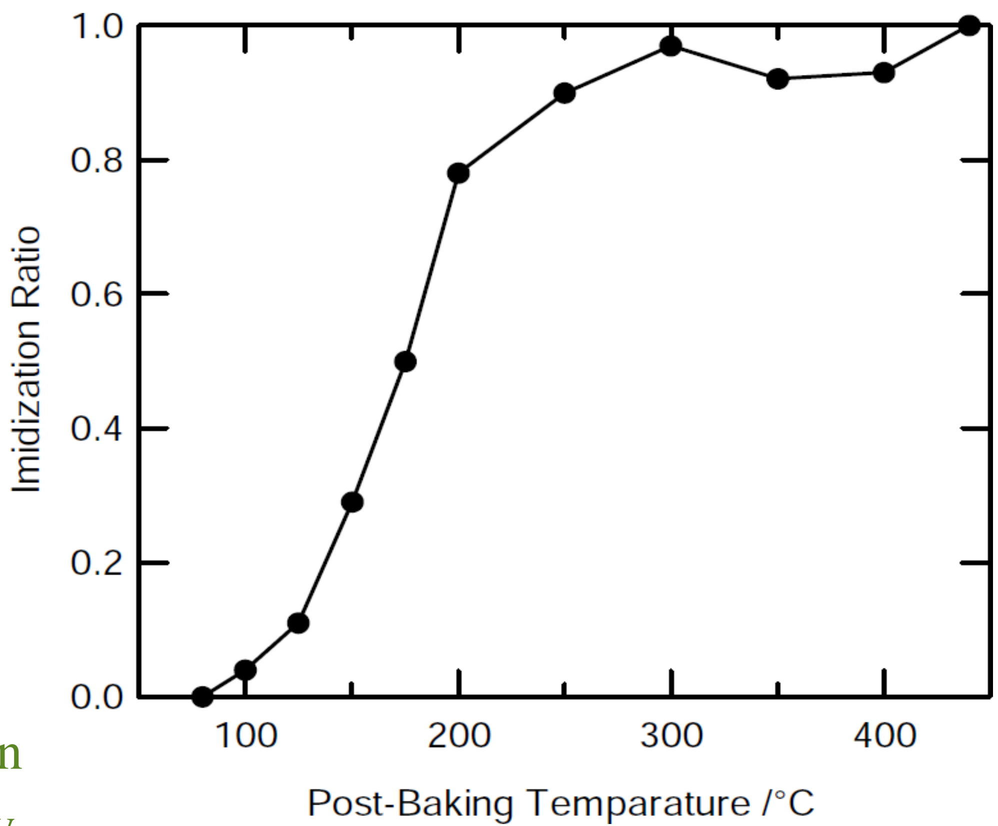

Rudolf Hermann Arndt Kohlrausch (November 6th 1809, Göttingen - March 8th 1858, Erlangen)

Kohlrausch relaxation

- This time dependence is known since 1854 at least. Also known as Curie-von Schweidler behaviour.

- Numerous models have been proposed
  - H. Kliem, *Kohlrausch relaxations: new aspects about the everlasting story*, doi: 10.1109/TDEI.2005.1511096.

- One of the simplest models specifically assumes ions (e.g. protons, not electrons) as charge carriers and has thin insulating barriers between dielectric medium and electrodes.

Ar^+ and Ne^+ mobility

- Avalanches take a few ns: http://cern.ch/garfieldpp/examples/gemgain
- Ion velocity at 3 kV/cm: Ar: ~20 µs/mm, Ne: ~8 µs/mm

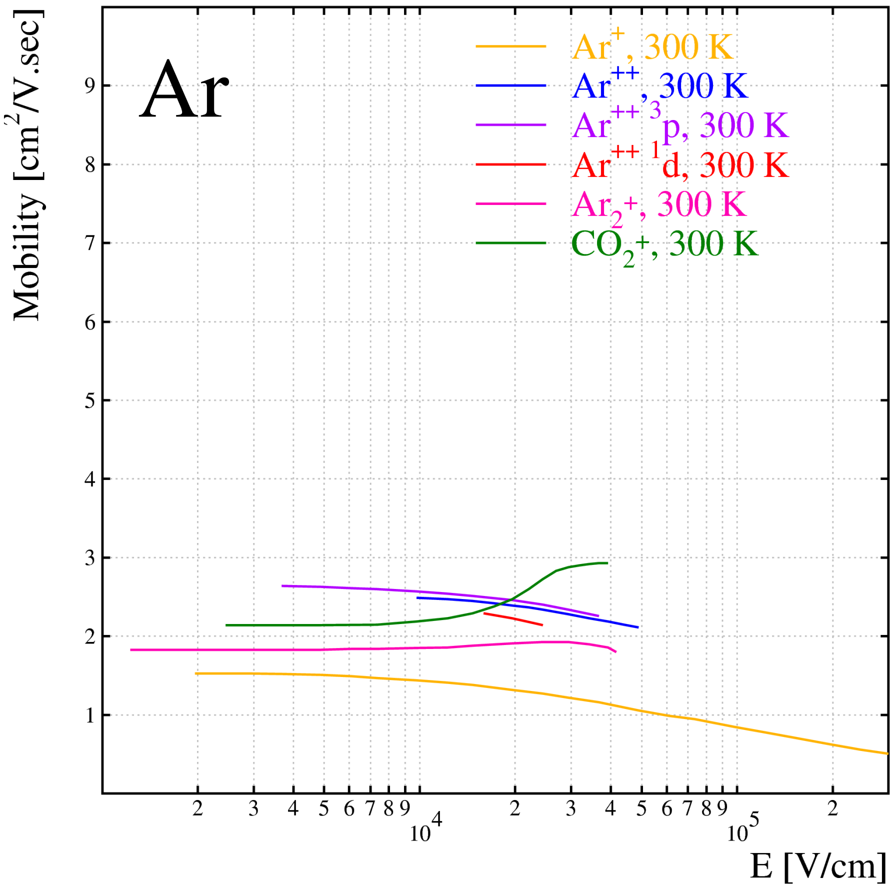

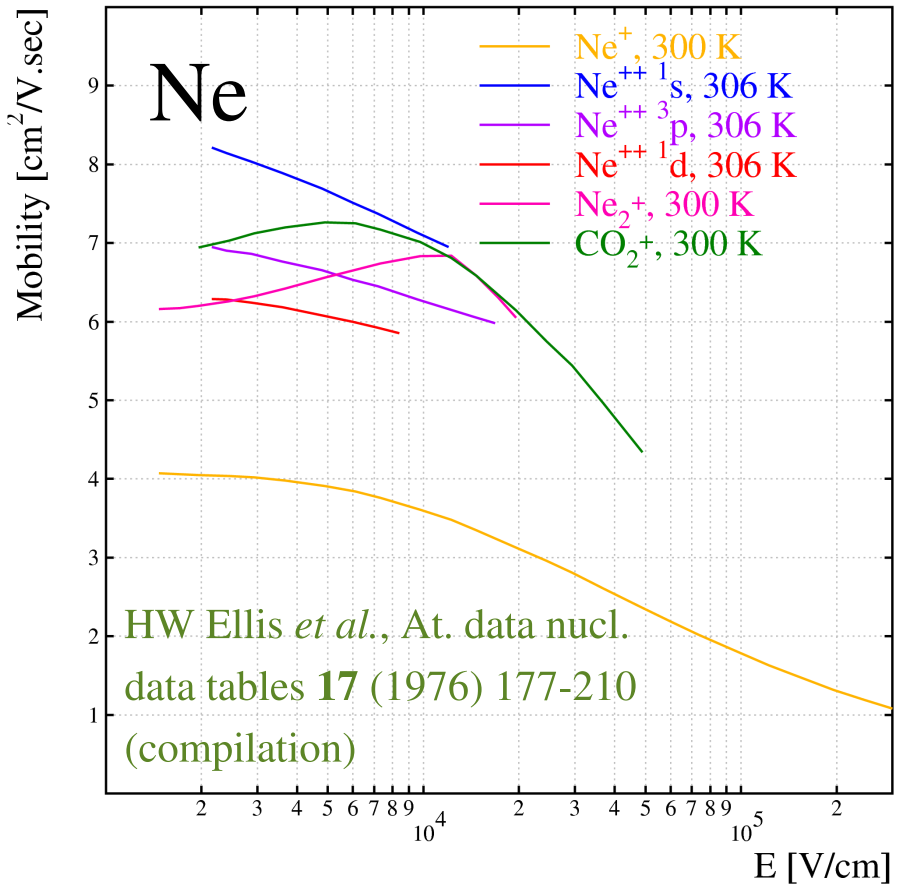

Ion chemistry – rate constants

- Ions react with the gas in which they move:
  - proton exchange: $AH^+ \; B \rightarrow A \; BH^+$
  - charge transfer: $A^+ \; B \rightarrow A \; B^+$
  - condensation reactions: new C-O and C-C bonds
  - molecular ion formation Ar^+_2
  - ...
- Rate constants range from 10^{-9} to 10^{-14} cm^3/s. At atmospheric pressure, in a pure gas, this corresponds to characteristic times of 40 ps to 4 μs.

Ion transport

- Ar 90 % - C_2H_6 10 %, at low pressure

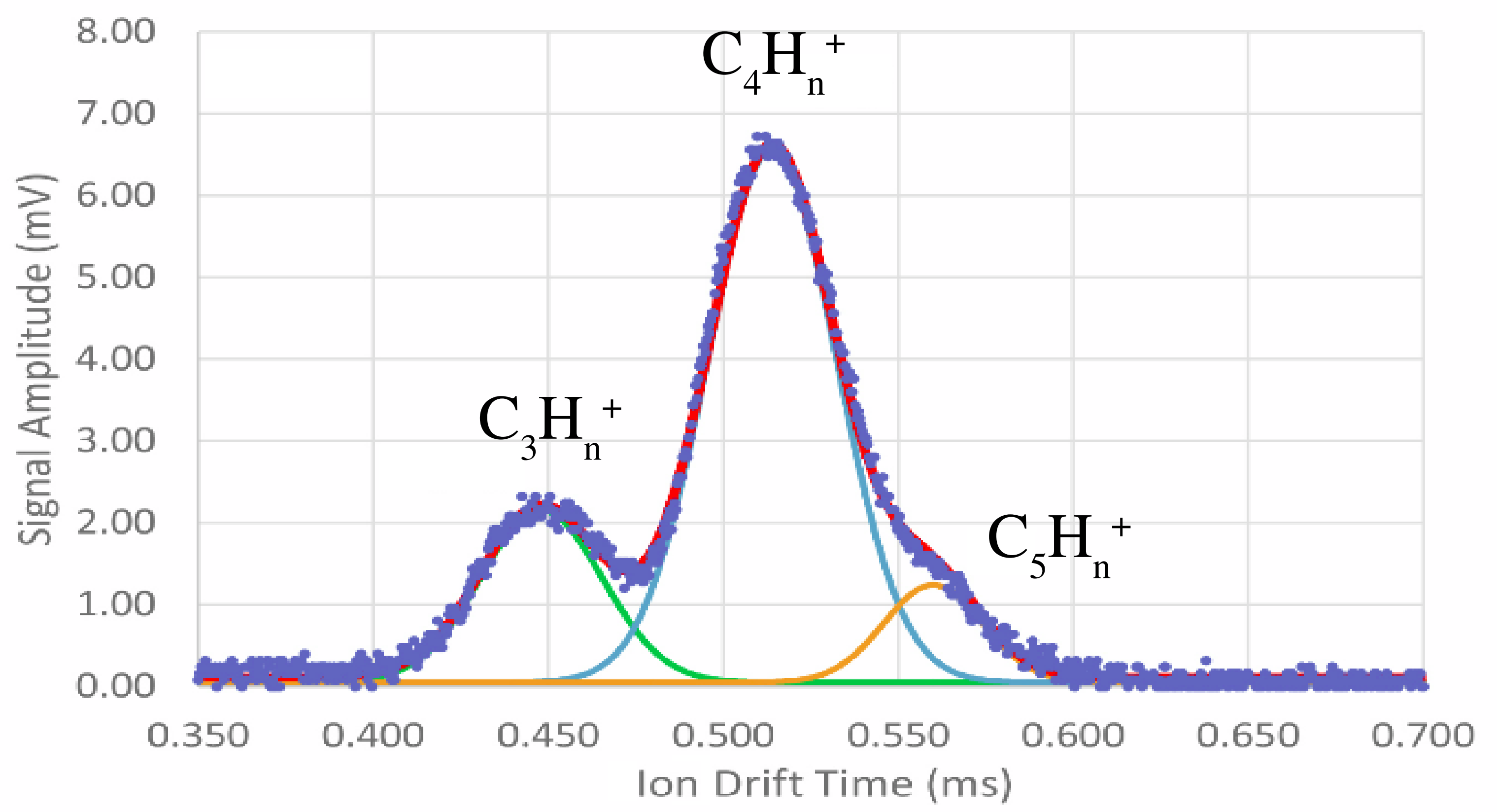

[André Cortez et al. 10.1088/1748-0221/8/12/P12012]

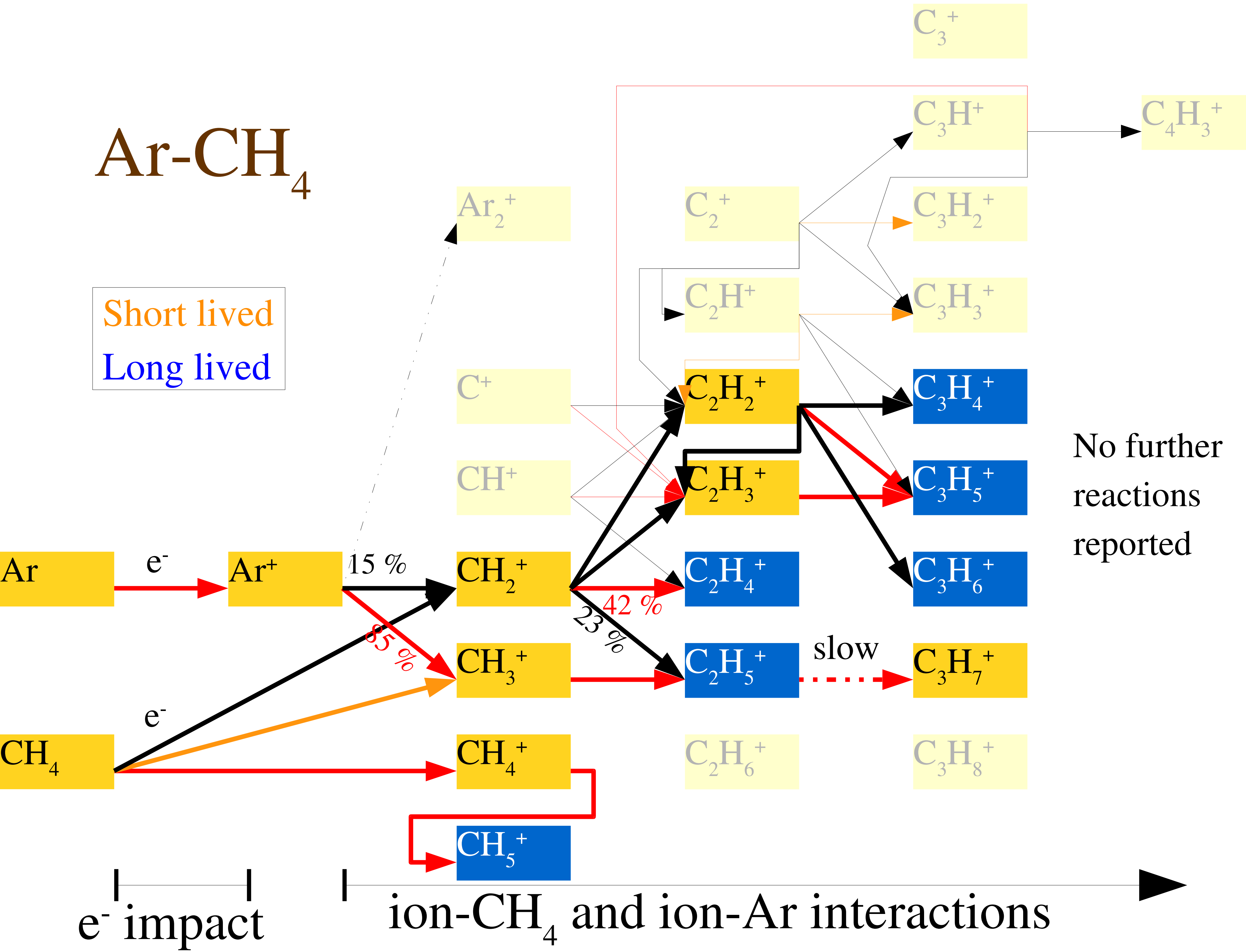

Ar-CH4
Short lived
Long lived
Ar
e-
Ar+
15 %
85 %
CH4
e-
Ar2+
C+
CH+
CH2+
CH3+
CH4+
CH5+
C2+
C2H+
C2H2+
C2H3+
C2H4+
C2H5+
C2H6+
42 %
23 %
slow
C3+
C3H+
C3H2+
C3H3+
C3H4+
C3H5+
C3H6+
C3H7+
C3H8+
C4H3+
No further reactions reported
e- impact
ion-CH4 and ion-Ar interactions

Diffusion of Ar^+ in Ar and Ne^+ in Ne

- Little experimental data, in particular at low fields. extrapolated from higher fields: ~10 μm for 1 mm

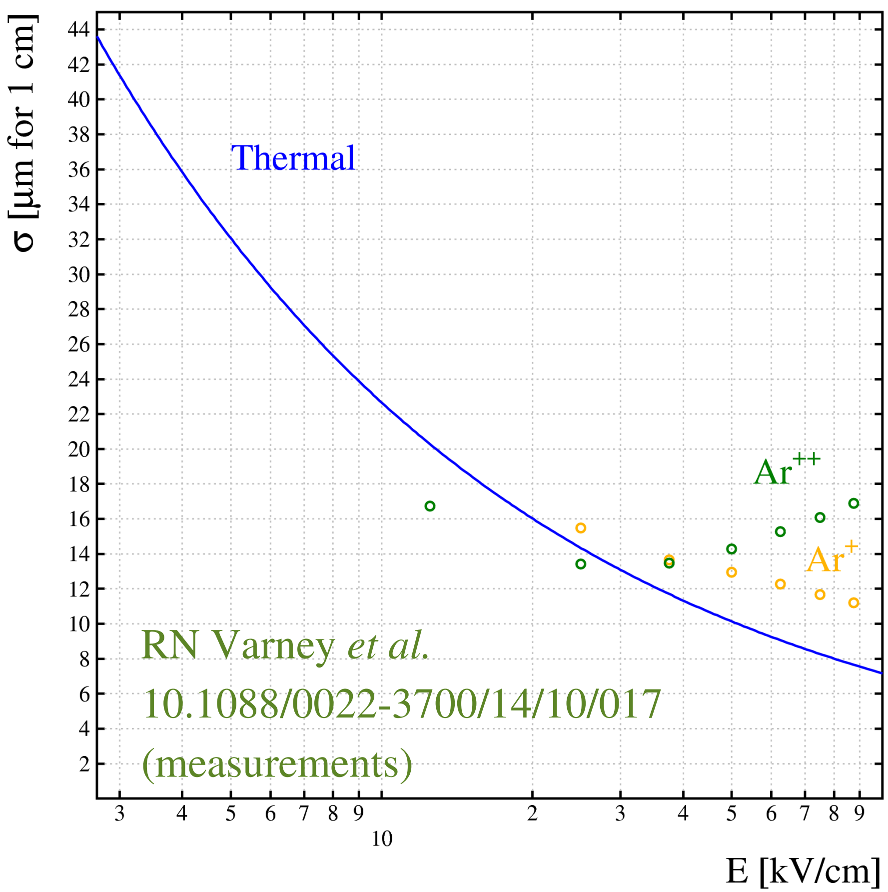

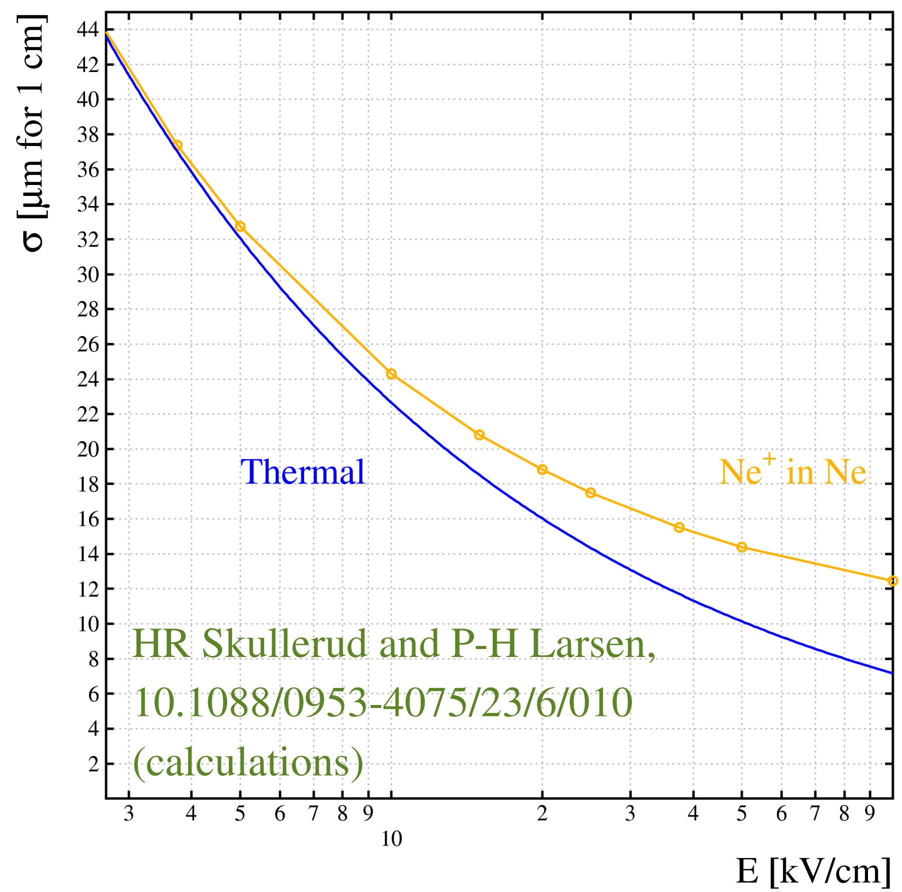

Changes

- Wires have fallen out of favour:
  - finite element and boundary elements.
- Electron transport:
  - transport and fields are coupled for small structures;
  - role of excited noble gas atoms, transfer measurements;
  - charges in dielectrics, surface charge, space charge.
- Current activities:
  - ion chemistry and measurement of ion transport;
  - semi-conductive layers.

Backup slides

GEM space charge – summary

- Space charge between GEMs pushes ions towards the cathode ("upper") GEM electrode. This reduces the ion back-flow.

- The trend of the measured rate dependence of ion back-flow is reproduced by simulations.

- By a stroke of luck, higher rates lead to improved ion back-flow reduction.

- Conical GEMs and misalignment can reduce ion back-flow.

GEM surface charge – summary

- Gain (effective and total) is modified by charging-up.

- Hole shape:
  - charge-induced increase is strongest in tapered holes;
  - gain is virtually stable in cylindric holes;
  - dependence on hole shape is non-linear.
- Voltage:
  - effect increases with voltage.

- Although the absolute gain is not yet understood, simulations do reproduce charging-up effects.

Square mesh wires ?

- Square wires are much simpler to model than cylindric wires – but this is an inadequate simplification.
- Calculations done using finite elements.

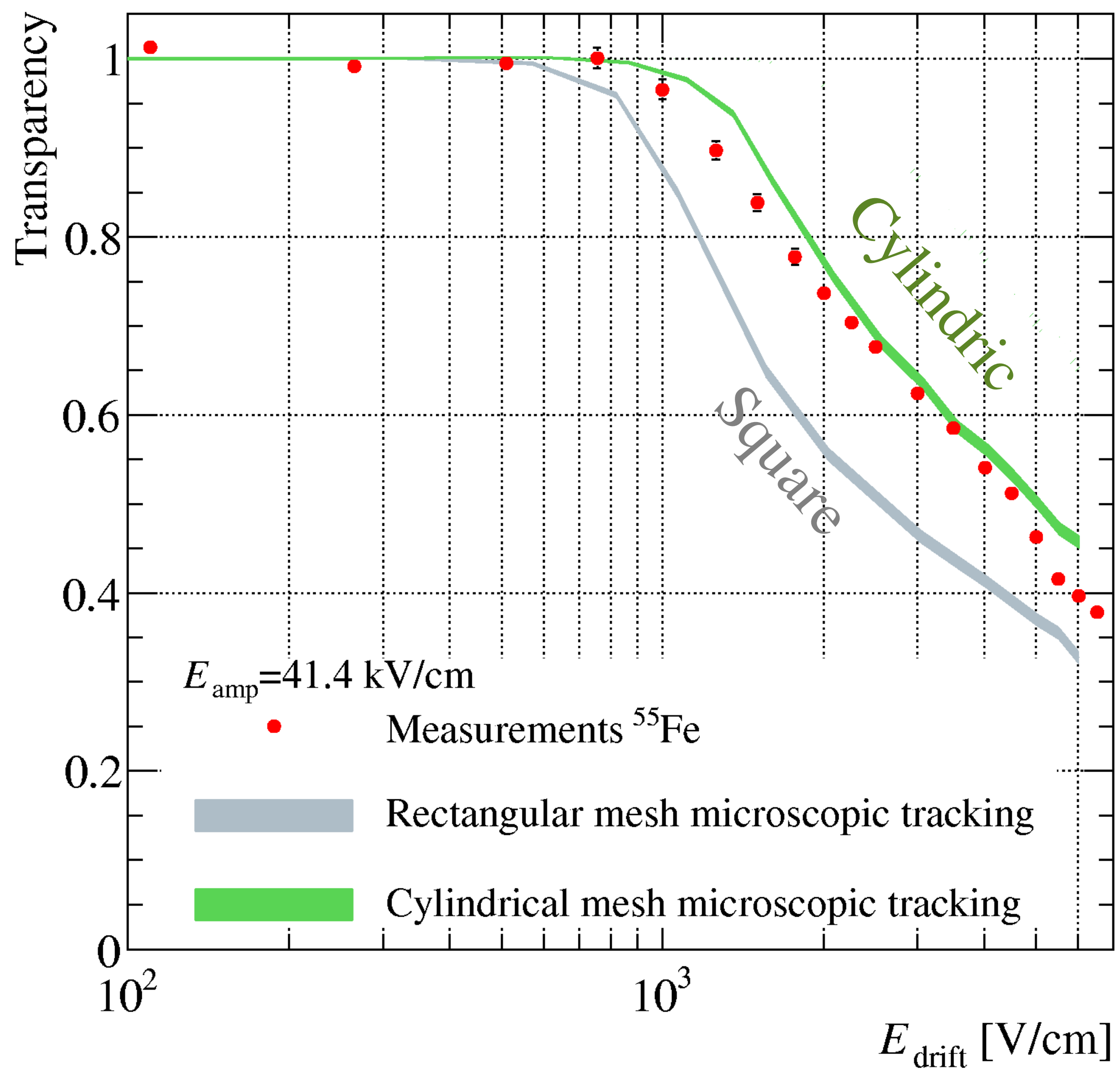

Dipole moment of the mesh

- Compare equipotentials at E_{drift} = 3.3 kV/cm: thin-wire elements overestimate the transparency by 15 %.

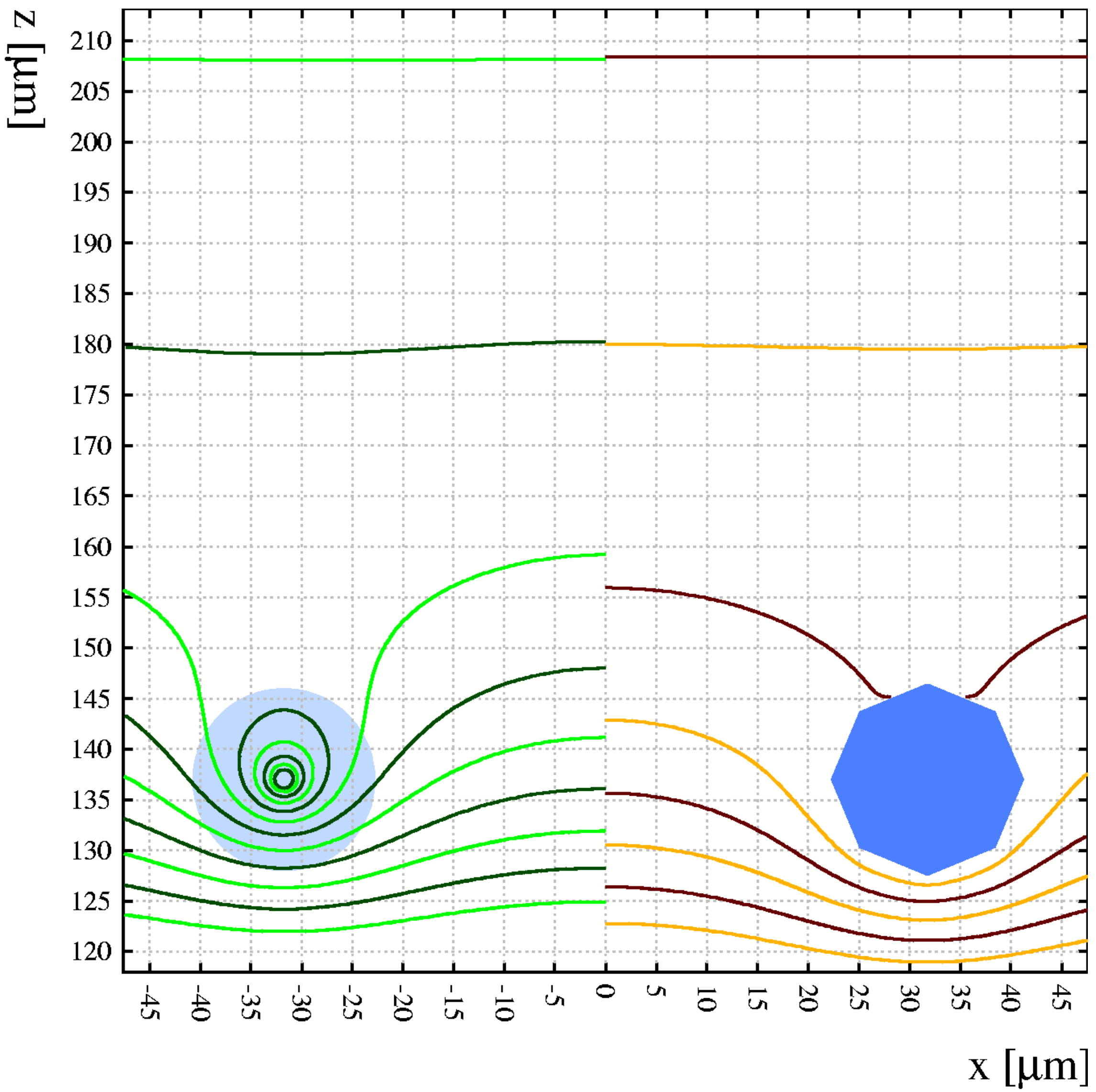

GEM – unit cell

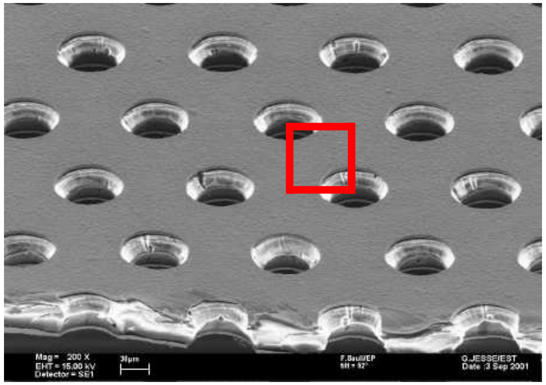

- Modelling more than ½ hole would be a waste: the rest is obtained as periodic copies.
- Only the gas and plastic are meshed.

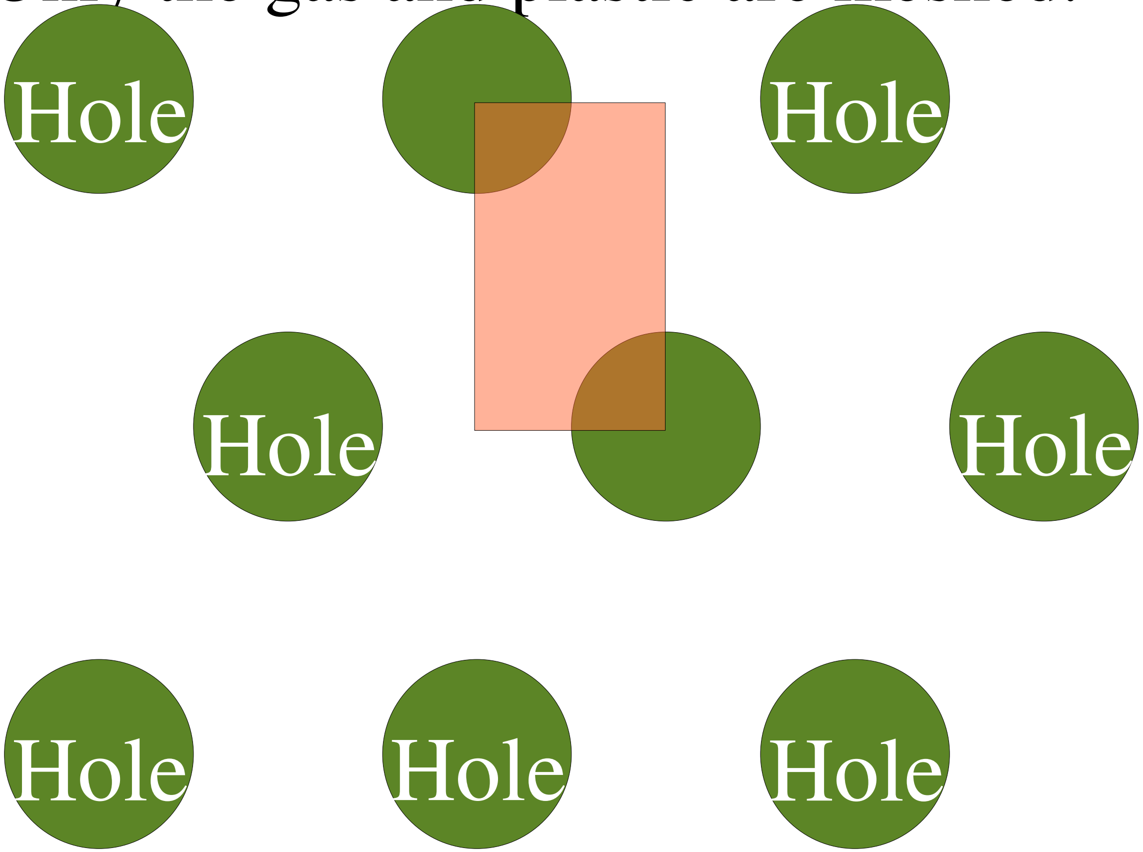

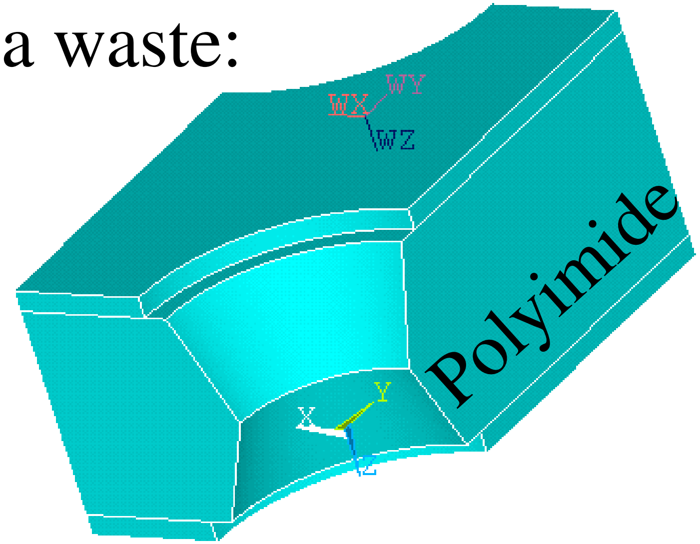

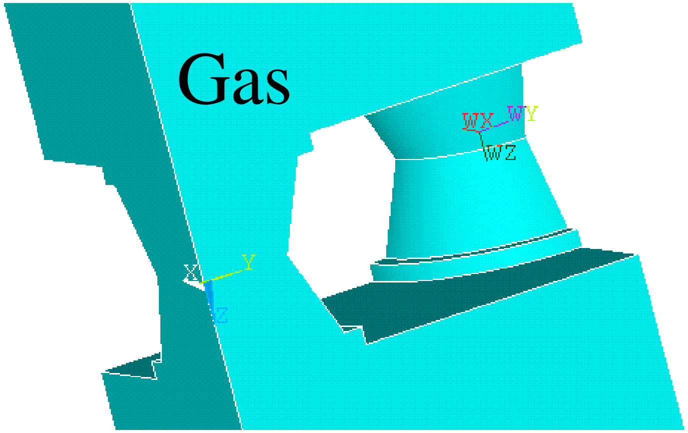

Steady-state resistivity

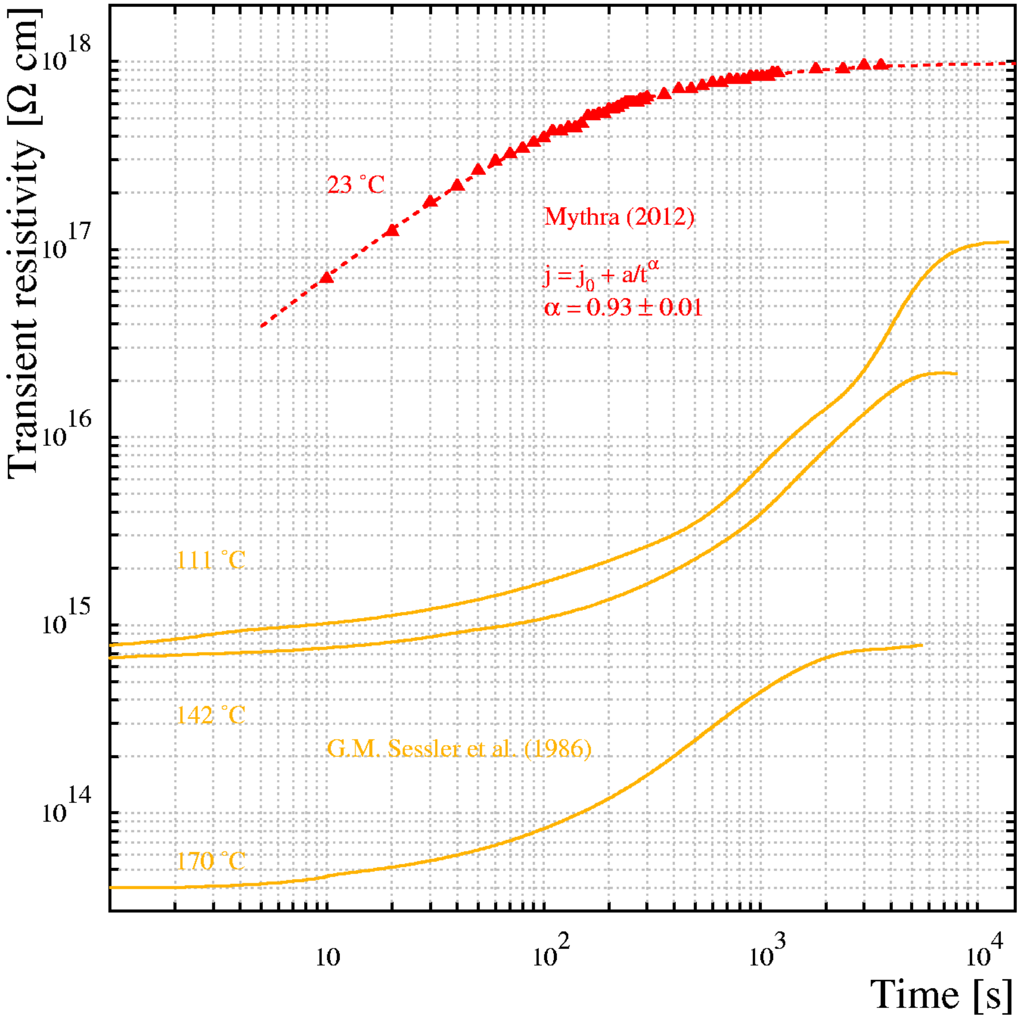

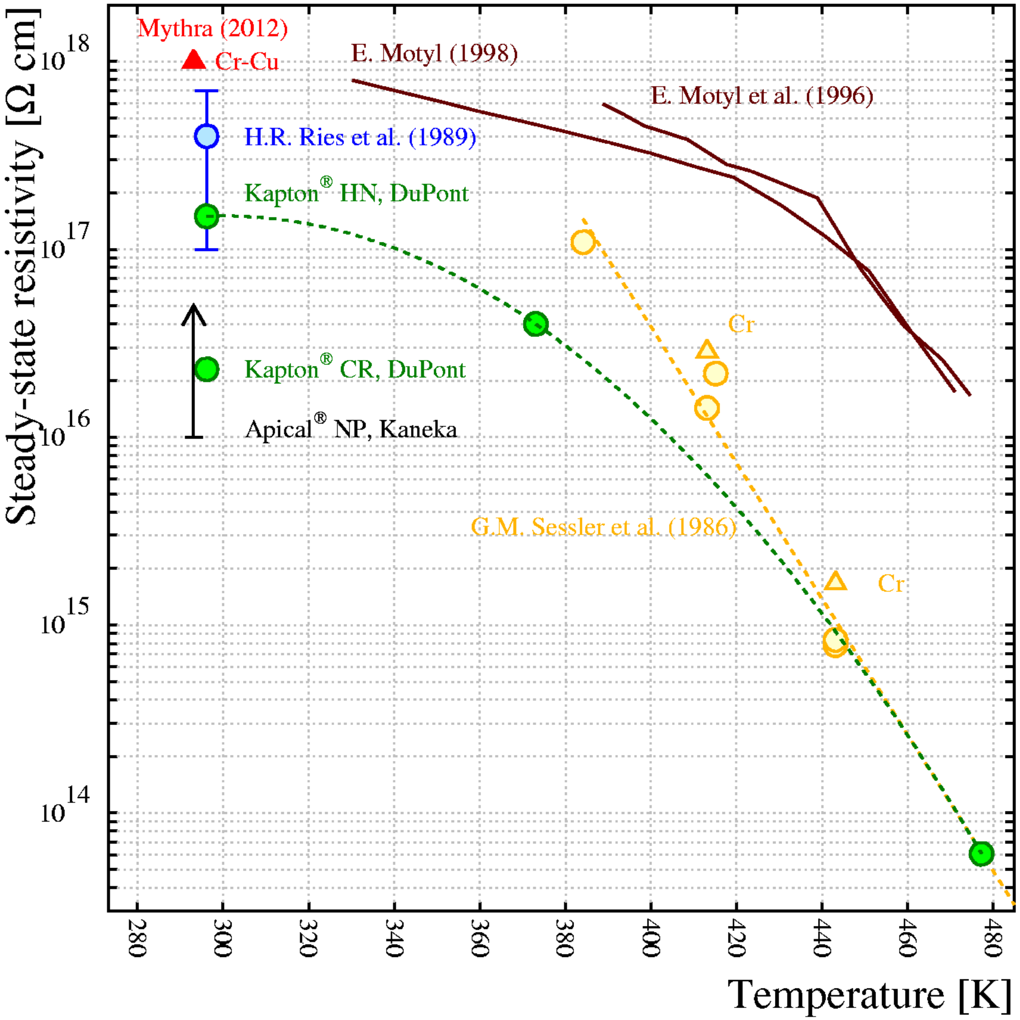

3 GEM configurations adding N_2

- 3 GEMs under $Ne/CO_2/N_2$=(90/5/10). GEM2 is mis-aligned.
- Townsend: ~ 2/cm at 6kV/cm. $\times 1.3$ gain in 2mm.
- 0.5% - 2% of IBF with $E_{T1} \sim$ 4-6kV/cm and $E_{T2} \sim$ 0.5kV/cm.

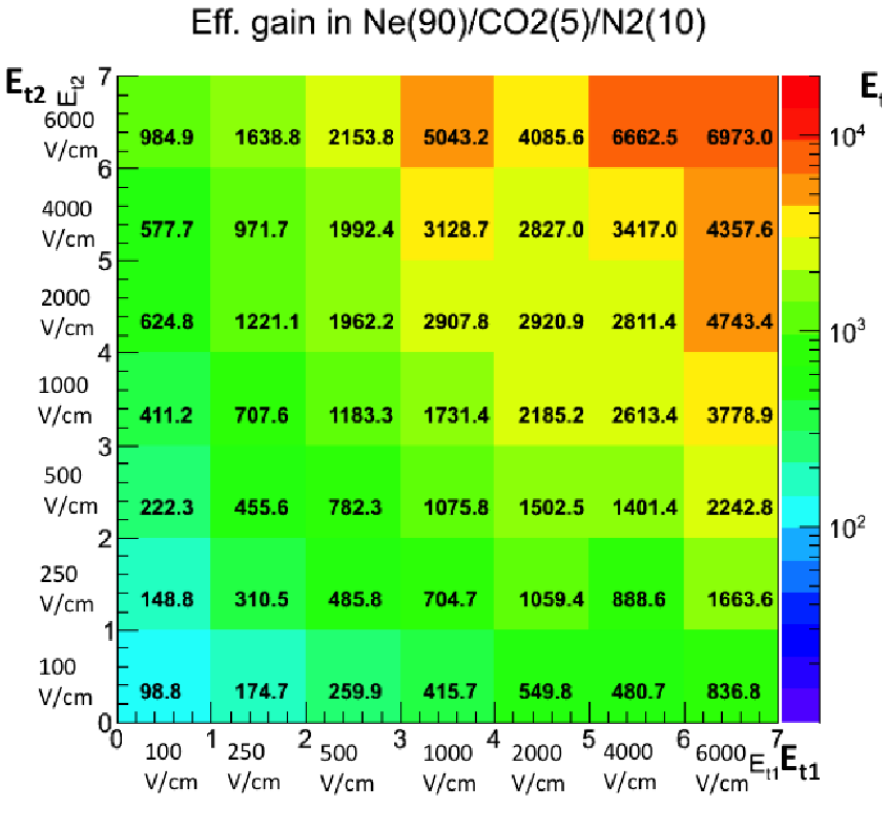

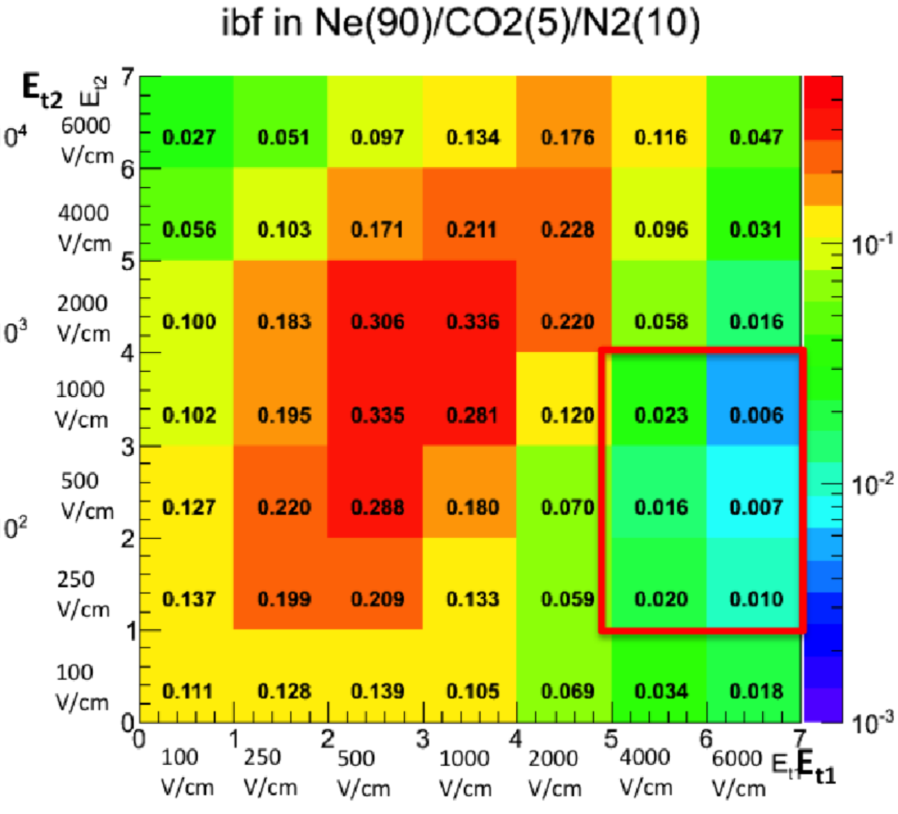

4 GEM configurations adding N_2

- 4 GEMs under $Ne/CO_2/N_2$=(90/5/10). GEM2 and GEM4 is mis-aligned. E_{T1}=4kV/cm
- 0.3% - 1% of IBF with $E_{T1} \sim$ 4-6kV/cm and $E_{T2} \sim$ 0.5kV/cm.
- ×2-3 improvement with 4 GEMs

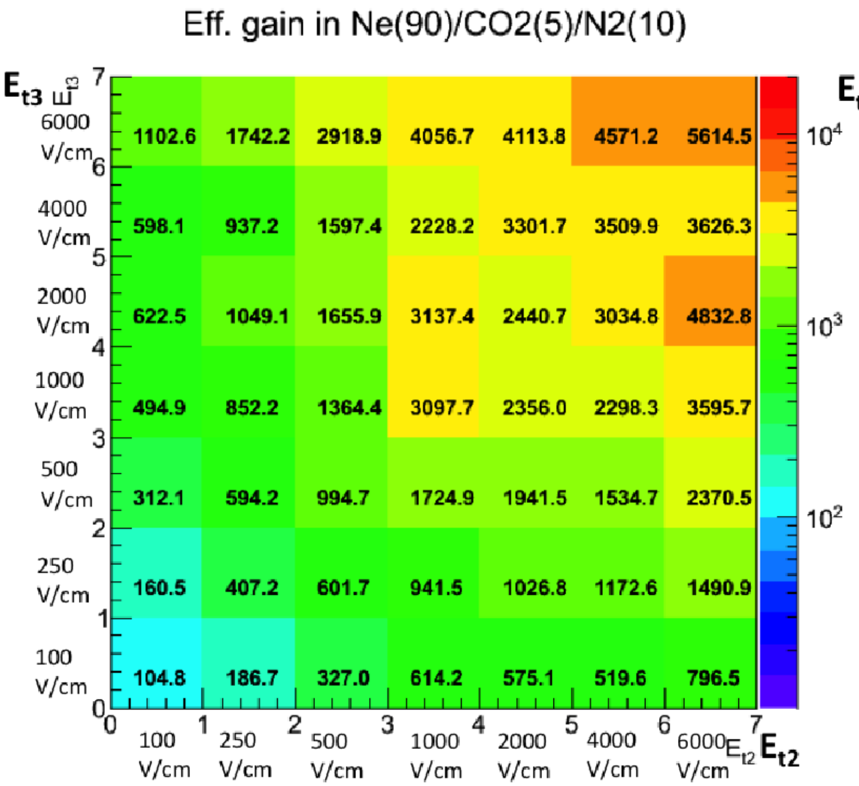

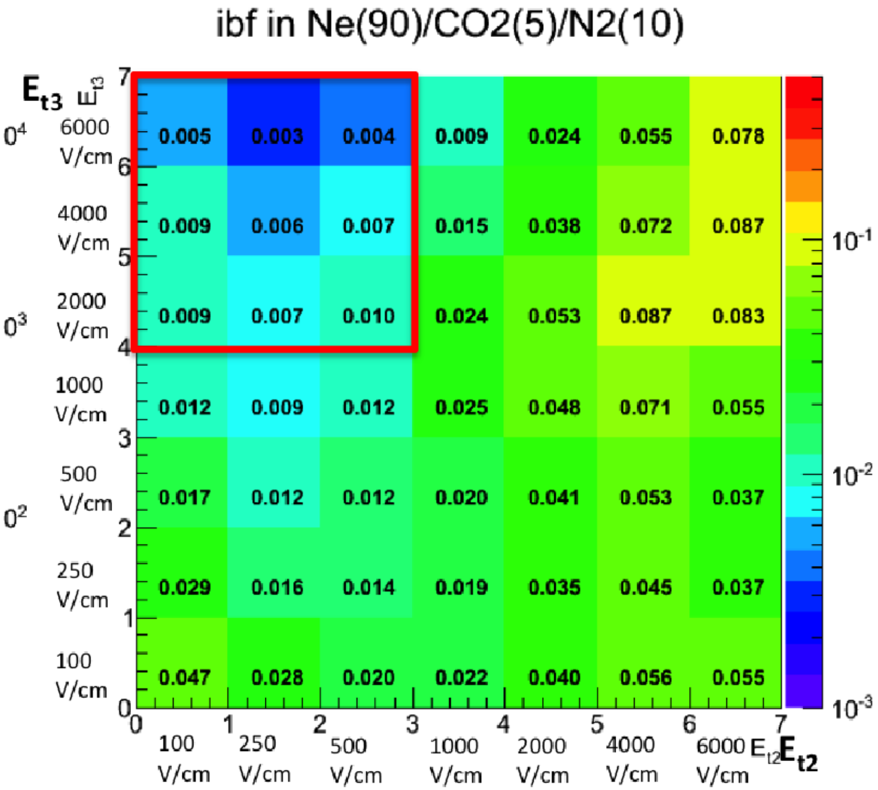

Gain measurement

- Care was taken:
  - GEM was kept in dry gas for weeks;
  - GEM had not been exposed to radiation for weeks;
  - no area of the GEM was used twice;
  - electrically insulated box, virtually no noise;

Gain curves

- Rise of gain is clearly visible at all voltages, in the range 5-20 %.
- An unexpected initial drop shows up.

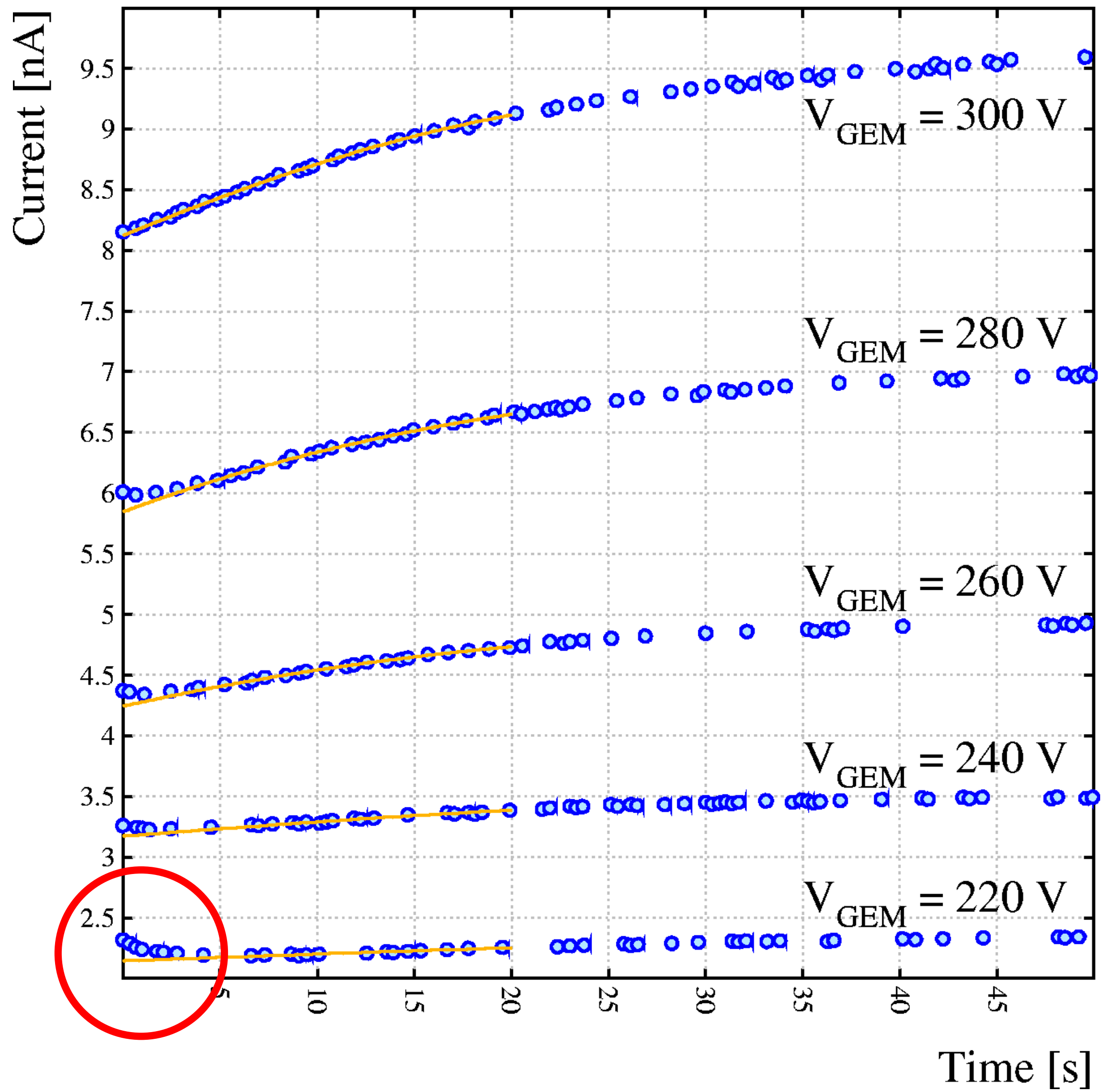

Initial drop

- Properties:
  - larger at low V_{GEM};
  - decays faster at high V_{GEM};
- Interpretation ?

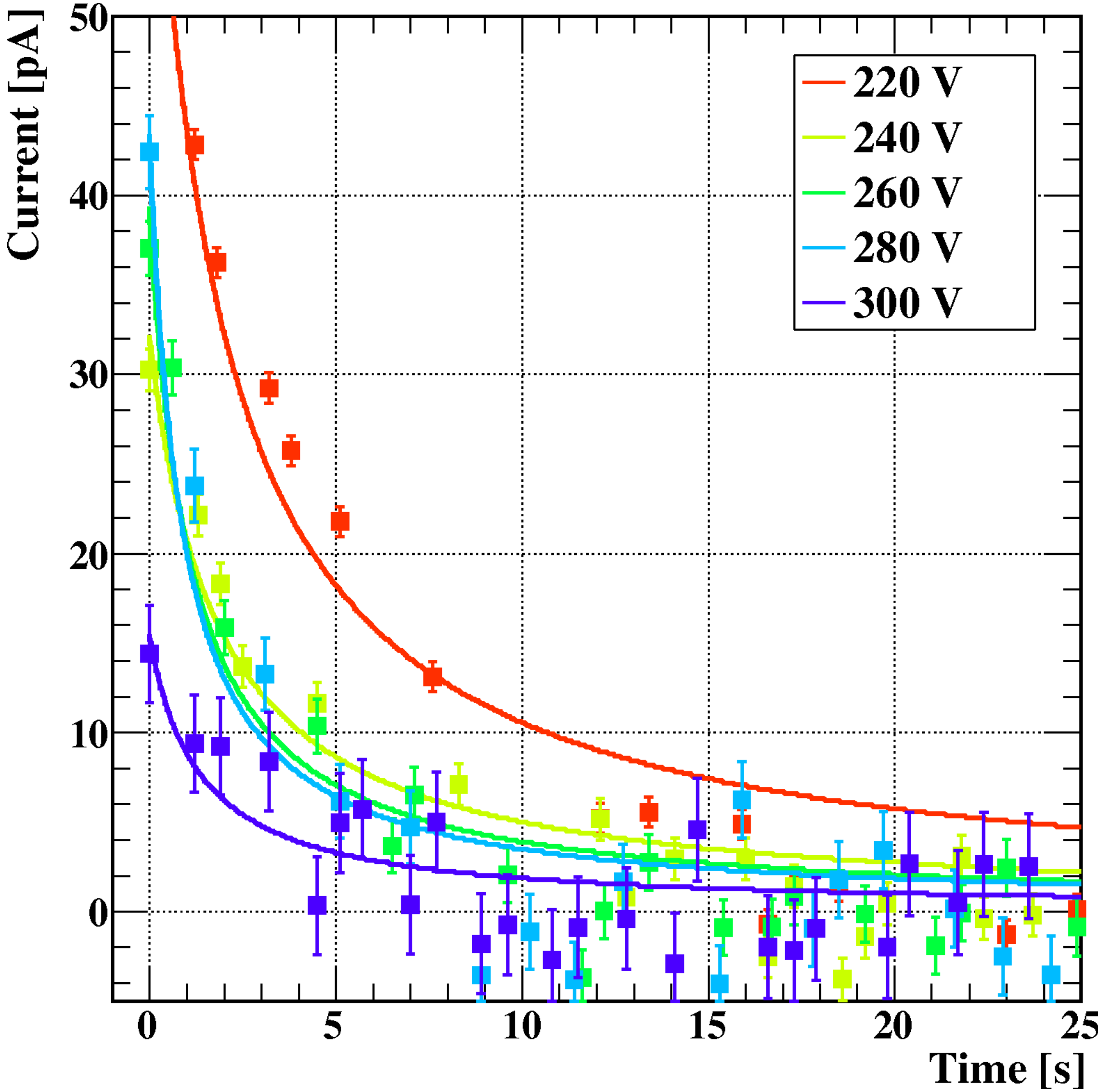

Effect of pre-charge

- Pre-charge proportional to the final equilibrium, gives an initial drop.
- Only works if the pre-charge is locally larger than the equilibrium.
- Typically requires a charge of 10^6-10^7 /hole.

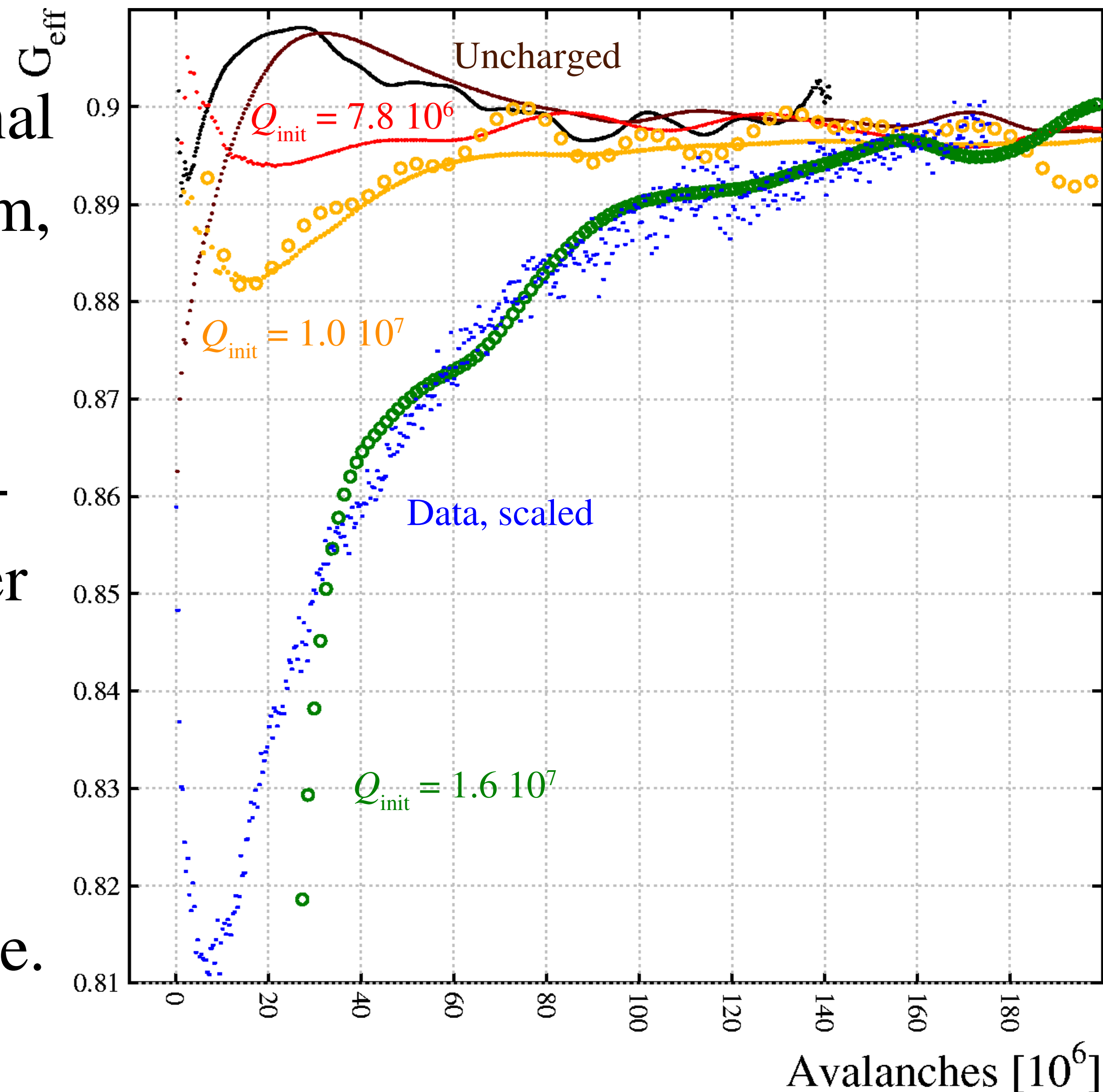

Volume or surface charge ?

- Volume:
  - Kohlrausch measurement, dividing the integrated moved charge by the PI volume: $n < 5\ 10^{12}$ / cm^3.
  - The volume from where charge can reach bare PI is $5\ 10^{-8}$ cm^3/hole.
  - Charge: $< 2\ 10^5\ q_e$/hole
- Surface:
  - Same measurements, but dividing the integrated charge by 5890 holes/cm^2.
  - Charge: $< 2\ 10^6\ q_e$/hole

r_P in Ar/CO_2 mixtures

- r_P for 30 % CO_2 currently requires an extrapolation

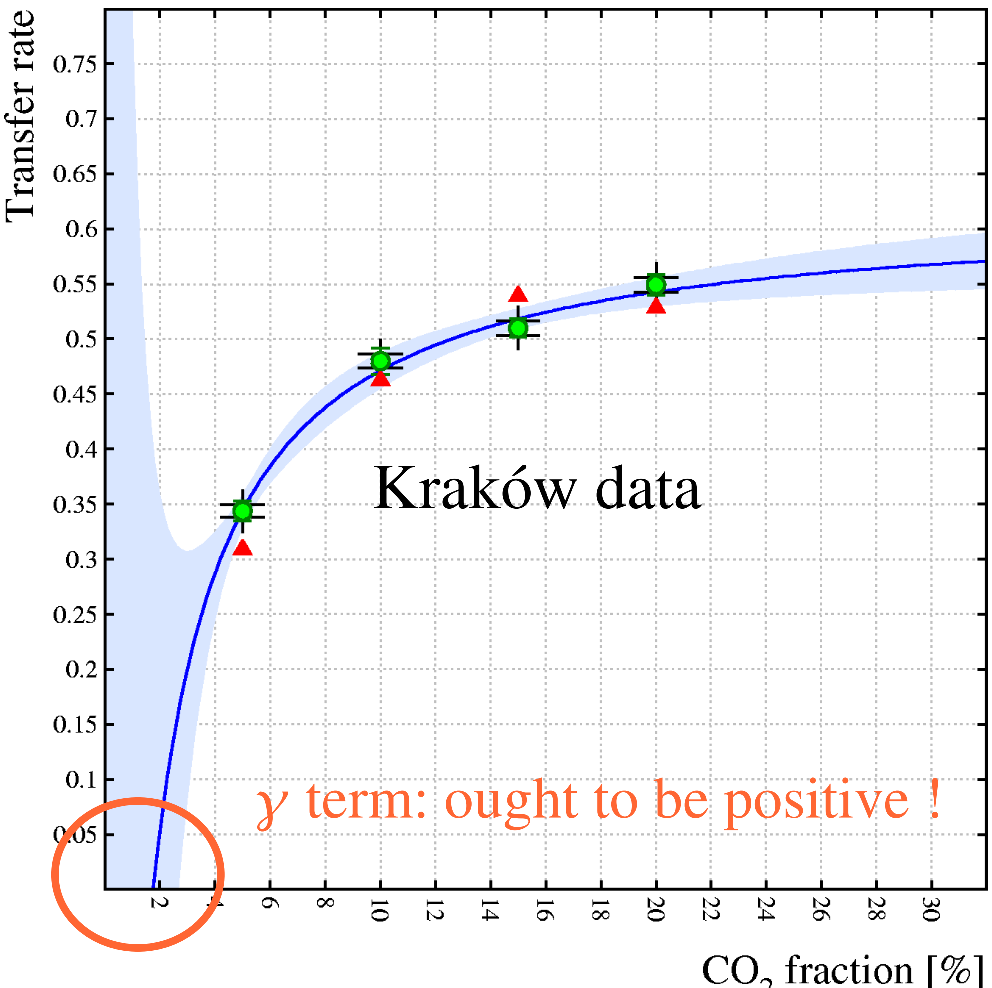

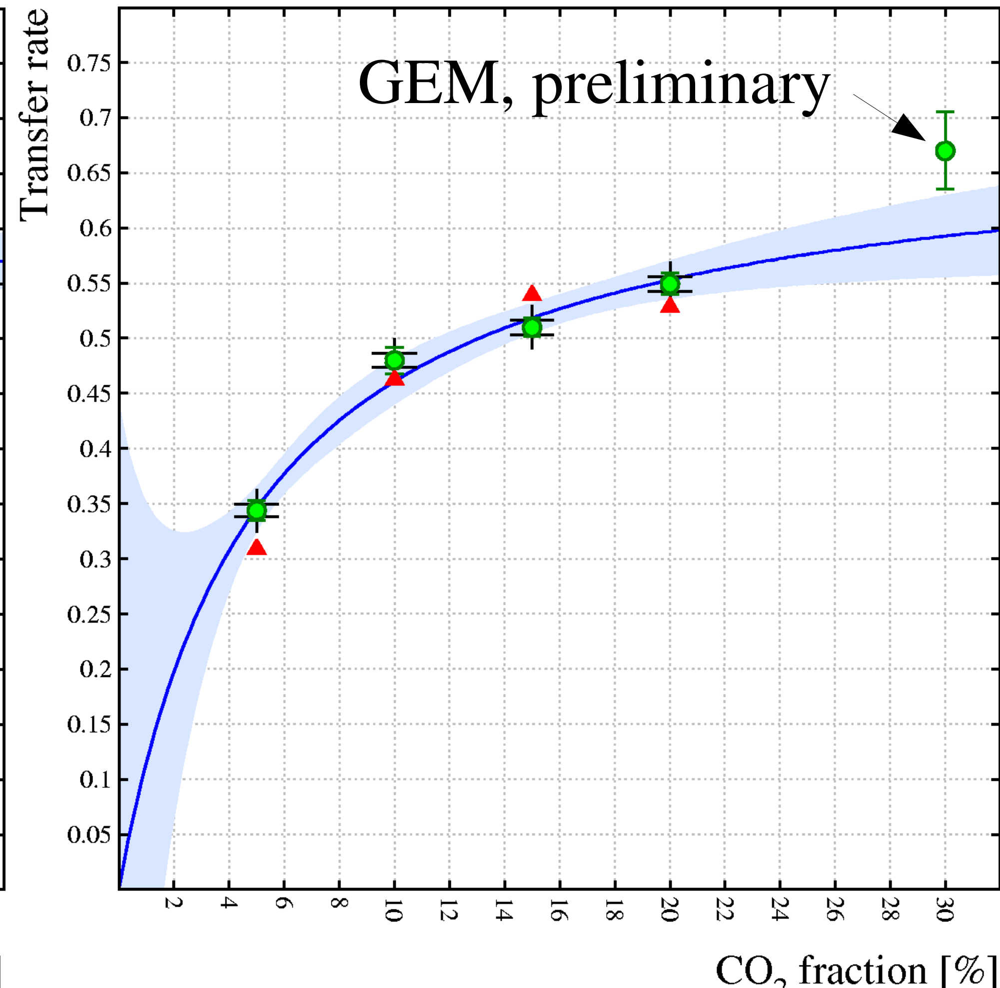

Transfer rate fit in GEM

- Extracting r_P from GEM data is more complicated than in tube data because of charging-up effects.
- The accuracy is inevitably smaller.
- Preliminary.

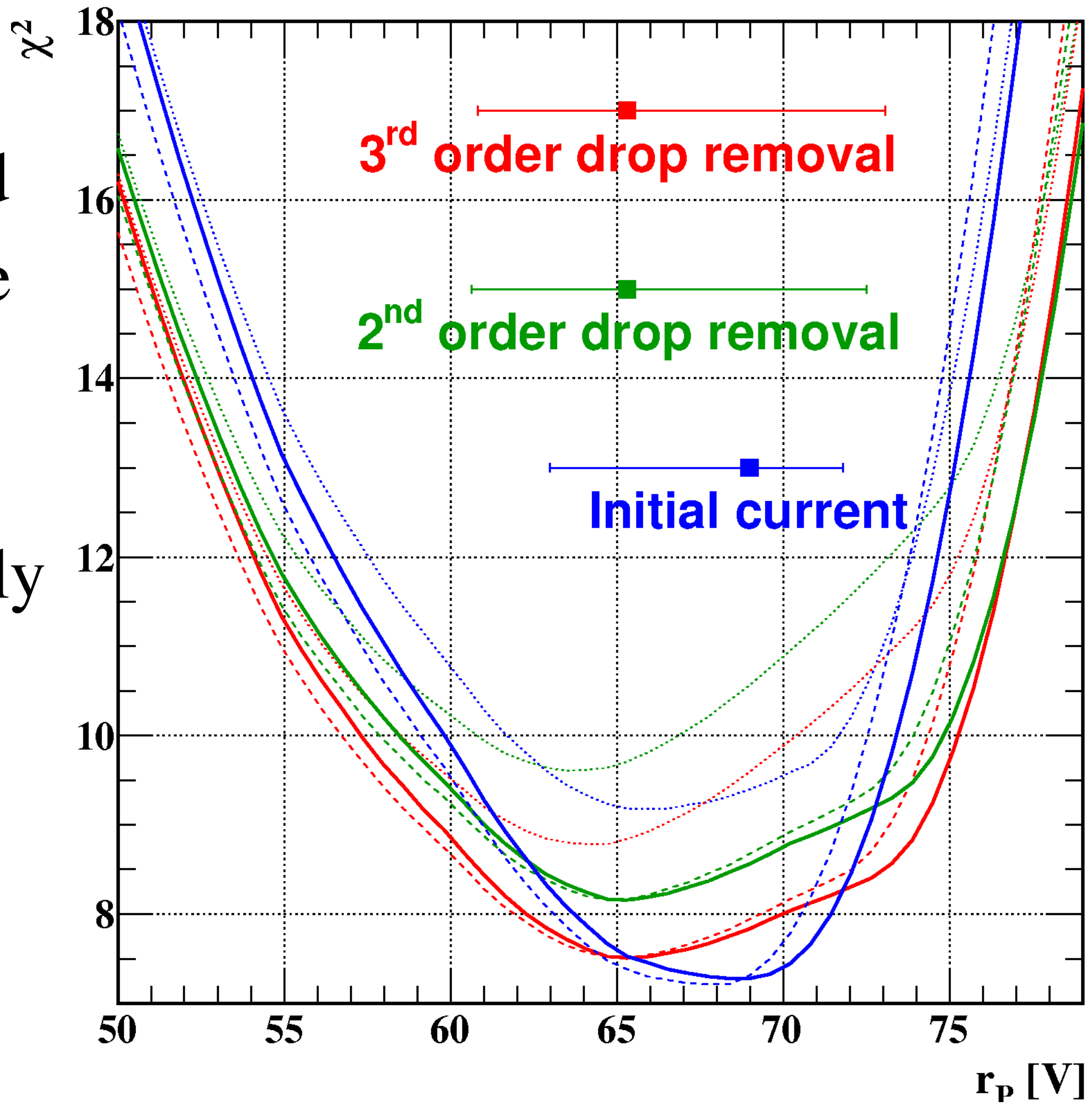

Solutions for 2-dimensional fields

- As ansatz for the potential function ϕ, we use:
  $\phi = \mathrm{Re} \log F$

- Required properties of F:
  - $\log F$ analytic function in the problem domain;
  - F has simple zeroes at the wires;
  - leads to finite field energy.

- Examples:
  - Single charge: $F = z$ hence: $\phi = \log(r)$
  - Row of charges: $F = \sin(\pi z/s)$, $F = \sinh(\pi z/s)$
  - Forest of charges: $F = \vartheta_1(\pi z / s_x, e^{-\pi s_y / s_x}) + \ldots$

Cross section of argon

- Cross section in a hard-sphere model:
  - Radius: ~70 pm (`http://www.webelements.com`)
  - Surface: $\sigma = \pi (70\ 10^{-10}\ \text{cm})^2 \approx 1.5\ 10^{-16}\ \text{cm}^2$
- Simplified cross sections used by Magboltz:

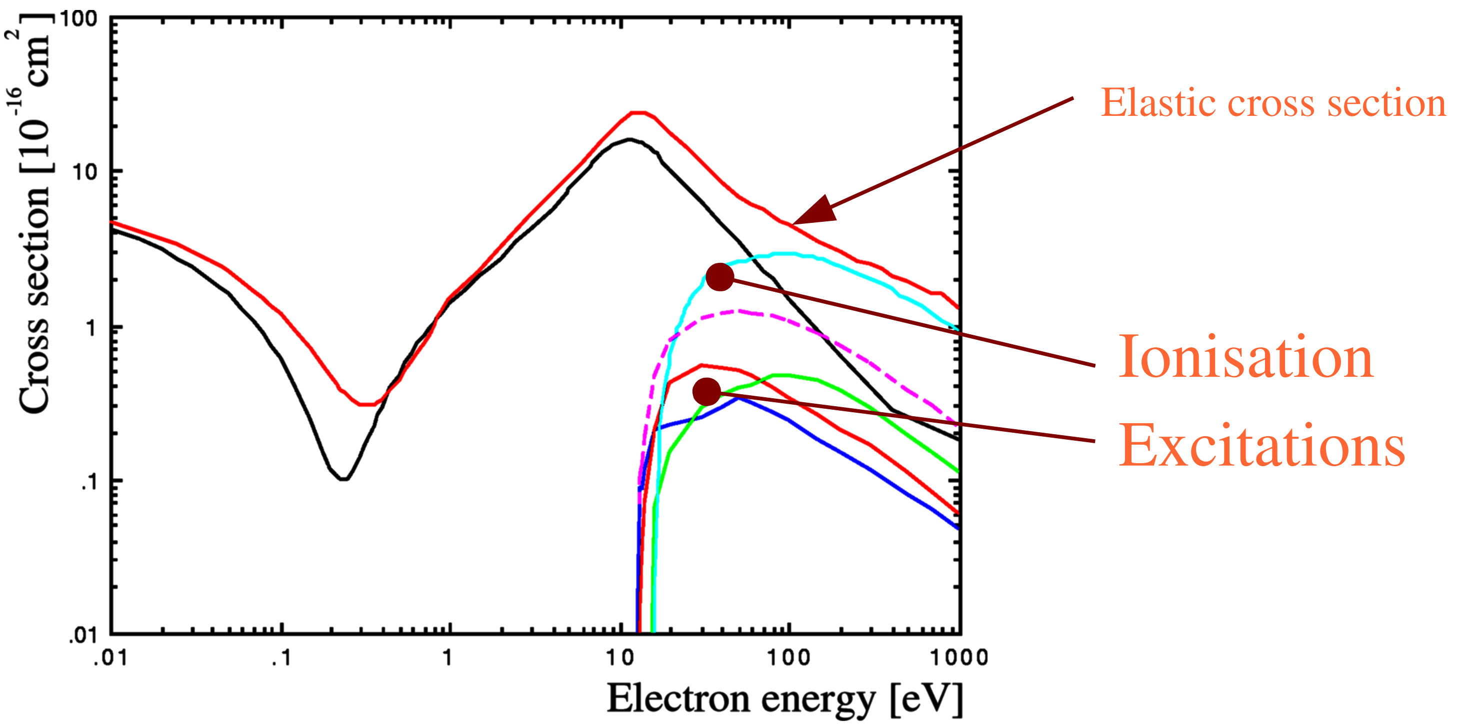

Mean free path in argon

- Given:
  - Cross section of 1 atom: $\sigma \approx 1.5\ 10^{-16}\ \mathrm{cm}^2$
  - Atoms per volume: $\mathscr{L} \approx 2.5\ 10^{19}$ atoms/cm^3

- Mean free path for an electron ?
  - An electron hits all atoms of which the centre is less than a cross section radius from its path
  - Over a distance L, the electron hits $\mathscr{L} \sigma\ L$ atoms
  - Hence, the mean free path is $\lambda_e = 1/(\mathscr{L}\sigma) \approx 2.7\ \mu\mathrm{m}$
  - Much larger than the distance between atoms, 3.5 nm and typical gas molecule diameters, 140-600 pm.

Drift velocity in electric fields

- Imagine that an electron stops every time it collides with a gas molecule and then continues along *E*.

- To cover a distance λ_e, it will need a time *t*:

$$\frac{1}{2}\frac{qE}{m_e}t^2=\lambda_e, \quad i.e. \quad t=\sqrt{\frac{2\lambda_e m_e}{qE}}, \quad i.e. \quad \bar{v}=\frac{\lambda_e}{t}=\sqrt{\frac{\lambda_e qE}{2m_e}}$$

- For example:

$$\bar{v}\approx 13\,\mathrm{cm}/\mu\mathrm{s} \quad \text{for } E=1\,\mathrm{kV/cm}$$

Drift velocity in argon

- Compare with a Magboltz c
  - *E* dependence is OK;

BUT

  - the velocity is *vastly* overes

$\bar{v} = 13\,\mathrm{cm}/\mu\mathrm{s}$

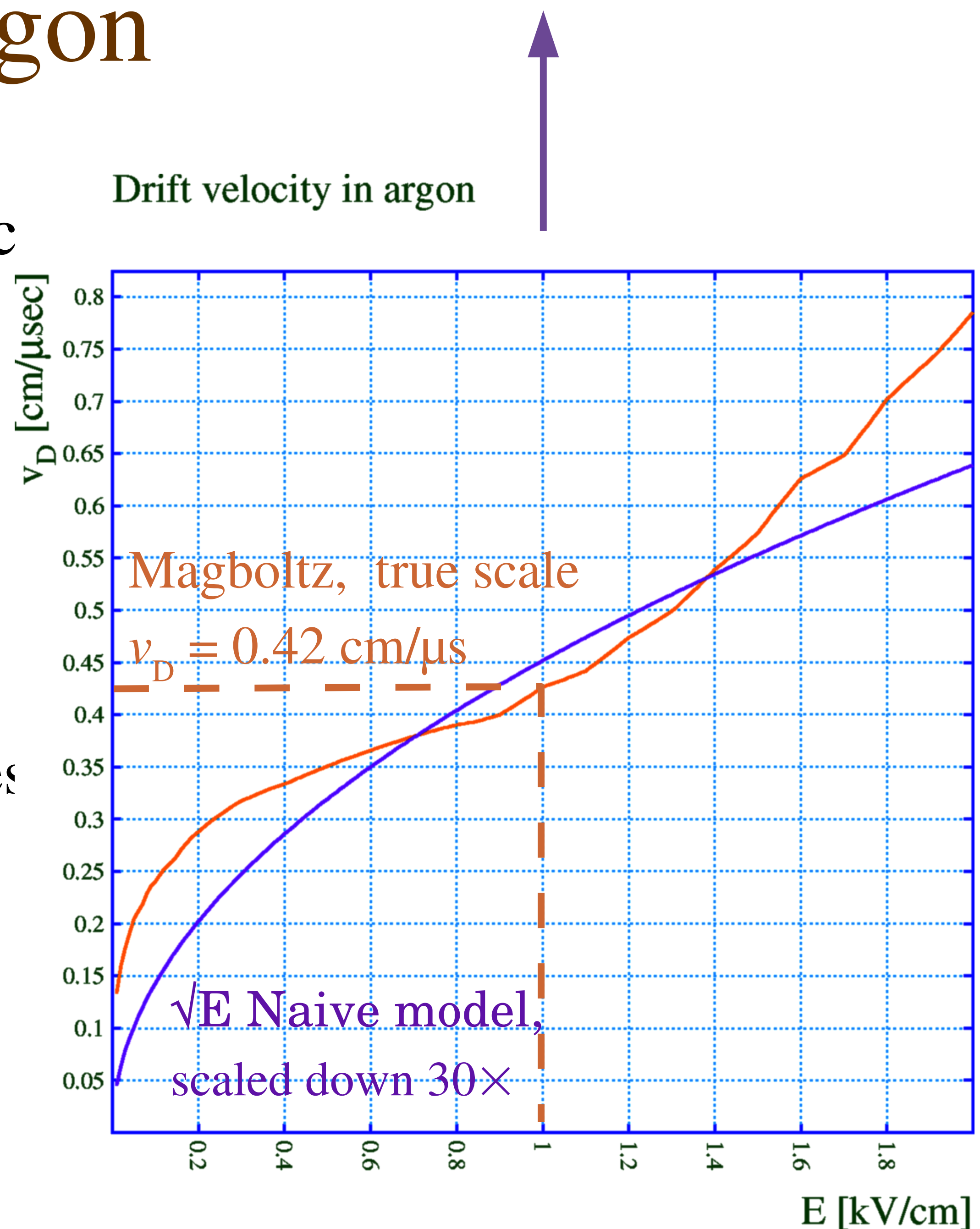

Adding CO_2

- CO_2 makes the gas faster, dramatically.

- Calculated by Magboltz for Ar/CO_2 at 3 bar.

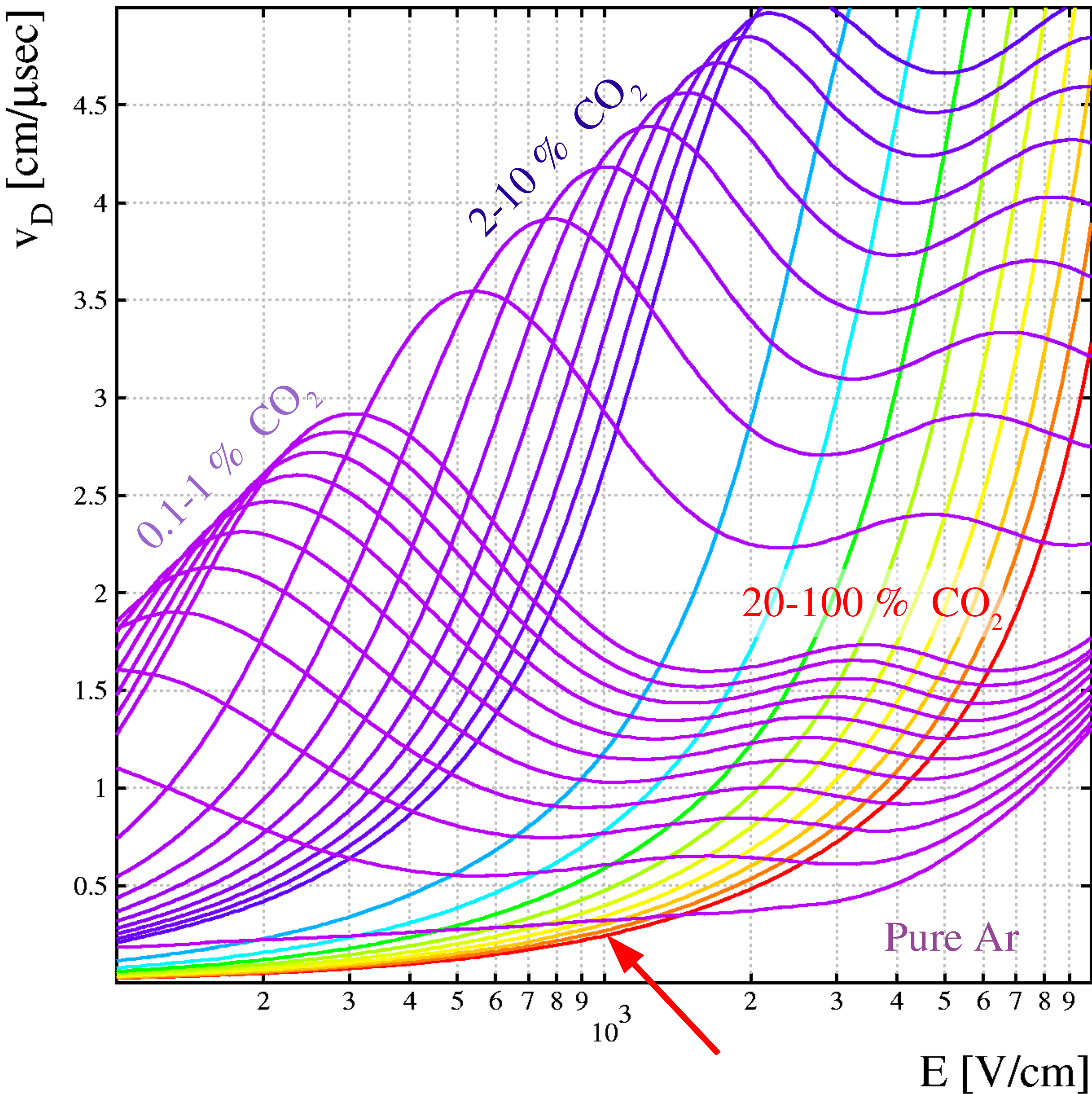

Electrons in Ar/CO_2 at E=1 kV/cm

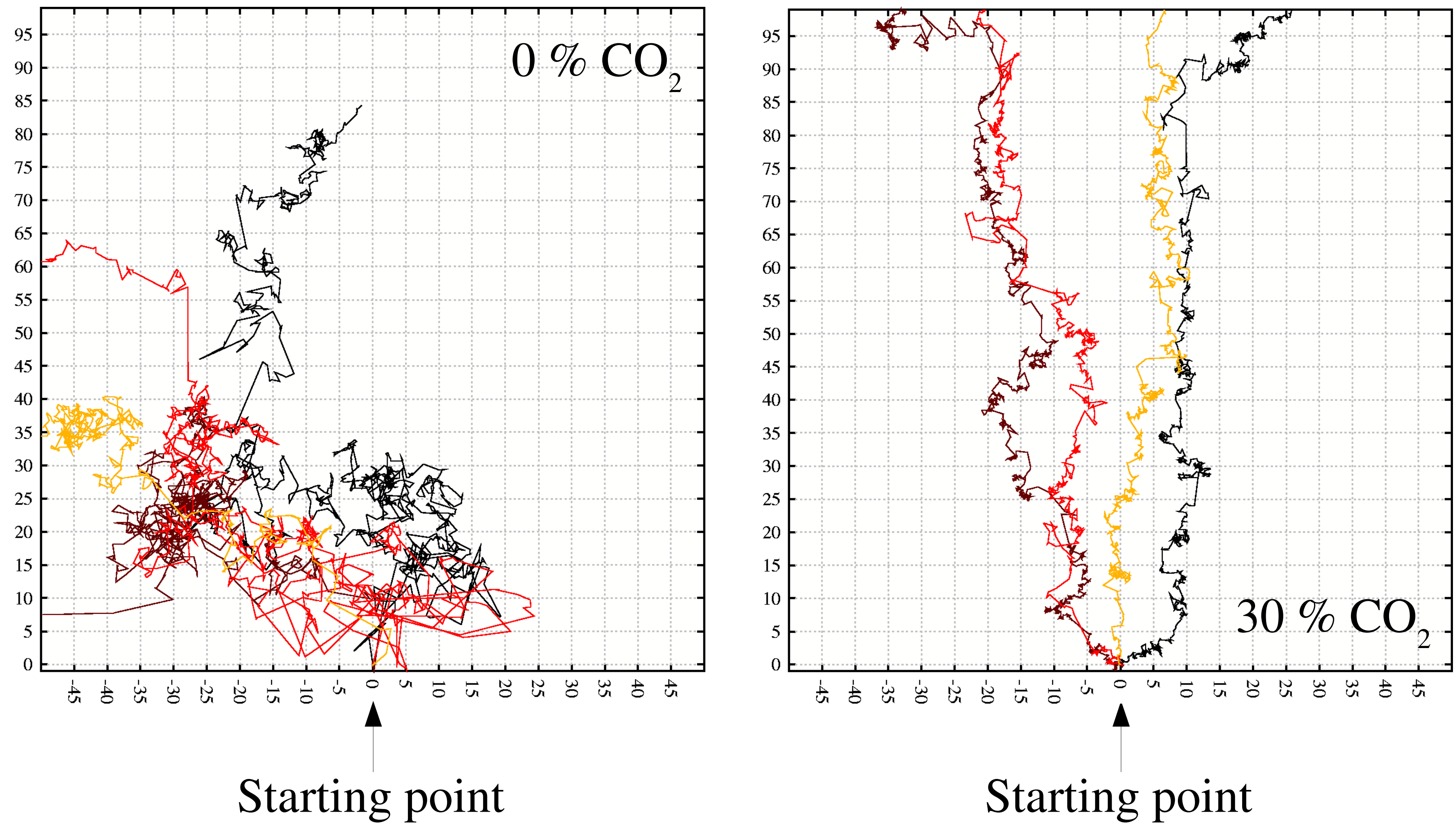

Drift velocity vs Mean velocity

- Drift velocity: distance effectively travelled divided by time needed.

- Imagine they take equal time:

$$v_D = \bar{v}$$

$$v_D \ll \bar{v}$$

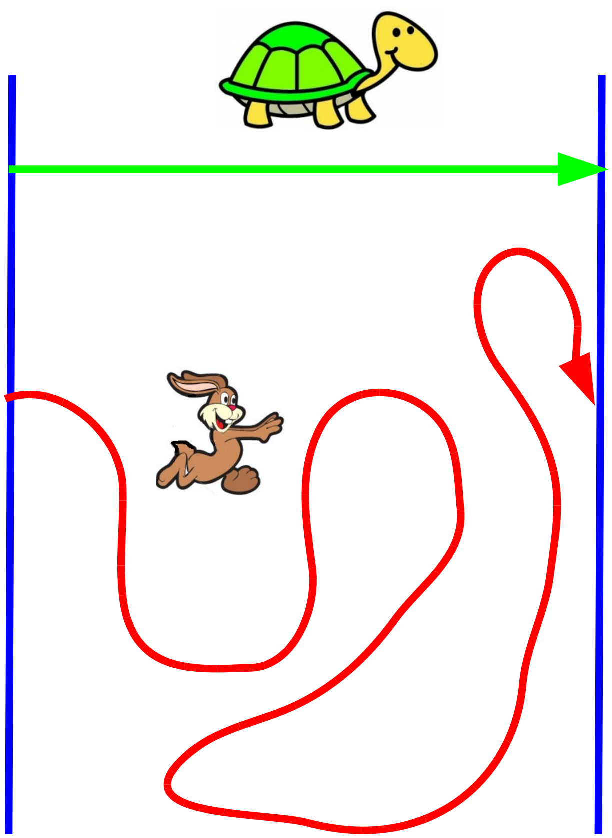

Adding CO_2

- Transverse diffusion is much reduced by CO_2.

- Calculated by Magboltz for Ar/CO_2 at 3 bar.

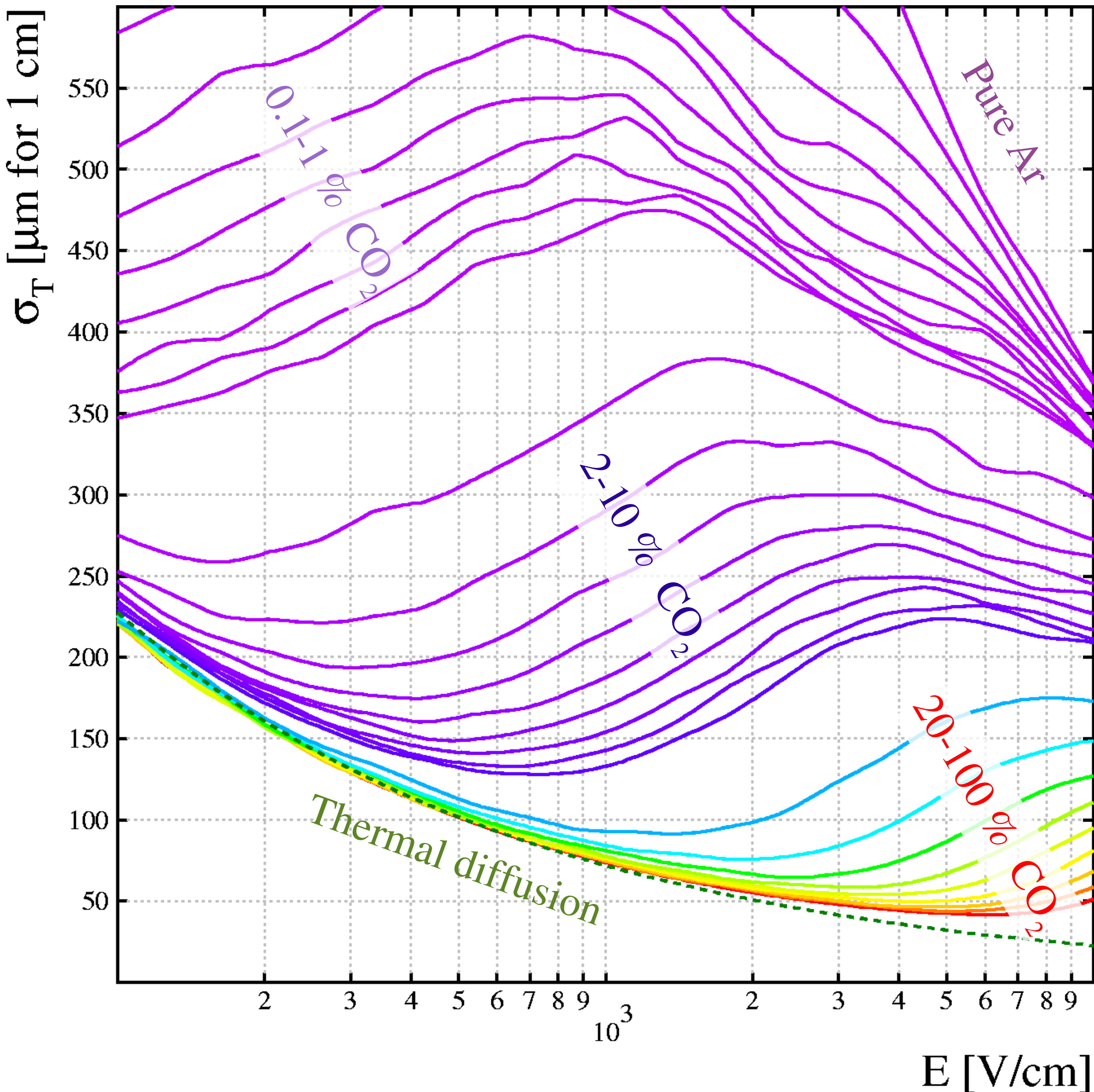

Transport - scale $\gg$ mean free path

- For practical purposes, electrons from a given starting point reach the same electrode – but with a spread in time and gain.

- Electrons transport is treated by:
  - integrating the equation of motion, using the Runge-Kutta-Fehlberg method, to obtain the path;
  - integrating the diffusion and Townsend coefficients to obtain spread and gain.

- This approach is adequate for TPCs, drift tubes etc.

First comparison of IBF between real and simulations

- Simulation (Penning factor) is tuned to reproduce the gain.
- However, IBF in simulation doesn't agree with the measurements.
- Strong dependence on V_{GEM} in the measurements

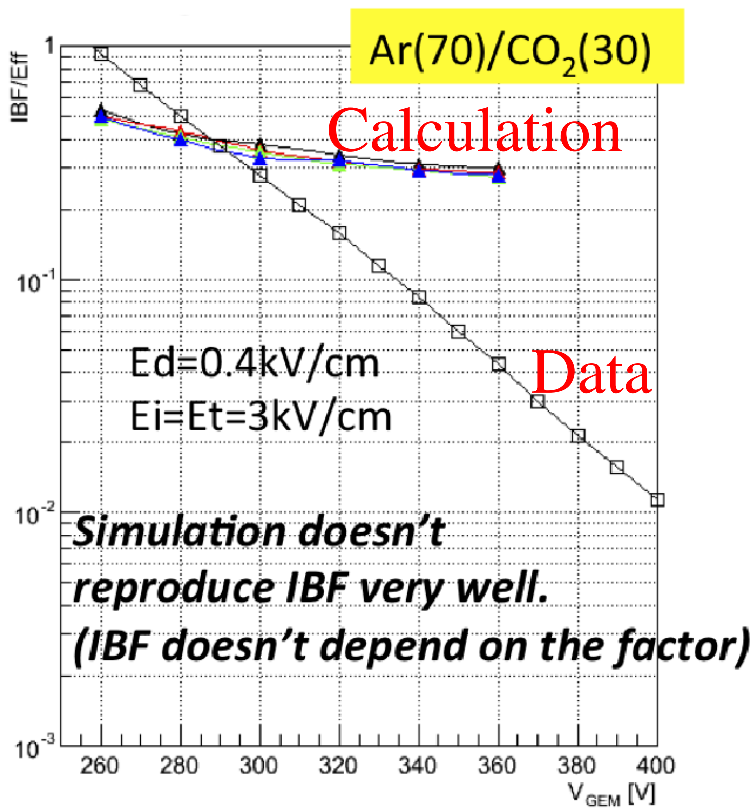

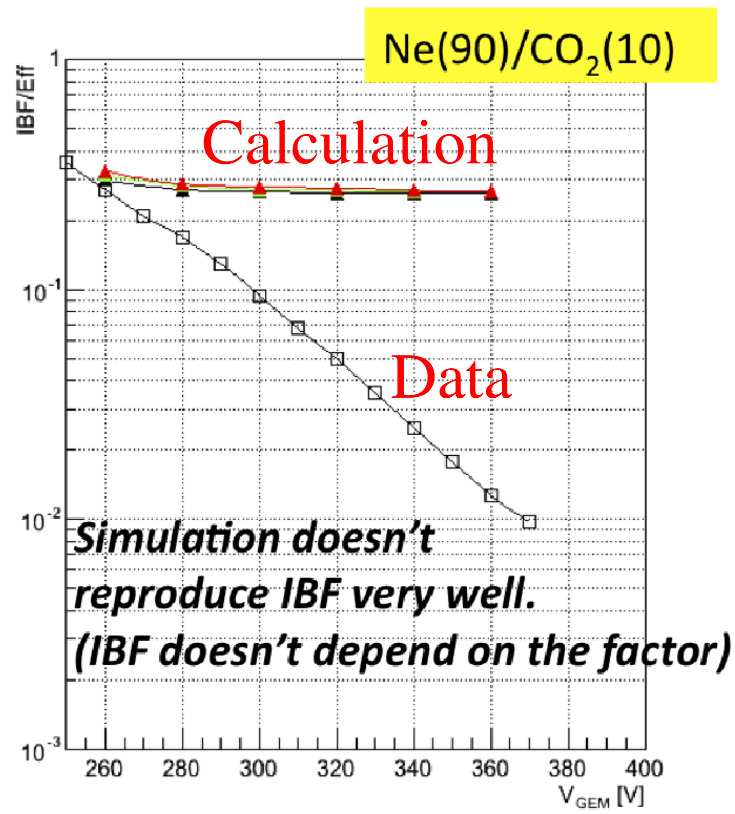

More results from the measurements

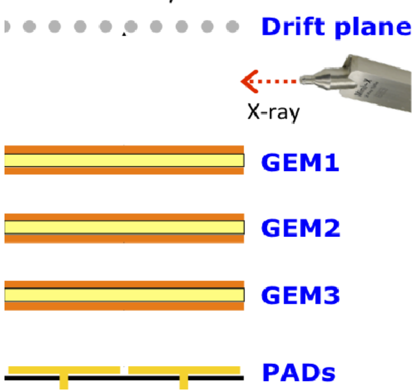

- Rate, Energy (target), drift-space (3 mm or 80 mm) dependence
- Clear rate and drift-space dependence of IBF.
- Indicating space-charge effect ($\propto$ rate$\times$gain$\times$seed) to IBF...

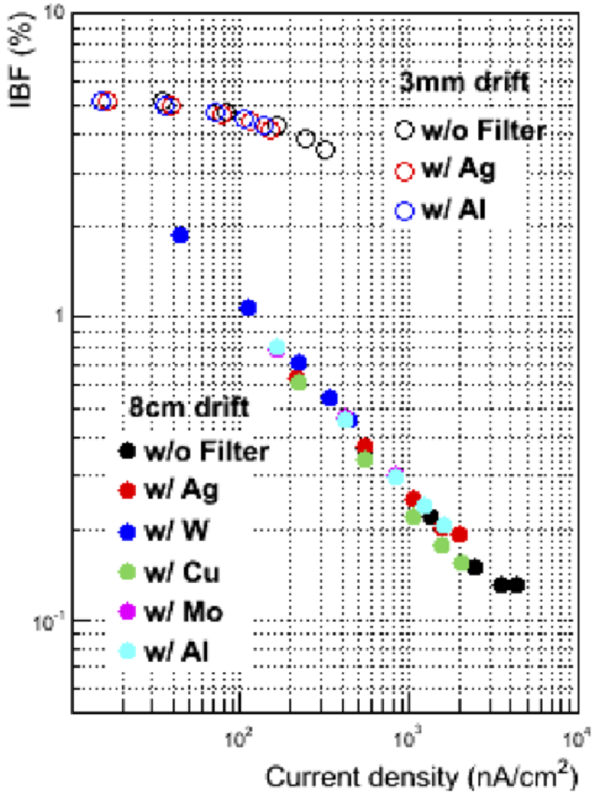

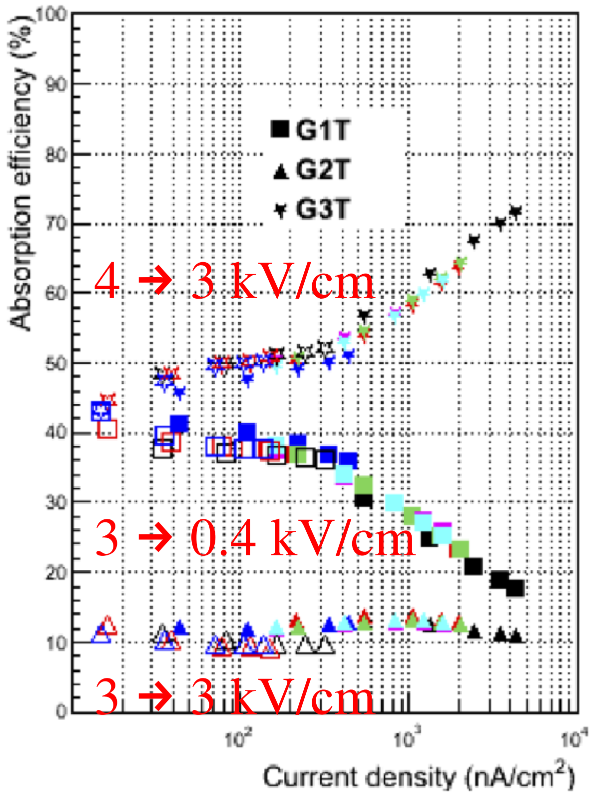

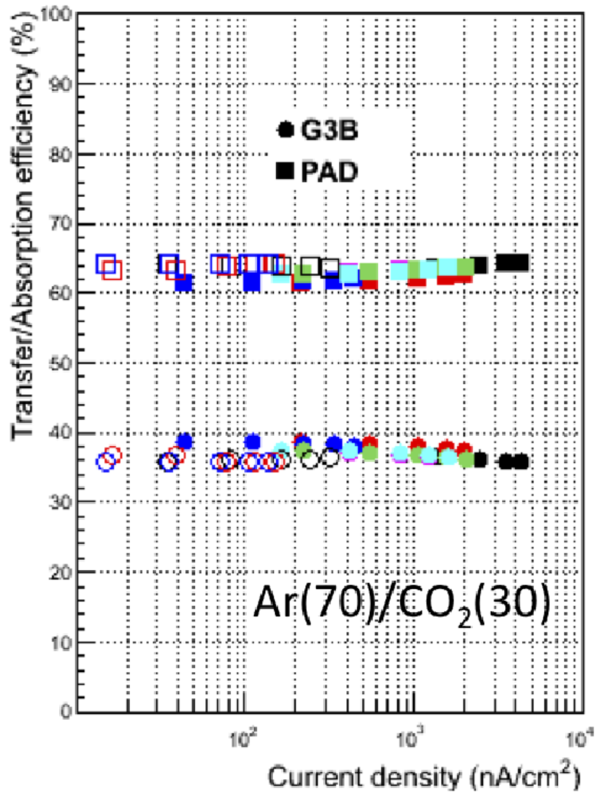

Space-charge above a single GEM

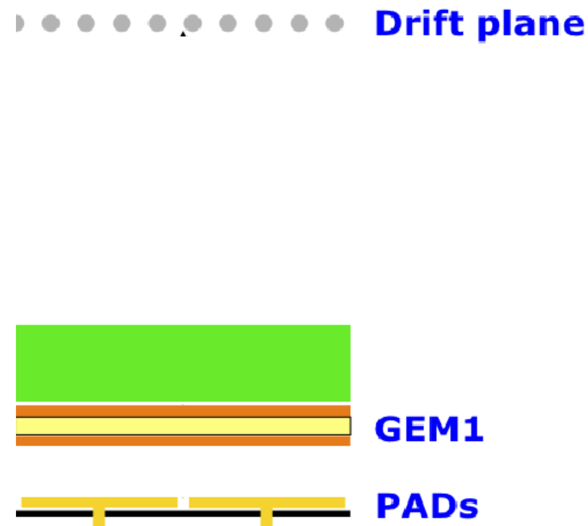

- Ions at $z \in [0,\ 100\ \mu m]$ above the GEM; $E_{dr} = 400$ V/cm; Ar/CO_2 70/30;
- Gain: Does not depend on the ion density;
- IBF: Onset of decrease at ~10^4 ions/hole,

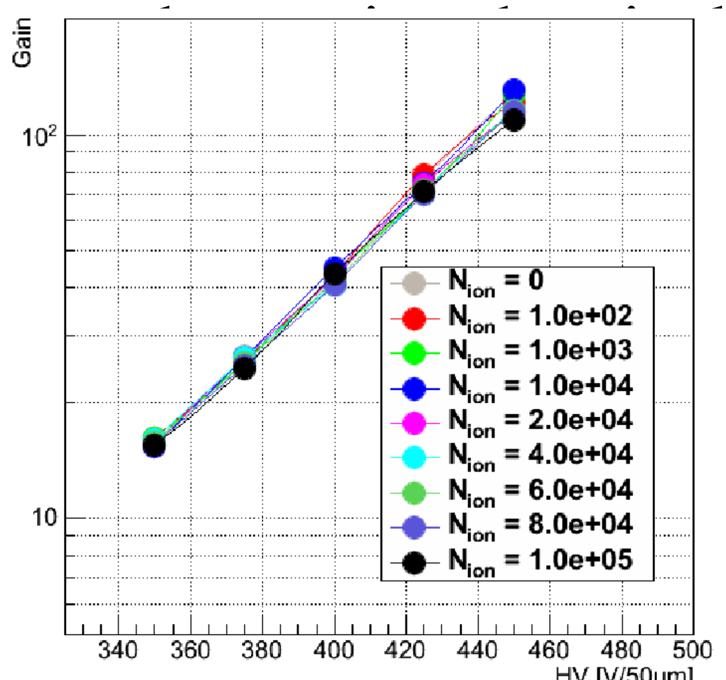

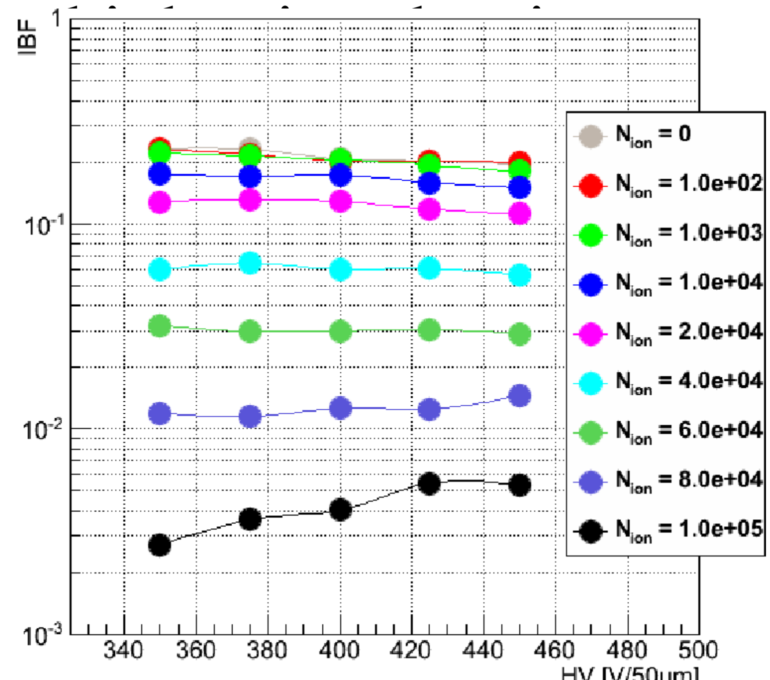

Note: N_{ions} is expressed in ions / ½ hole

Hole Alignment

- IBF with 3 GEMs. Ne/CO_2=(90/10).
- IBF vs. hole distance between GEM1 and GEM2.
- Strong alignment dependence (×10) for E_{T1} ≥2-4 kV/cm.
- No alignment dependence for E_{T1} ∼1 kV/cm. But IBF is worse.

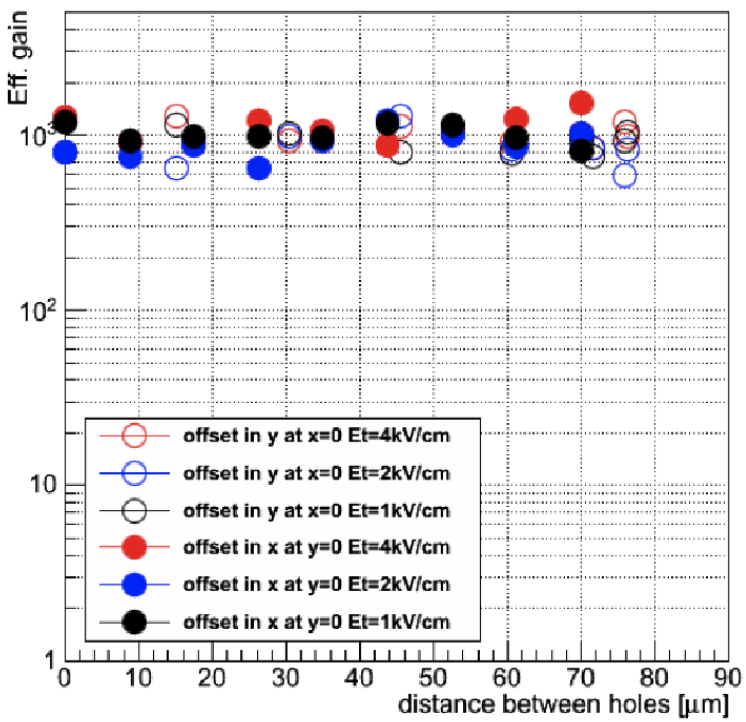

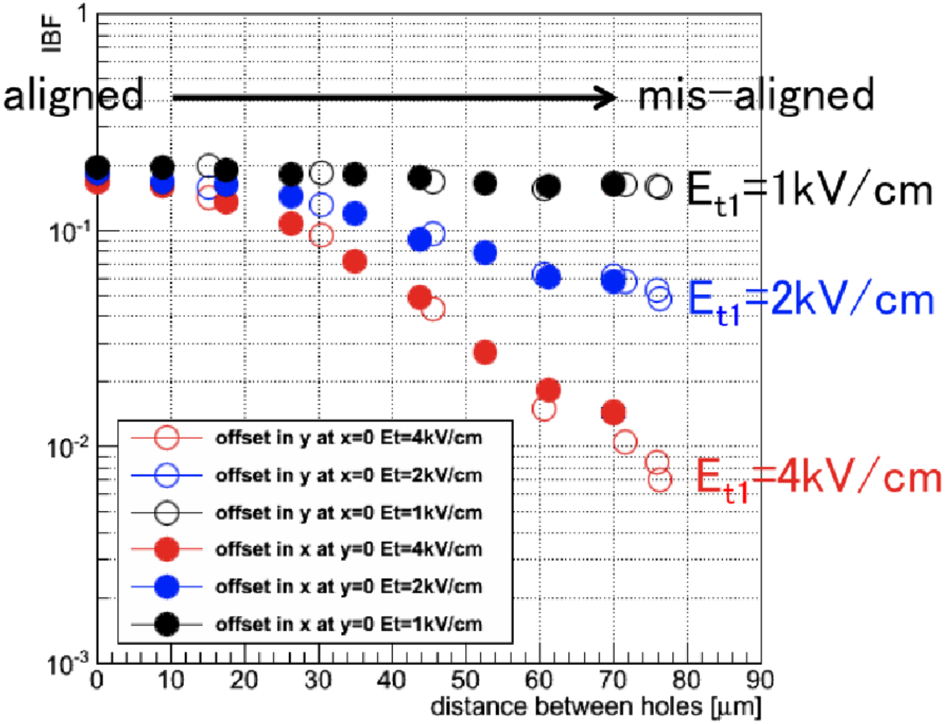

The mediæval solution ... arrow slits !

Absorbing photo- & Auger-electrons

- Both typically have enough energy to ionise:
  - $E_{\text{pe}} = E_\gamma - E_{\text{shell}}$,
  - $E_{\text{Auger}} = E_{\text{knock-out}} - E_{\text{filling}} - E_{\text{emitted}}$

- The energy is dissipated by scattering, excitation and ionisation of the outer shells, producing electrons serving for detection → transport. This consumes ~20-30 eV per electron produced – much more than the ionisation energy.

- In the process, δ-electrons are scattered extensively, leaving an erratic trace of ionisation electrons.

Geiger counter

- Detects radiation by discharge
- Can count α and β particles (at low rates ...)
- No tracking capability

- Around 1928: Hans Geiger and Walther Müller

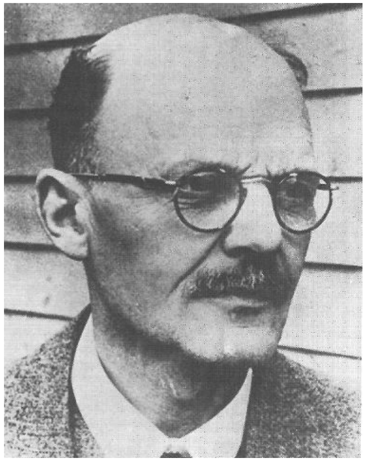

Hans Geiger
(1882-1945)

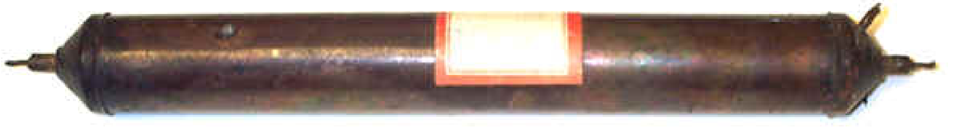

A Geiger-Muller counter built in 1939 and used in the 1947-1950 for cosmic ray studies in balloons and on board B29 aircraft by Robert Millikan et al.

Made of copper, 30 cm long

Muon mass estimate

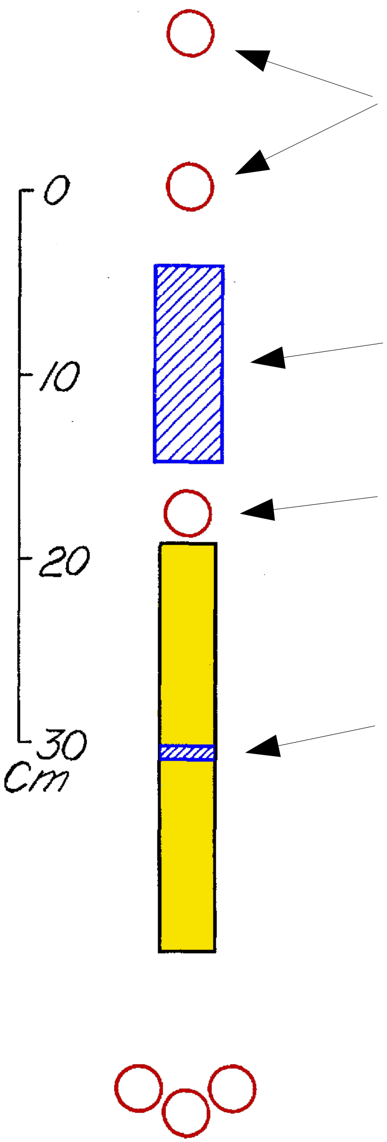

Trigger counters

Lead absorber

Trigger counter

Cloud chamber,
lead filter in the middle,
0.35 T magnetic field

Veto counter

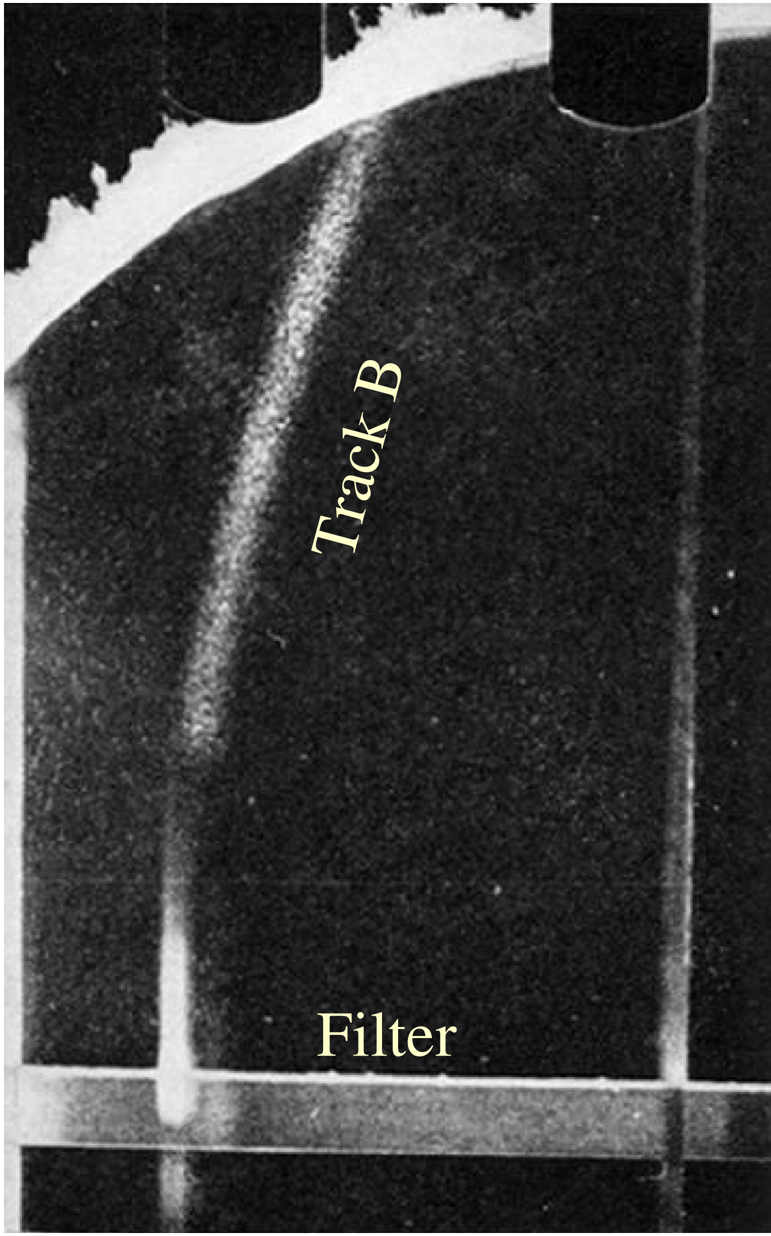

[J. C. Street and E. C. Stevenson, Phys. Rev 52 (1937) 1003]

Findings $\mu^{\pm}$ experiment 1937

- Curvature of "track B" is consistent with a charged, negative particle.

- Ionisation density 6 × density of "usual thin tracks", *i.e.* high energy charged particles.

- Assuming ionisation $\propto 1/v^2$, and using the curvature, the estimated mass was $130 \pm 33\ m_e$ or 66 ± 17 MeV (*cf.* PDG 2012 value: 105.6583715 ± 0.0000035 MeV).

Spark chambers

- Popular in the 1960s and 1970s
- Parallel plates between which a spark develops when an ionising particles passes
- Read out optically or acoustically (!)

- Precursor in a way to the RPC

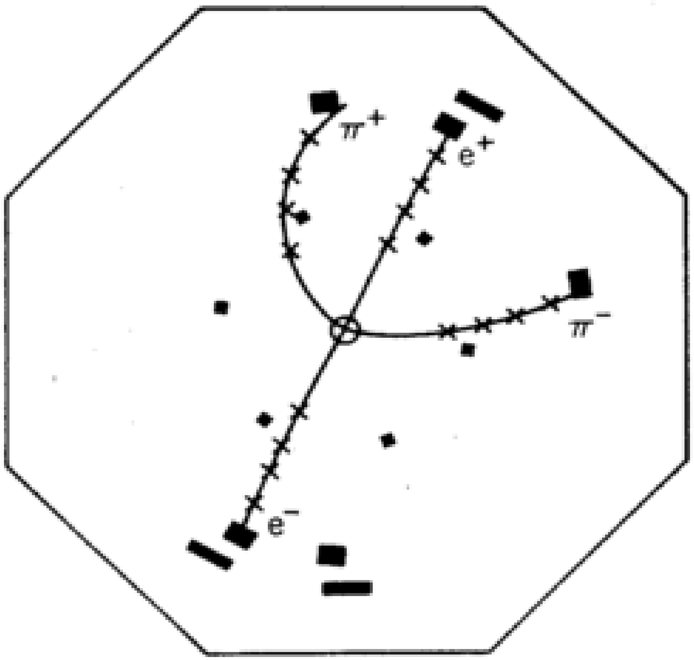

A J/ψ event from SPEAR (1974)

Attachment in CO_2

Thin-wire approximation ?

- The thin-wire approximation is usual in wire chambers – but is not adequate here.

Field calculations: neBEM.

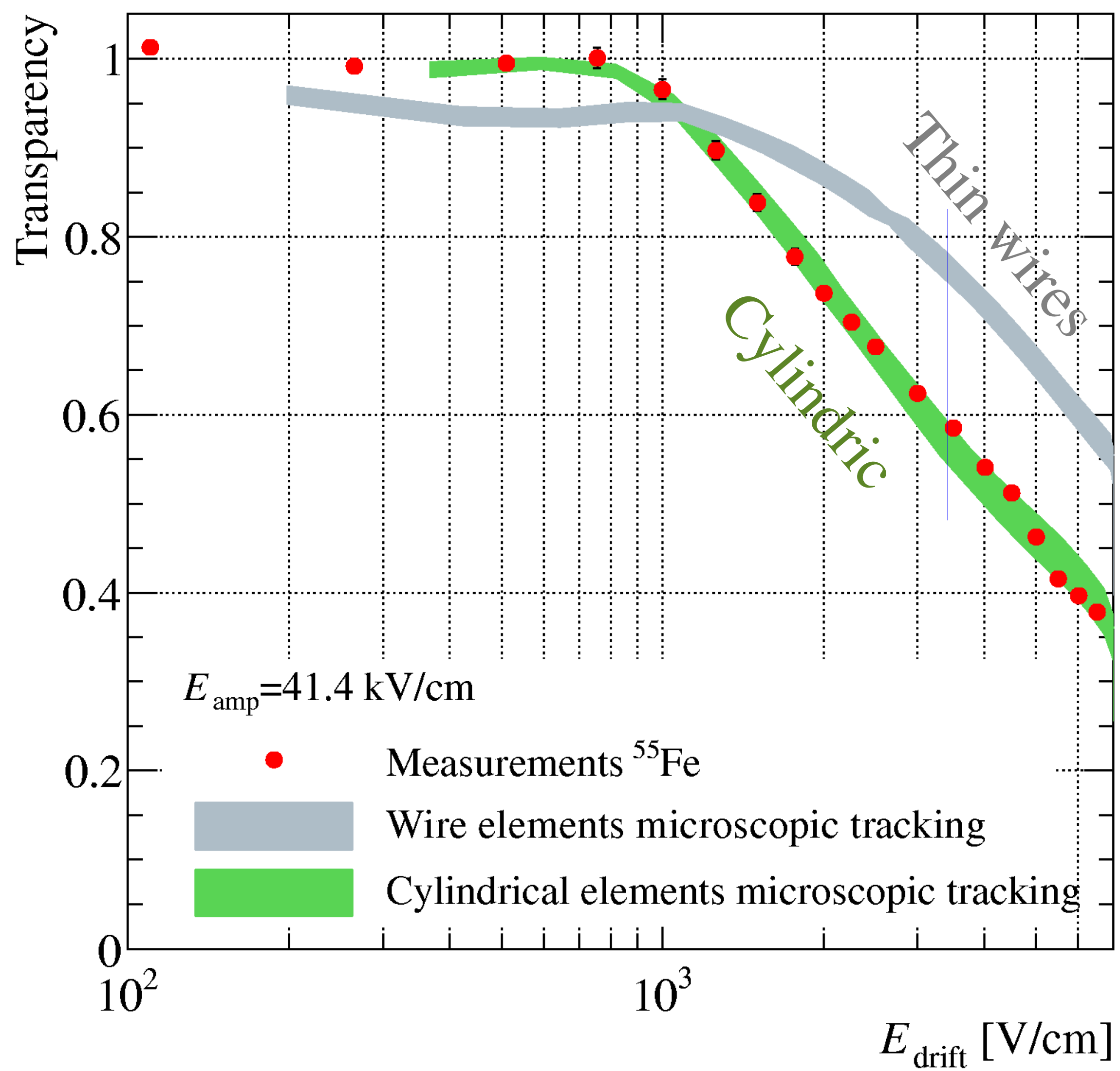

Surface charge

- GEMs violate the 1st law of gas-based detectors: active gas must not be in contact with an insulator.
- Electrons and ions will therefore land on the insulating material.
- Polyimide as used in GEMs is an extraordinarily good insulator: once on the surface, charge stays there.

GEMs with surface charge

- The polyimide surface area inside the holes is sliced.
- Start: uncharged GEM;
- iterate:
  - simulate avalanches;
  - histogram electron and ion deposition patterns;
  - add surface charges and recalculate the field;
- convergence when electron and ion deposits balance.

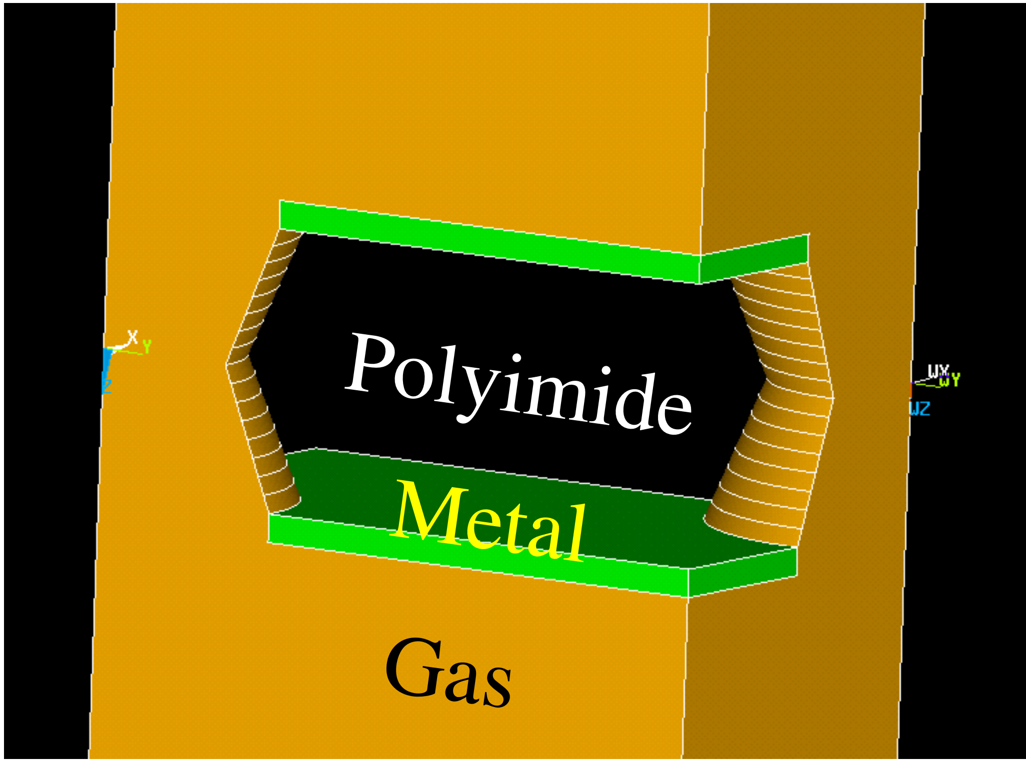

Conclusions

- Microscopic simulations, although time consuming, are capable of reproducing e.g. the transparency of Micromegas meshes.

- GEMs have insulating material in contact with active gas. As a result, the insulator collects charge and the surface charges modify the detector behaviour.

- Evacuation of ions from multiple GEMs is sufficiently slow for space charge effects to become noticeable at high rates. This modifies the ion back-flow rate.

Ion back flow and space charge

- Alice plans using a triple GEM for TPC read-out with:
  - ion back flow < 0.5 % (< 0.25 % in some sources)
  - effective gain 2000

- https://cdsweb.cern.ch/record/1475243/files/LHCC-I-022.pdf

Gas-based detectors

- Tracking + identification devices for charged particles, that rely on the ionisation of gas molecules and the currents due to the movement of electrons and ions.

- Common features:
  - gas
  - high electric fields
  - electric signals due to electron and ion motion

- Simplest way to generate high fields: wires. However, the present-day detectors use more intricate electrodes.

Micromegas

- Fast, rate tolerant tracking device
- 1994: Yannis Giomataris and Georges Charpak

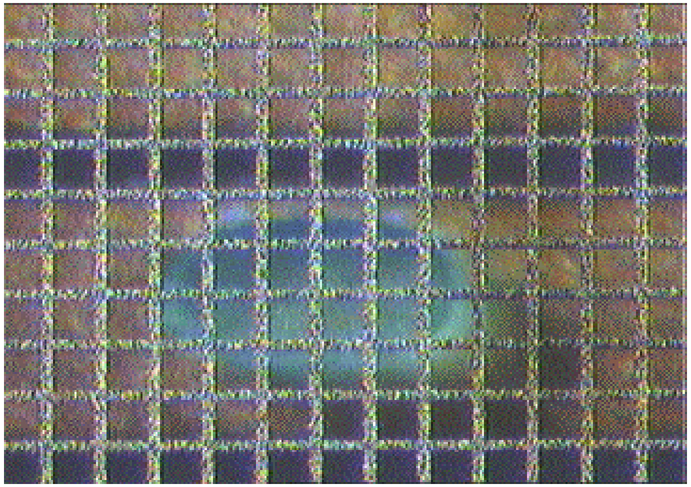

A mesh – holes of 30 μm

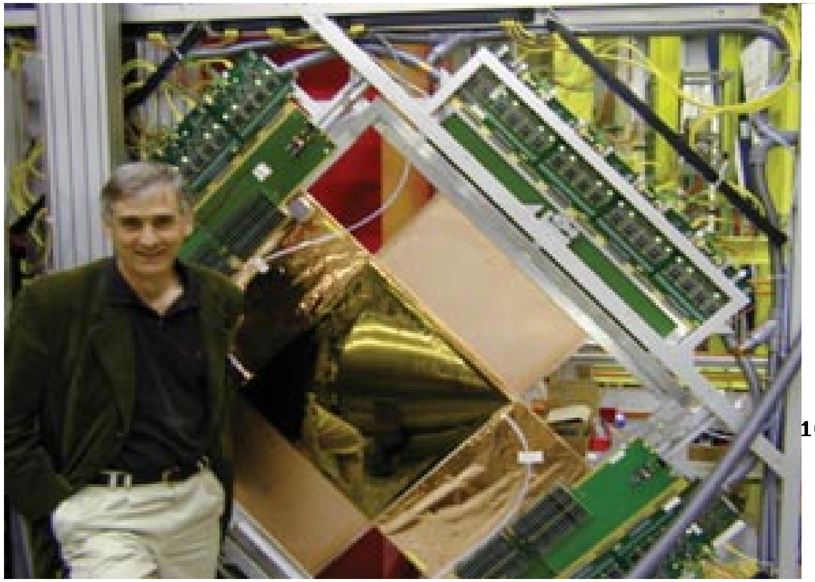

Yannis Giomataris

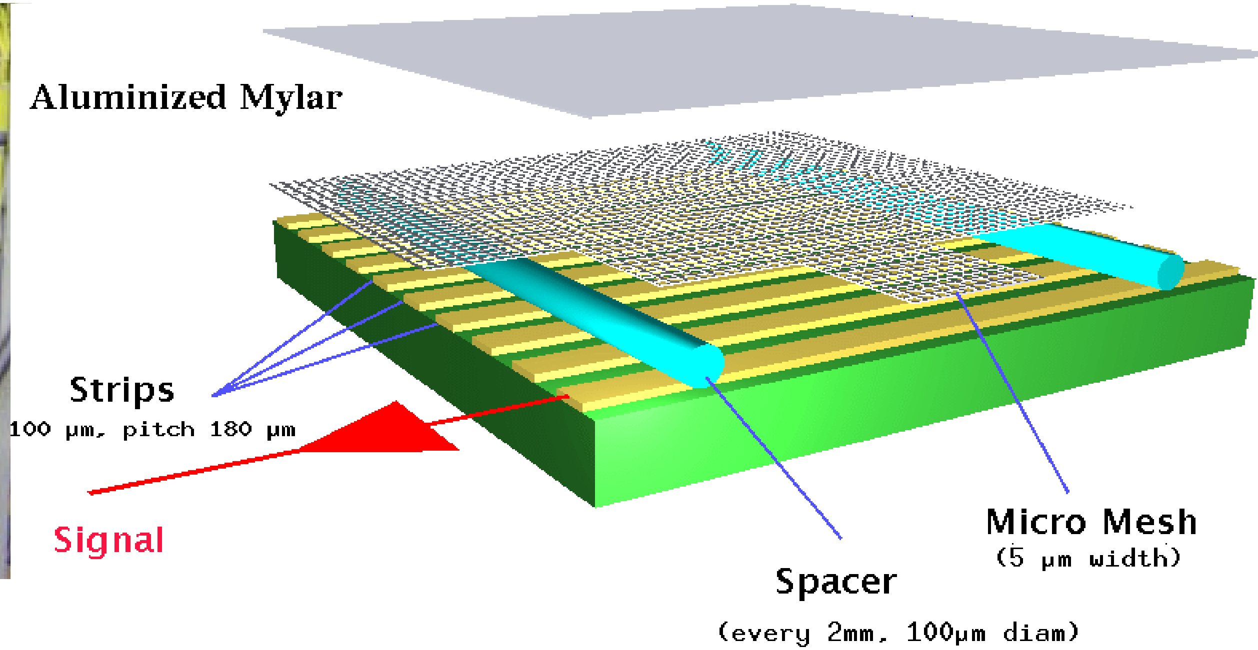

GEMs

- Acts as a “pre-amplifier”
- 1996: Fabio Sauli

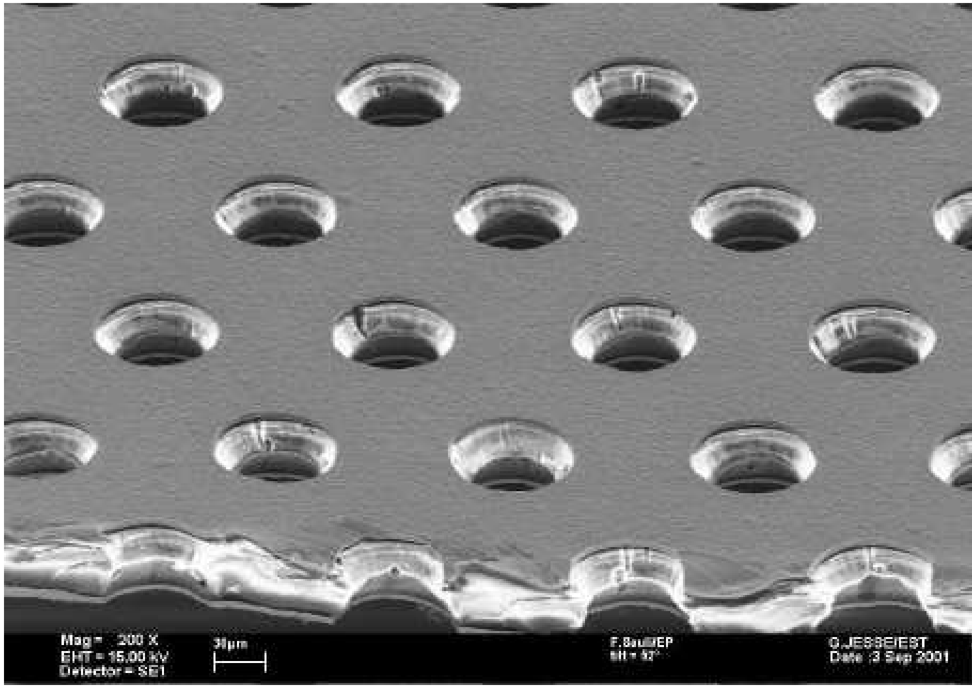

A few electrons enter here

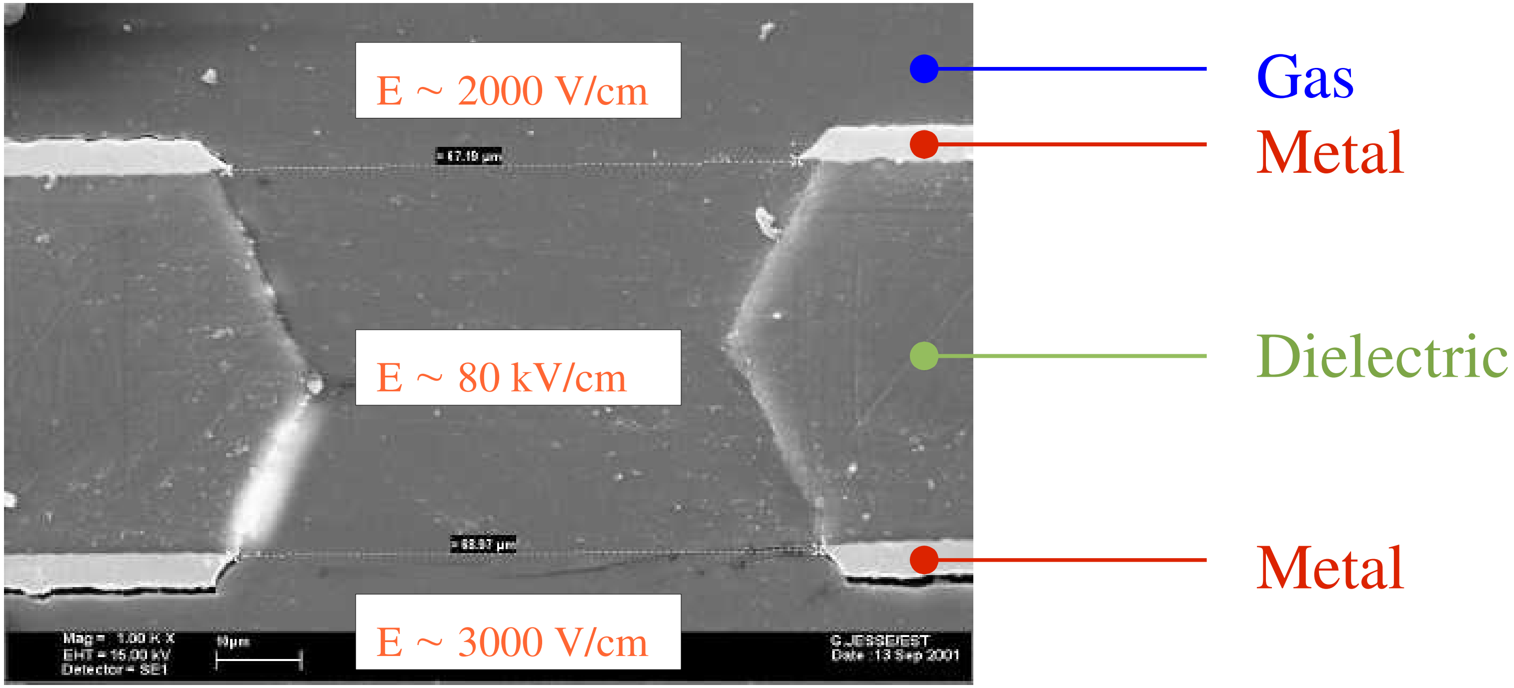

Many electrons exit here

Fabio Sauli

[Four Curies: Pierre, Marie, Irène and Pierre's father, around 1904 at the BIPM]

1896: Ionisation by radiation

- Early in the study of radioactivity, ionisation by radiation was recognised:

" Becquerel discovered in 1896 the special radiating properties of uranium and its compounds. Uranium emits very weak rays which leave an impression on photographic plates. These rays pass through black paper and metals; they make air electrically conductive."

[Pierre Curie, Nobel Lecture, June 6th 1905]

"A sphere of charged uranium, which discharges spontaneously in the air under the influence of its own radiation, retains its charge in an absolute vacuum. The exchanges of electrical charges that take place between charged bodies under the influence of the new rays, are the result of a special conductivity imparted to the surrounding gases, a conductivity that persists for several moments after the radiation has ceased to act."

[Antoine Henri Becquerel, Nobel Lecture, December 11th 1903]

IBF Measurements at CERN

- Systematic measurements at RD51 lab. in CERN.
  - Field dependence (ΔV_{GEM}, T1, T2, Induction)
  - Rate, x-ray position dependence (charge current density)

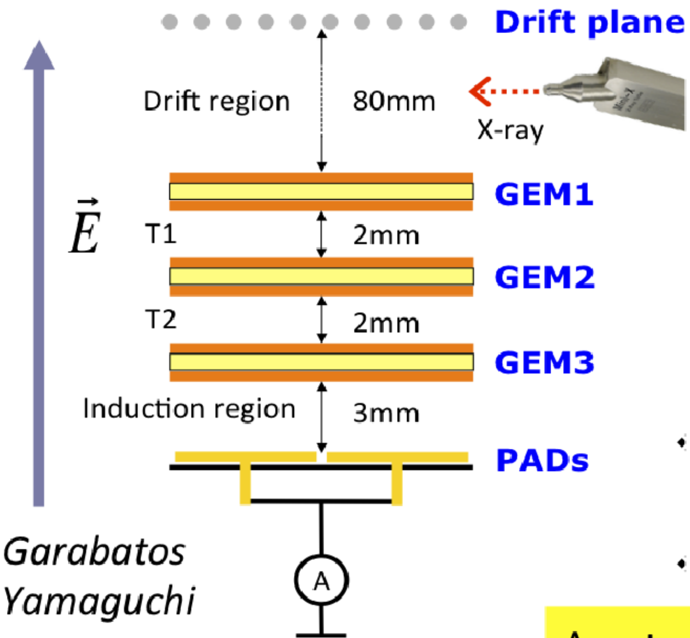

C. Garabatos
Y. Yamaguchi

❖ Currents at readout pads & drift plane are measured.
❖ The current of primary ions is measured with only HV ON for drift plane.
  ✓ Gain = $I_{pad}/I_{prim.ion}$
❖ Always E_{drift} = 400V/cm

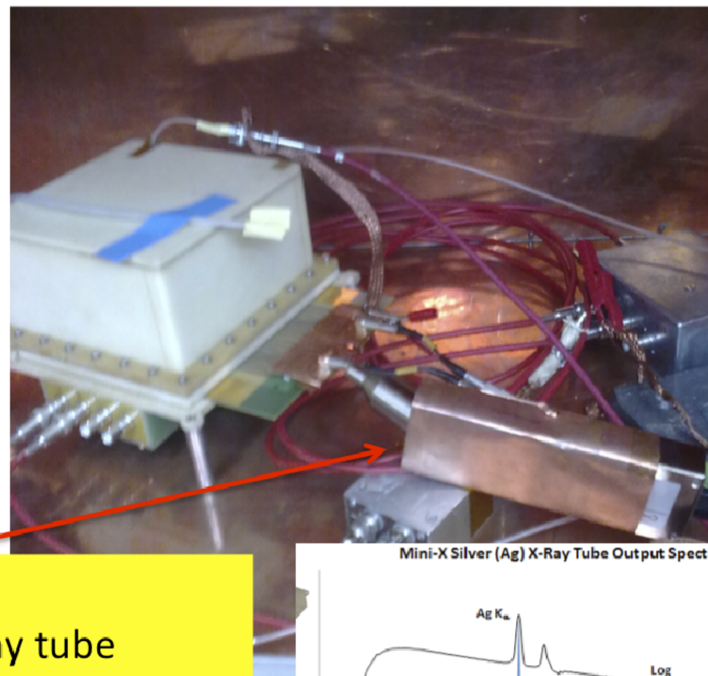

Ampteck
Mini X-ray tube

Ag target: Kα=22KeV
Rate (Ar(70)/CO2(30)) = 5e7 estimated by I_d

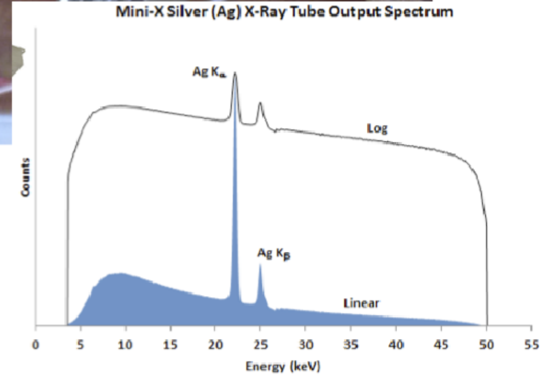

[Slide made by Taku Gunji]

Herbert Kliem

Kohlrausch relaxation

- Hopping model (3d, MC) including Coulomb force of neighbouring ions, *mirror charges* and external field.

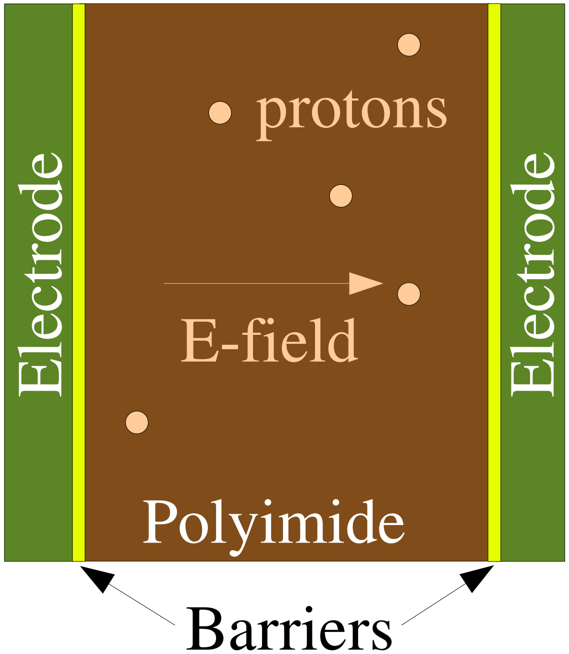

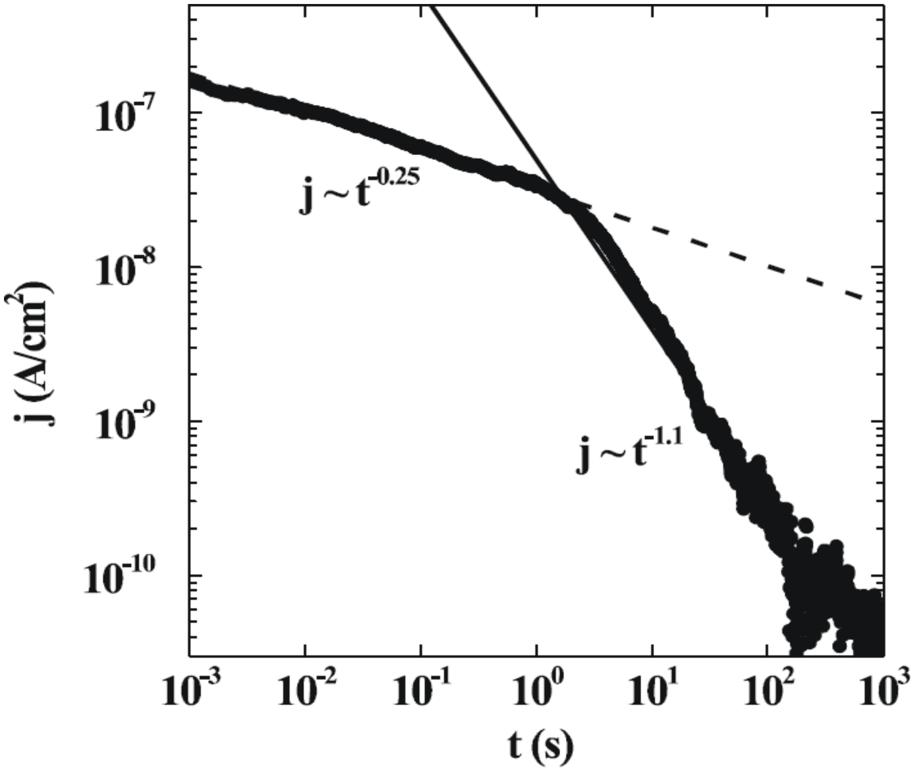

De-excitation

Ralph de Laer Kronig
(1904-1995)

Dirk Coster
(1889-1950)

Lise Meitner
(1878-1968)

Pierre Victor Auger
(1899-1993)

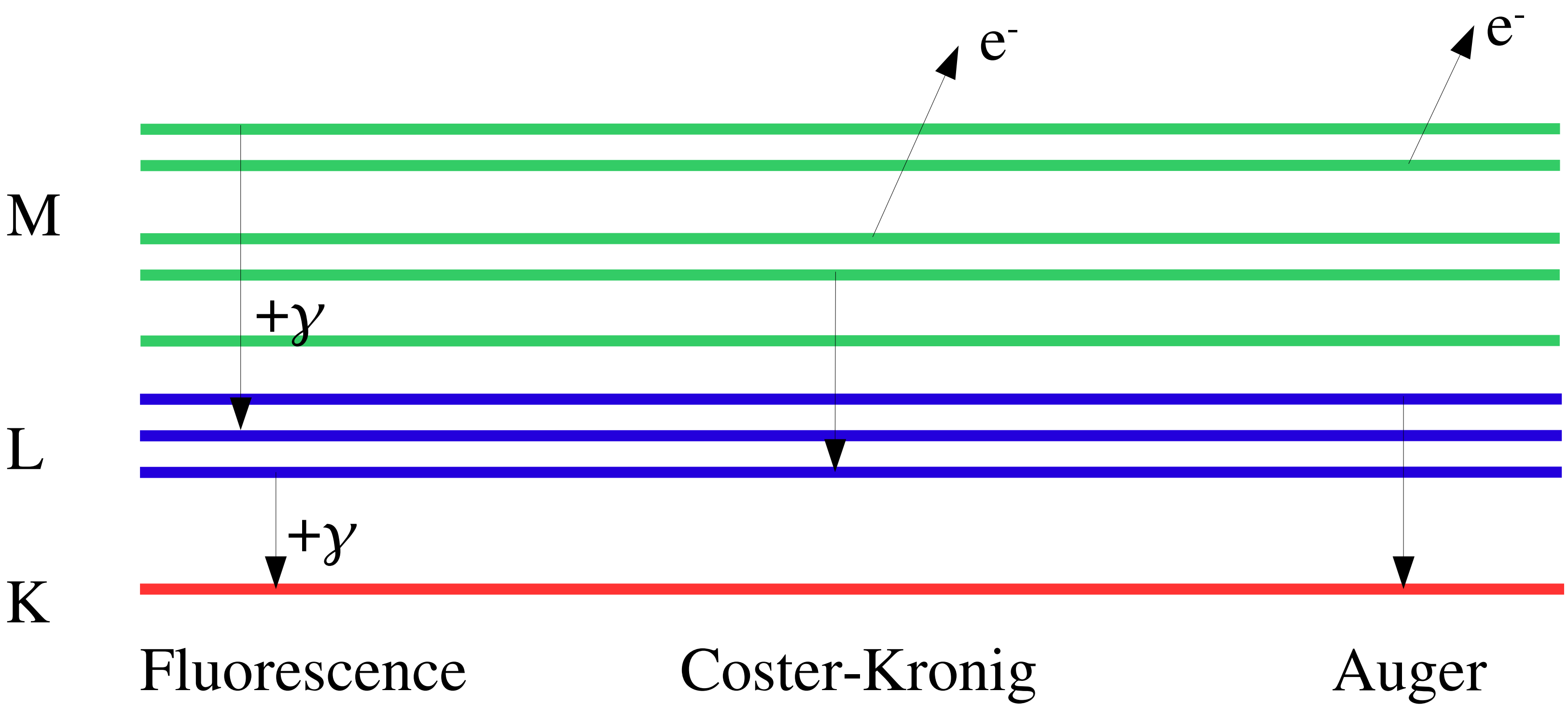

References:

D. Coster and R. de L. Kronig, Physica **2** (1935) 13-24.

Lise Meitner, *Über die β-Strahl-Spektra und ihren Zusammenhang mit der γ-Strahlung*, Z. Phys. **11** (1922) 35-54.

L. Meitner, *Das β-Strahlenspektrum von UX_1 und seine Deutung*, Z. Phys. **17** (1923) 54-66.

P. Auger, J. Phys. Radium **6** (1925) 205.

Which shells matter ?

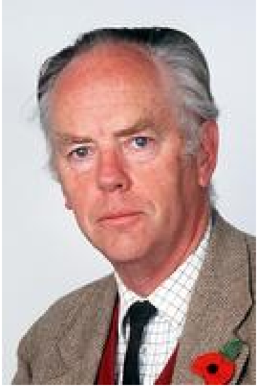

Wade Allison

John Cobb

- All electron orbitals (shells) participate:
  - outer shells: frequent interactions, few electrons;
  - inner shells: few interactions, many electrons.

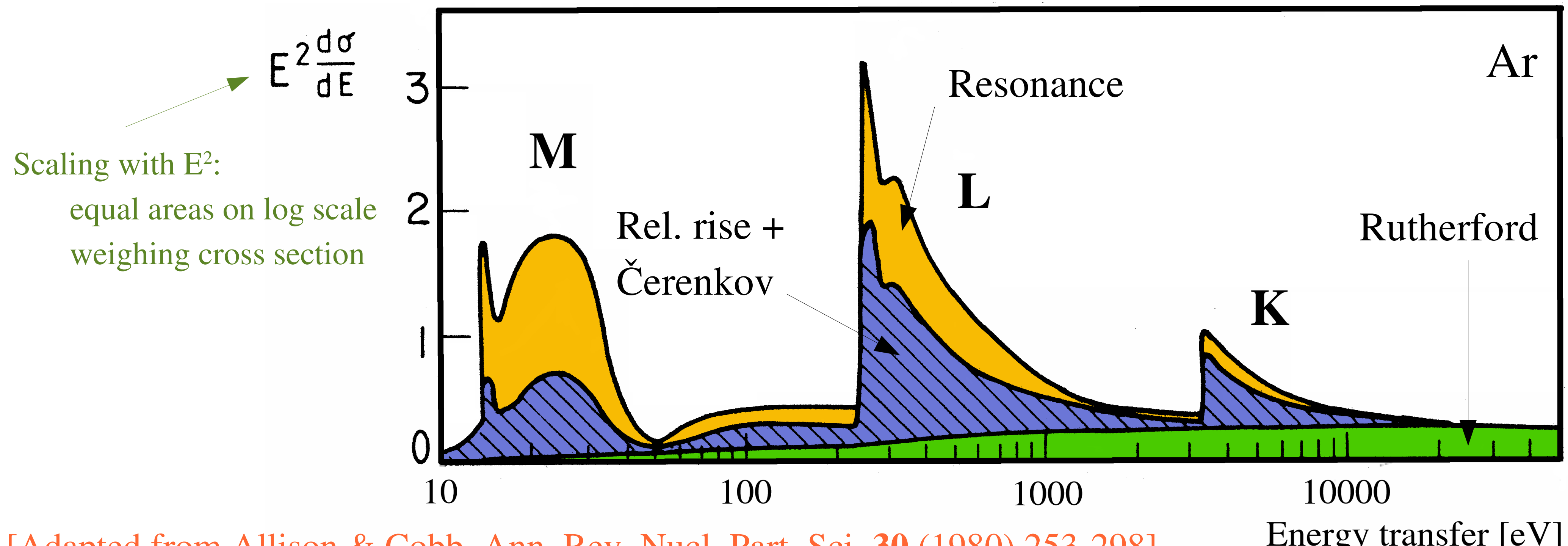

[Adapted from Allison & Cobb, Ann. Rev. Nucl. Part. Sci. **30** (1980) 253-298]

V_{GEM} = 220 V and V_{GEM} = 300 V

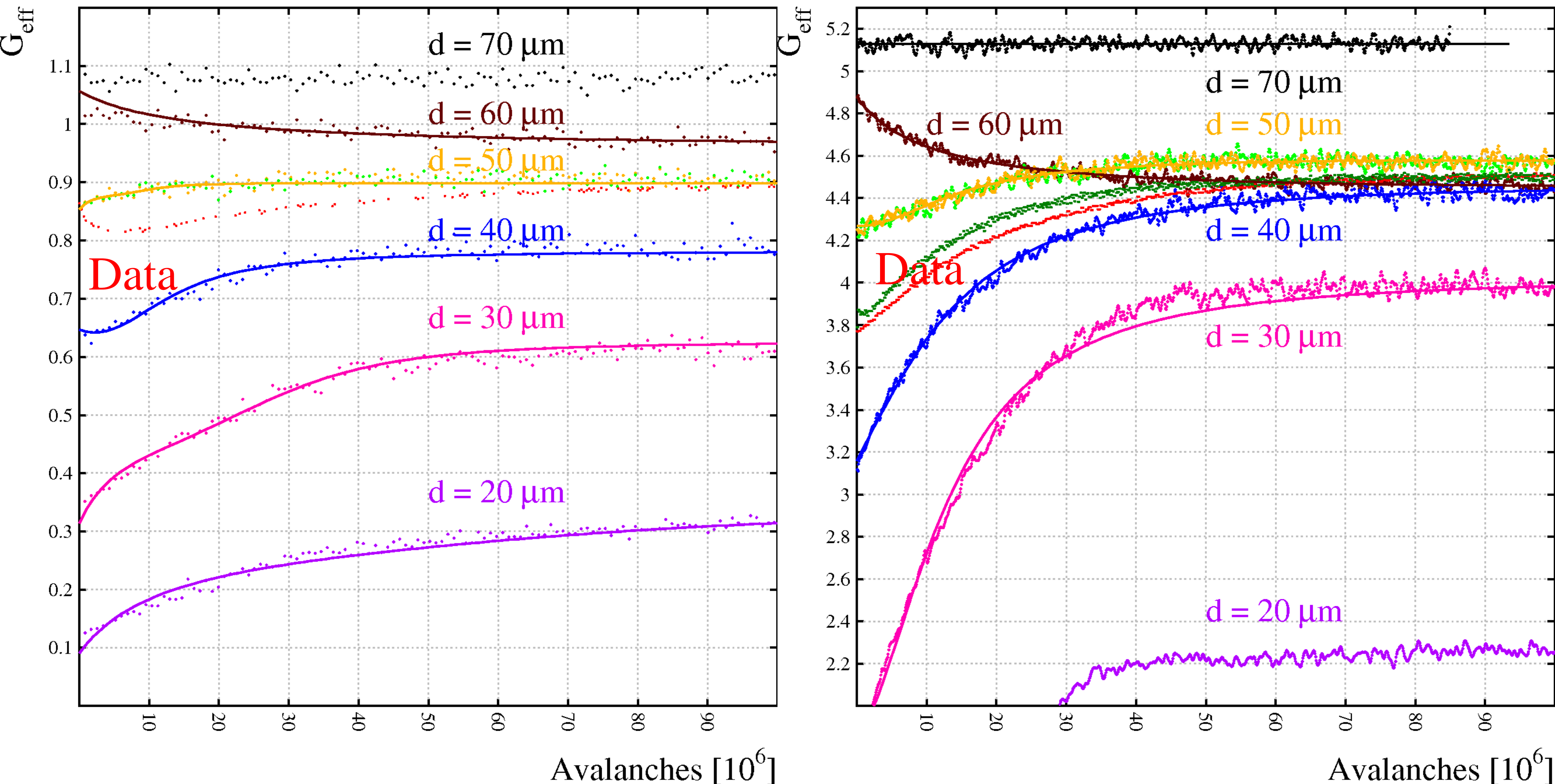

V_{GEM} = 400 V and V_{GEM} = 500 V

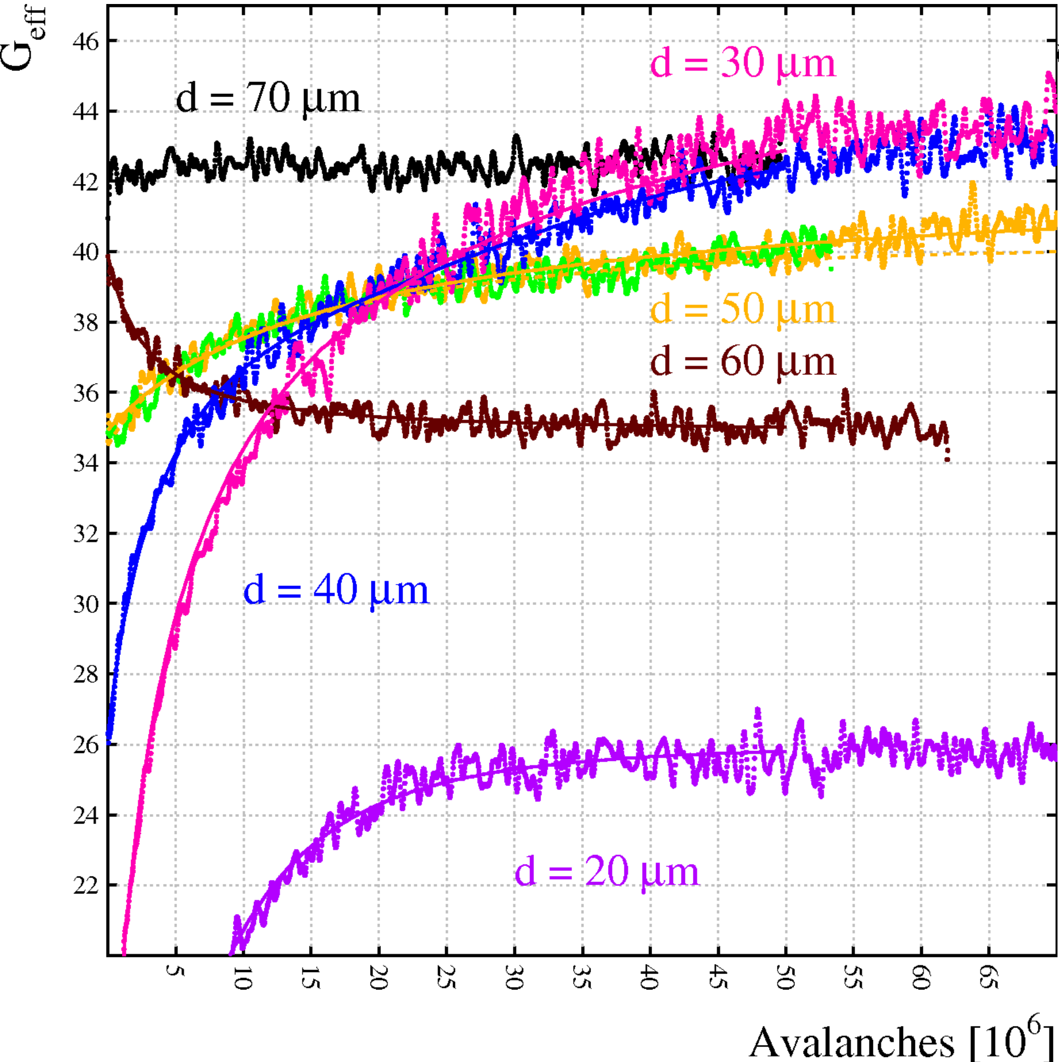

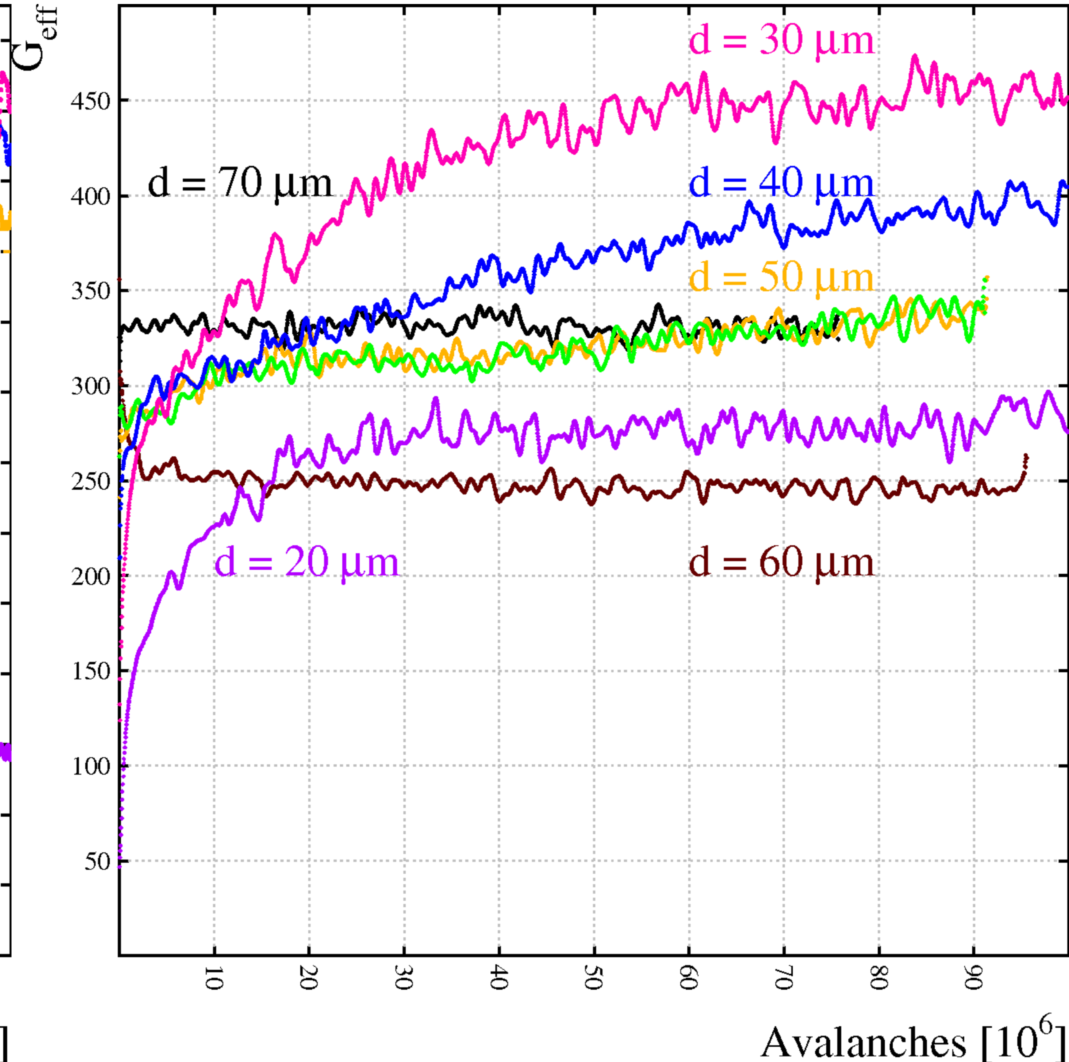

Space-charge simulations: Method

- Slice the space in drift direction by 100 μm
- Uniformly distribute ions in space $z \in [Z, Z + 100\mu\text{m}]$
- Calculate the field by ANSYS and evaluate gain/IBF by Garfield++
- Example of the field around GEM1 with N_{ions}=0, 10^5, 10^6 with E_{drift}=0.4kV/cm. less IBF with huge N_{ions}?

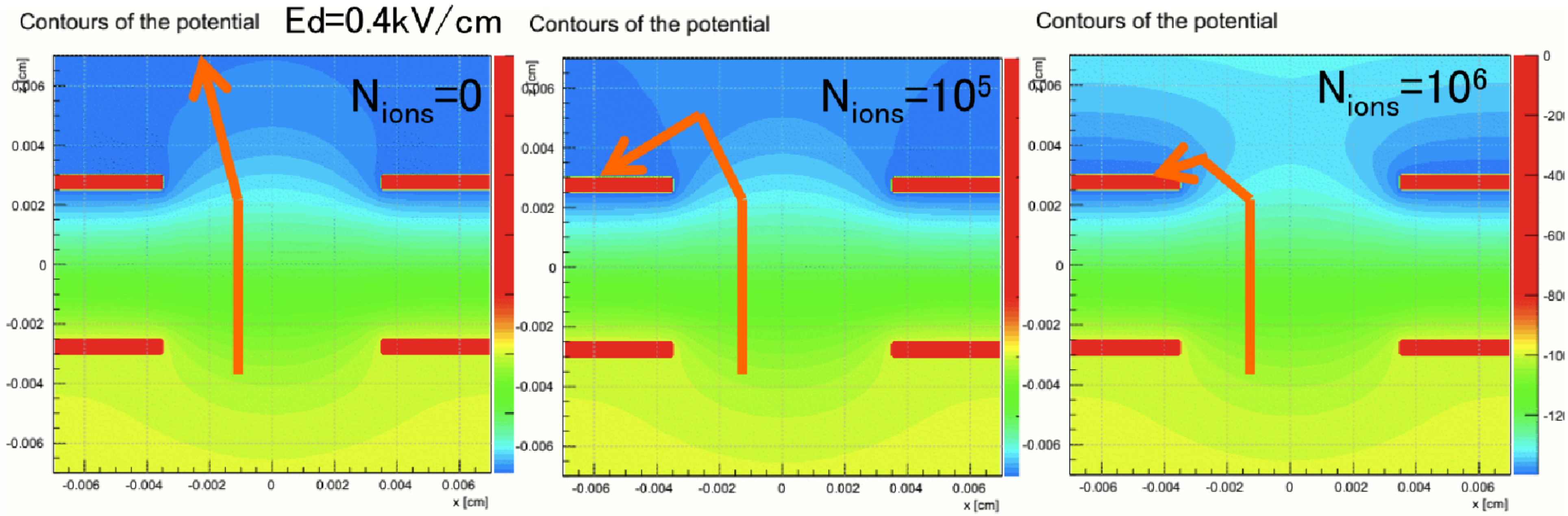

[Slide made by Taku Gunji]

Space-charge above a double GEM

- Ions at $z \in [0, 100\ \mu m]$ above GEM2;
- Gain changes by a factor 2: smaller electron collection losses at GEM1 ?
- IBF decreases from ~5 10^4 ions/½ hole, depending on underlying field.

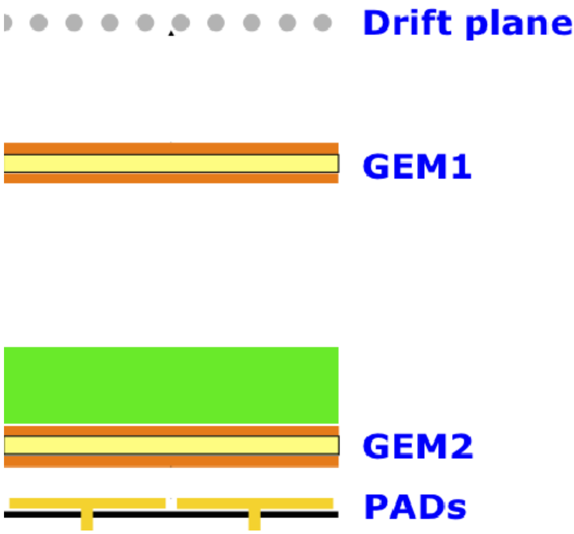

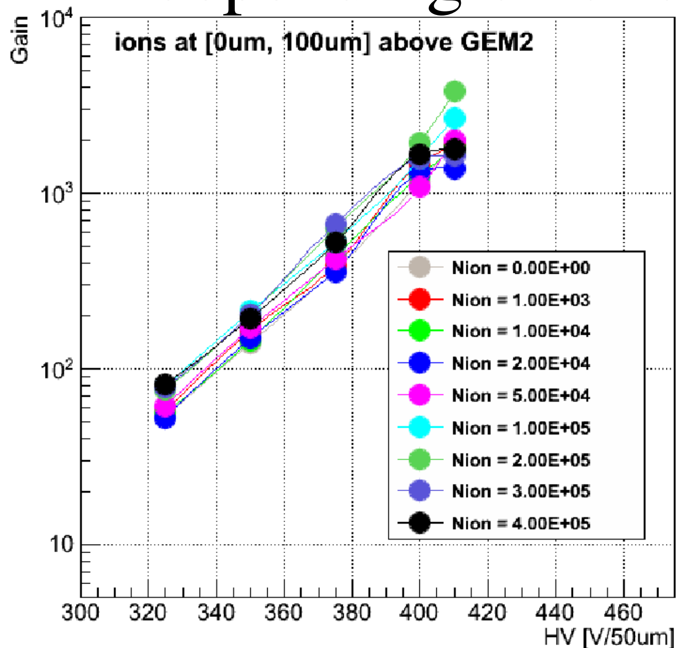

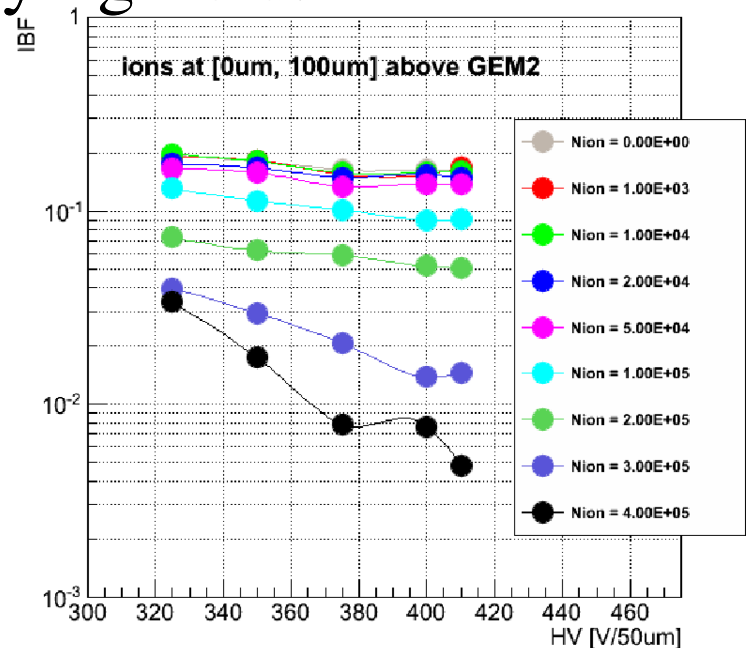

Note: N_{ions} is expressed in ions / ½ hole

[Slide: Taku Gunji]

Penning mechanism (cont'd)

- Once produced, the excited noble gas atom can:
  - decay (cascade towards a radiative or metastable, which may or may not ionise);
    independent of the quencher concentration
  - collide and ionise a quencher molecule;
    linear in the quencher concentration
  - form a molecular ion or an excimer (usually not capable of ionising)
    linear resp. quadratic in the pressure.

- Hence, except at high pressure, the transfer probability should rise with the quencher concentration.